Graduate School ETD Form 9
(Revised 12/07)

PURDUE UNIVERSITY
GRADUATE SCHOOL
Thesis/Dissertation Acceptance

This is to certify that the thesis/dissertation prepared

By Cherie Nicole Billingsley

Entitled Developmental Differences and Altered Gene Expression in the Ts65Dn Mouse Model
of Down Syndrome

For the degree of   Master of Science

Is approved by the final examining committee:

Randall J. Roper
_____
Chair

Ellen Chernoff

Teri Belecky-Adams

To the best of my knowledge and as understood by the student in the *Research Integrity and Copyright Disclaimer (Graduate School Form 20)*, this thesis/dissertation adheres to the provisions of Purdue University's "Policy on Integrity in Research" and the use of copyrighted material.

Approved by Major Professor(s): Randall J. Roper

Approved by: Norman Lees   7/16/10
                       Head of the Graduate Program   Date

PURDUE UNIVERSITY
GRADUATE SCHOOL

Research Integrity and Copyright Disclaimer

Title of Thesis/Dissertation:

Developmental Differences and Altered Gene Expression in the Ts65Dn Mouse Model of Down Syndrome

For the degree of Master of Science

I certify that in the preparation of this thesis, I have observed the provisions of *Purdue University Teaching, Research, and Outreach Policy on Research Misconduct (VIII.3.1)*, October 1, 2008.*

Further, I certify that this work is free of plagiarism and all materials appearing in this thesis/dissertation have been properly quoted and attributed.

I certify that all copyrighted material incorporated into this thesis/dissertation is in compliance with the United States' copyright law and that I have received written permission from the copyright owners for my use of their work, which is beyond the scope of the law. I agree to indemnify and save harmless Purdue University from any and all claims that may be asserted or that may arise from any copyright violation.

Cherie Nicole Billingsley
_____
Printed Name and Signature of Candidate

7/16/10
_____
Date (month/day/year)

*Located at http://www.purdue.edu/policies/pages/teach_res_outreach/viii_3_1.html

DEVELOPMENTAL DIFFERENCES AND ALTERED GENE EXPRESSION IN THE
TS65DN MOUSE MODEL OF DOWN SYNDROME

A Thesis

Submitted to the Faculty

of

Purdue University

by

Cherie Nicole Billingsley

In Partial Fulfillment of the

Requirements for the Degree

of

Master of Science

August, 2010

Purdue University

Indianapolis, Indiana

ACKNOWLEDGMENTS

I would like to thank my advisor, Randall Roper, for his insight and motivation throughout my research. I would also like to thank my committee members, Ellen Chernoff and Teri Belecky-Adams, for taking the time to offer their advice towards my research. I would also like to acknowledge Abby Newbauer, Josh Blazek, Andy Darrah, Brady Harman, and Jared Allen for their contributions to my research. Finally, I'd like to thank all of my fellow lab members for their encouragement and support and also for baking amazing treats.

TABLE OF CONTENTS

LIST OF FIGURES

ABSTRACT

Billingsley, Cherie Nicole. M.S., Purdue University, August 2010. Developmental Differences and Altered Gene Expression in the Ts65Dn Mouse Model of Down Syndrome. Major Professor: Randall Roper.

Trisomy 21 occurs in approximately 1 out of 750 live births and causes brachycephaly, a small oral cavity, a shortened mid-face, and mental impairments in individuals with Down syndrome (DS). Craniofacial dysmorphology occurs in essentially all individuals with trisomy 21 and causes functional difficulties. Mouse models are commonly used to study the etiology of human disorders because of the conserved phenotypes between species. The Ts65Dn Down syndrome mouse model has triplicated homologues for approximately half the genes on human chromosome 21 and exhibits many phenotypes that parallel those found in individuals with DS. Specifically, newborn and adult Ts65Dn mice display similar craniofacial defects as humans with DS. Ts65Dn embryos also exhibit smaller mandibular precursors than their euploid littermates at embryonic day 9.5 (E9.5). Furthermore, Ts65Dn mice exhibit reduced birth weight which suggests a possible generalized delay in overall embryonic growth.

Based on previous research at E9.5, it was hypothesized that Ts65Dn E13.5 embryos would have reduced mandibular precursors with altered gene expression. It was also hypothesized that other neural crest derived structures would be reduced in trisomic

embryos. Using morphological measurements it was determined that the mandible, Meckel's cartilage, and hyoid cartilage were significantly reduced in E13.5 trisomic embryos. The tongue was of similar size in trisomic and euploid embryos while cardiac and brain tissue volumes were not significantly different between genotypes. Analysis of total embryonic size at E9.5 and E13.5 revealed smaller trisomic embryos with developmental attenuation that was not related to maternal trisomy.

A microarray analysis performed on the mandibular precursor revealed 155 differentially expressed non-trisomic genes. *Sox9* was of particular interest for its role in cartilage condensation and endochondral ossification. It was hypothesized that the overexpression of *Sox9* in the developing mandible would be localized to Meckel's and hyoid cartilages. Immunohistochemistry performed on the mandibular precursor confirmed an overexpression of *Sox9* in both Meckel's and the hyoid cartilages. This research provides further insight into the development of trisomic tissues, both neural crest and non-neural crest-derived, and also the specific molecular mechanisms that negatively affect mandibular development in Ts65Dn mice and presumably individuals with Down syndrome.

CHAPTER 1   INTRODUCTION

1.1   <u>Down Syndrome Etiology and History</u>

Down syndrome (DS or trisomy 21) is caused by the triplication of chromosome

21 (FRACCARO 1960; JACOBS 1959; LEJEUNE 1959) and affects approximately 1 of 750

newborns each year (CANFIELD 2006; CHRISTIANSON 2006; LEJEUNE 1959; WEIJERMAN

2008) (Figure 1.1.1). The majority of DS cases are caused by an error during meiosis

(95%), but other incidences of DS result from a translocation (4%) or mosaicism (1%)

(ALLEN 2009; FREEMAN 2007; MUTTON 1996). When DS results from a meiotic error, it

is most commonly caused by nondisjunction of chromosome 21 during meiosis I in the

oocyte (MUTTON 1996) (Figure 1.1.2). Translocations that result in trisomy 21 are most

often Robertsonian translocations (BEREND 2003; GIRAUD 1975). Robertsonian

translocations are whole-arm rearrangements between acrocentric chromosomes and

rob(14q21q) is the most common arrangement resulting in Down syndrome (BEREND

2003). In cases of mosaicism, a percentage of cells contain a normal karyotype while the

other cells have a third copy of chromosome 21 (MUTTON 1996). It is not fully

understood why these errors occur, but increased maternal age is known to increase the

risk for meiotic errors in the oocyte (FREEMAN 2007; HASSOLD 1985).

Down syndrome was first recognized as a separate condition from other cognitive

impairments in 1866 by John Langdon Down (DOWN 1866). Although it was not

recognized as a syndrome until somewhat recently, ancient art indicates that individuals with DS have existed since at least 2500 years ago (BERNAL 2006). Little is known about the quality of life for individuals with trisomy 21 before the 19th century, but advances in medical knowledge and technology continue to improve the life expectancy and functional capabilities of individuals with DS. For example, life expectancy for people with trisomy 21 has increased from an average age of 9 years in 1929, to 12 years in 1949, to 35 years in 1982, and to 55 years or older currently (BARNHART and CONNOLLY 2007; BITTLES and GLASSON 2004). Modern technology also improves physical functioning in individuals with DS through occupational and other therapies (VAN CLEVE *et al.* 2006). With ongoing research, the life expectancy and functional capabilities of individuals with DS will continue to improve.

1.2   Down Syndrome Phenotypes Cause Functional Difficulties

Even with advances in medical knowledge and technology, the phenotypes caused by trisomy 21 still cause functional difficulties in the lives of individuals with DS. The phenotypes caused by trisomy 21 vary greatly among individuals with DS, but the most common features are cognitive impairment, craniofacial dysmorphology, and cardiac malformations (BROWN 1990; CUNNIFF 2001; FREEMAN 1998; GUIHARD-COSTA 2006). Individuals with DS generally have an IQ ranging from 30-70 which causes intellectual difficulties on several different levels (CHAPMAN 2000). Specifically, people with trisomy 21 have short and long-term memory deficits, deficiencies in language production, and early onset Alzheimer disease (BROWN 1990; CARLESIMO 1997; CHAPMAN 2000; DALTON 1986; NADEL 2003). Along with altered neurological development, individuals

with DS also have brachycephaly which develops during gestation and remains throughout adulthood (ALLANSON 1993; GUIHARD-COSTA 2006). Further complicating learning difficulties, approximately 35-76% and 64% of children with DS experience ophthalmological disorders and hearing loss, respectively (BALKANY 1979; CUNNIFF 2001; DAHLE 1986; ROIZEN 2003).

Trisomy 21 not only affects intellectual development, but also increases the risk for cardiac deformities, Hirschsprung disease, and childhood onset leukemia (CUNNIFF 2001; FERENCZ et al. 1989; PUFFENBERGER et al. 1994). Approximately half of children with DS are born with a cardiovascular malformation which most commonly presents as an atrioventricular septal defect (FREEMAN 1998). Nearly 1% of individuals with trisomy 21 also suffer from leukemia or Hirschsprung disease (CUNNIFF 2001).

As adults, individuals with DS have a higher incidence of obesity that is exacerbated by lower resting metabolic rates (ALLISON et al. 1995; RUBIN et al. 1998). Craniofacial dysmorphology also complicates dieting and weight issues by causing difficulties with chewing and swallowing (VAN CLEVE and COHEN 2006). The most common craniofacial abnormalities in individuals with DS are a flattened nose bridge, small oral cavity, shortened mid-face, and a hypoplastic mandible (EPSTEIN 2001; ROIZEN 2003; SHOTT 2006; VAN CLEVE and COHEN 2006). The small oral cavity results in a proportionally larger tongue and relative macroglossia which complicates important daily functions such as speaking and eating (GUIMARAES 2008). Approximately 50-75% of patients with trisomy 21 also suffer from sleep apnea which is exacerbated by craniofacial deformities (CUNNIFF 2001; MARCUS 1991; TROIS et al. 2009). Craniofacial dysmorphology develops prenatally and persists throughout adulthood which indicates

that individuals with Down syndrome may struggle with functional difficulties for the entirety of their lives (ALLANSON 1993; DAGKLIS *et al.* 2006; GUIHARD-COSTA 2006).

1.3   Down Syndrome Mouse Models

Mice serve as beneficial model organisms for the study of human disease because considerable homology exists between the murine and human genomes (DAVISSON 1993) (Figure 1.3.1). Specifically, mice have served as useful models for DS because of the homology between *Homo sapiens* 21 (Hsa21) and *Mus musculus* 16, 17, and 10 (Mmu16, Mmu17, and Mmu10) (DIERSSEN 2001). In humans, chromosome 21 is the smallest autosome and represents only about 1-1.5% of the human genome (HATTORI 2000). Approximately 364 genes have been identified on Hsa21 and about 170 of these genes are highly conserved human/mouse orthologues (GARDINER 2003; HATTORI 2000). One of the first trisomic mouse models, Ts16, was created by a bilateral Robertsonian translocation of Mmu16 (DAVISSON 1993; DIERSSEN 2001). This mouse model had limited usefulness because Mmu16 has many genes that were not present on Hsa21 and is also missing several important genes found on human chromosome 21. It was also impossible to study the later development of Ts16 mice because they died *in utero* (DAVISSON 1993; DIERSSEN 2001). Since then, several segmental trisomic mouse models have been created including the Ts(12;16C-tel)1Cje, Dp(16Cbr1-ORF9)1Rhr, Ts[Rb(12.Ts17^{16}65Dn)]2Cje, Ts(17^{16})65Dn, Dp(16)1Yu, and *Dp(10)1Yey/+;Dp(16)1Yey/+;Dp(17)1Yey/+* (Ts1Cje, Ts1Rhr, Ts2Cje, Ts65Dn, Dp16, and Ts1Yey;Ts2Yey;Ts3Yey, respectively) (LI 2007; MOORE 2007; VILLAR 2005; YU *et al.* 2010). The Ts65Dn mouse model has three copies of Mmu16 from *App* to *Mx1* and is

homologous to approximately half of Hsa21 genes (DAVISSON 1993; DIERSSEN 2001; GARDINER 2003; REEVES 1995) (Figure 1.3.2). It is the most widely used mouse model for DS because it displays many phenotypes that parallel those found in individuals with trisomy 21 such as reduced birth weight, cognitive and behavioral impairments, neurological structural deficiencies, craniofacial dysmorphology, and cardiovascular abnormalities (MOORE 2007).

Initial research on the Ts65Dn mouse model revealed reduced birth weight in newborns and functional sterility in males (REEVES 1995). More recent research has also shown that only ~35% of the offspring from Ts65Dn mothers are trisomic at weaning (MOORE 2006; ROPER 2006a). Much research on the Ts65Dn mouse model has focused on neurological development and function because of the intellectual disabilities that occur in individuals with DS. Specifically, Ts65Dn mice were found to exhibit impaired functioning in complex learning and memory tasks that correlates with the intellectual difficulties displayed by humans with DS (REEVES 1995). To more specifically study the cause of learning and memory disabilities, many researchers focused on the structure and function of the hippocampus. One study found reduced long term potentiation (LTP) in the hippocampus (HOLTZMAN 1996; SIAREY 1997) while another study discovered significantly enlarged presynaptic and postsynaptic elements in Ts65Dn brains (BELICHENKO 2004). Furthermore, Ts65Dn embryos were shown to exhibit altered growth of the hippocampus due to abnormal proliferation of embryonic precursor cells (CHAKRABARTI 2007). Extended research on hippocampal development revealed reduced cell proliferation in the Ts65Dn dentate gyrus and cell cycle differences between trisomic and euploid cells (CONTESTABILE 2007). The altered growth and development in the

Ts65Dn hippocampus parallels the reduced hippocampal size found in individuals with DS which further supports the use of the Ts65Dn mouse model to study human trisomy 21 (AYLWARD *et al.* 1999; CHAKRABARTI 2007).

Cerebellar development has also been of particular interest because of motor impairments exhibited by individuals with DS. The cerebellar volume in adult Ts65Dn mice was shown to be significantly reduced because of a reduction in both granule and molecular layers of the cerebellum (BAXTER 2000). The cerebellum was found to be significantly reduced as early as postnatal day 6 (P6) in Ts65Dn mice (BAXTER 2000; ROPER 2006b). As with the hippocampus, the reduced cerebellar volume in Ts65Dn mice correlates with the smaller cerebellar size found in individuals with DS (CROME 1966).

In addition to altered hippocampal and cerebellar growth, Ts65Dn mice also demonstrate early signs of Alzheimer disease similar to those found in individuals with DS. Trisomic mice were found to have age-related degeneration of septohippocampal cholinergic neurons and elevated amyloid precursor protein (APP) levels in the hippocampus which are indicative of Alzheimer disease found in elderly individuals with DS (HOLTZMAN 1996; SEO 2005).

Trisomy in the Ts65Dn mouse model not only affects the development of the brain but also the growth of many other structures. One study found that cell proliferation of fibroblasts was impaired in Ts65Dn mice which suggests that expansion of body tissues occurs at a slower rate in trisomic mice when compared to euploid littermates (CONTESTABILE 2009a). Other studies have revealed a high rate of heart defects in Ts65Dn pups. Specifically, one study found that 17% of trisomic pups had aortic arch defects and enlarged foramen ovales (WILLIAMS 2008).

Trisomy in the Ts65Dn mouse model also causes defects in craniofacial structures that are analogous to those found in individuals with DS (RICHTSMEIER 2000) (Figure 1.3.3). In both neonatal and adult trisomic mice, differences in craniofacial shape and reductions in size of the anterior face, palate, and mandible parallel those found in individuals with trisomy 21 (HILL 2007). Specifically, the mandible inTs65Dn mice at P0 was found to be significantly reduced (HILL 2007). In E9.5 Ts65Dn embryos, a reduced first pharyngeal arch (PA1) with fewer cranial neural crest (CNC) cells indicates an early origin to the mandibular abnormalities seen postnatally (ROPER 2009).

The Ts65Dn mouse model has been found to exhibit many neurological, cardiovascular, and craniofacial abnormalities that parallel those found in humans with DS (BAXTER 2000; CHAKRABARTI 2007; CROME 1966; HILL 2007; WILLIAMS 2008). Since the development of many structures is conserved between humans and mice, abnormalities found in both Ts65Dn mice and individuals with DS suggest common developmental pathways that are affected by trisomy.

1.4   Craniofacial Development

In normal embryonic development, the mandible is derived mainly from CNC cells and paraxial mesoderm (KNIGHT 2006; MINA 2001). CNC are pluripotent cells that delaminate from the ectoderm overlying the dorsal neural tube and migrate to form skeletal structures, connective tissue, and peripheral nervous system components (KNIGHT 2006; MINA 2001; TRAINOR *et al.* 2002) (Figure 1.4.1). Paraxial mesoderm is responsible for forming craniofacial muscles and some skeletal elements of the skull (MINA 2001).

The CNC cells migrate in three distinct streams from the hindbrain to colonize the pharyngeal arches (PAs). After migration, each PA consists of a core of mesoderm surrounded by CNC cells that are encompassed by endodermal and ectodermal epithelia (KNIGHT 2006). The first pharyngeal arch (PA1) gives rise to the mandibular and maxillary processes while the PA2 contributes to hyoid development (MINA 2001) (Figure 1.4.2). The ventral portion of the PA1 becomes Meckel's cartilage and contributes to the formation of the lower jaw while the distal portion becomes the maxilla (KNIGHT 2006). Meckel's cartilage, a transitory structure in the jaw that provides the template for mandibular growth, undergoes endochondral ossification to form the incus, malleus, and part of the mandible (ASLING 1973; BERESFORD 1975; BHASKAR 1953; FROMMER 1971; ISHIZEKI 1999; RAMAESH 2003). Excluding secondary cartilages, the rest of the mandible develops through intramembranous ossification (BERESFORD 1975; BHASKAR 1953; FROMMER 1971).

Bone is formed through intramembranous ossification when mesenchymal cells develop directly into osteoblasts. In endochondral ossification, undifferentiated mesenchymal cells first condense and then differentiate into chondrocytes. The chondrocytes proliferate and become hypertrophic. Hypertrophic chondrocytes then create a calcified matrix and undergo apoptosis so that blood vessels can invade the matrix and osteoblasts can enter to lay the bone matrix. Hypertrophic chondrocytes are particularly important in regulating chondrogenesis and osteogenesis because they form the scaffold for bone formation (PROVOT and SCHIPANI 2005).

Several genes and other molecules are known to regulate or affect both osteogenesis and mandibular development. For example, *Hox* genes are thought to

coordinate A-P patterning of the hindbrain with corresponding pharyngeal arches (KNIGHT 2006). CNC cells that migrate to the PA1 do not express *Hox* genes while the CNC that fill the PA2 express *Hox* group 2 genes (KNIGHT 2006). While *Hox* genes are responsible for the A-P patterning of PAs, the nested expression of *Dlx* genes is contribute to D-V specification (KURAKU *et al.* 2010). Specifically, *Dlx3, Dlx5,* and *Dlx5* are expressed in the mandibular processes, and *Dlx5* and *Dlx6* are also expressed in developing bones, cartilage, and teeth and may play an important role in mandibular formation (MINA 2001). *Dlx* genes in PAs are regulated by endothelin-1 (Edn-1), a signaling molecule that has conserved functions in the formation of the mandible (KIMMEL *et al.* 2003; KNIGHT 2006; KURAKU *et al.* 2010).

Sonic hedgehog (Shh) is also thought to have an important function in craniofacial development and has been shown to be expressed during epithelial-mesenchymal interactions (MINA 2001). Fibroblast growth factor 8 (Fgf8) is another key molecule in epithelial-mesenchymal interactions, and it has been shown that a deficit of Fgf8 results in loss of skeletal mandibular elements (KNIGHT 2006). Bone morphogenetic proteins (BMPs) also play a crucial role in osteogenesis of the mandible, and the Wnt gene family also affects endochondral ossification by regulating chondrocyte differentiation (MERRILL *et al.* 2008; MINA 2001). Normal development of the mandible depends heavily on the expression of these genes and molecules, but the dysregulation of other genes may also indirectly affect mandibular development.

1.5 *Sox9* Affects Endochondral Bone Development

One gene of particular interest to the development of the mandible is *Sox9* (Sry-box containing gene 9), a transcription factor located on Hsa17 that regulates testis development and chondrogenesis (BELL *et al.* 1997; BI 1999; FOSTER *et al.* 1994; WAGNER *et al.* 1994) (Figure 1.5.1). Sox9 initiates chondrogenesis by binding specifically to sequences in the first intron of collagen, type II, alpha 1 (*Col2a1*) (BELL *et al.* 1997; BI 1999; LEFEBVRE *et al.* 1997; NG 1997; WAGNER *et al.* 1994; ZHAO 1997). *Col2a1* encodes for type-II collagen which is a major cartilage matrix protein (BELL *et al.* 1997; NG 1997). Expression of *Sox9* occurs mainly in mesenchymal condensations throughout the embryo where cartilage or bone formations develop, but it is also present in other areas such as the central nervous and urogenital systems (BI 1999; WRIGHT 1995). *Sox9* expression is necessary for the differentiation of CNC into cartilage and endochondral bone structures but not for the correct migration and localization of CNC into pharyngeal arches (MORI-AKIYAMA *et al.* 2003). Haploinsufficiency of *Sox9* in humans results in campomelic dysplasia which is characterized by skeletal malformation and XY sex reversal (FOSTER *et al.* 1994; WAGNER *et al.* 1994).

In mice, the homologue of human *Sox9* is located on Mmu11 (DIETRICH *et al.* 1994; SCHMITT *et al.* 1996). Haploinsufficiency of *Sox9* in murine models results in a phenotype characteristic of the human syndrome campomelic dysplasia. Mice with only one copy of *Sox9* display hypoplasia and premature mineralization of endochondral bones (BI *et al.* 2001). When *Sox9* is completely absent in undifferentiated mesenchymal cells of limb buds, both cartilage and endochondral bone fails to develop which indicates that *Sox9* has an important role in the differentiation of mesenchymal cells into

chondrocytes (AKIYAMA *et al.* 2002). *Sox9* also inhibits the transition of proliferating chondrocytes into hypertrophic chondrocytes, but *Sox9* expression is not actually present in hypertrophic chondrocytes (AKIYAMA *et al.* 2002; HARGUS *et al.* 2008; ZHAO 1997). Dysregulation of *Sox9* could have deleterious effects on both Meckel's cartilage and the hyoid bone, which develop through endochondral ossification (MINA 2001).

1.6   Microarrays Used to Determine Abnormal Gene Expression

The DNA microarray is a relatively new form of technology that emerged in the early 1990's and allows for comprehensive genetic analysis of an organism (BILITEWSKI 2009; ROGERS and CAMBROSIO 2007). Microarrays utilize probes, either spotted cDNAs or oligonucleotides, which are specific to an organism, gene, or genetic variant. This specific design allows for genotyping, expression analysis, and studies of protein-DNA interactions. Microarrays are unique from traditional blot analysis because the nucleic acids hybridize to immobilized probes and are separated and identified based on their affinity to each specific probe rather than by their size (BILITEWSKI 2009).

Microarrays are beneficial to the study of DS because they provide a method to uncover the gene dosage effects caused by a triplicated chromosome. Two separate hypotheses have been formulated to explain the pathogenesis of trisomy 21. The gene dosage effect hypothesis proposes that the DS phenotype is caused by the overexpression of genes located on the triplicated chromosome. Alternatively, the amplified developmental instability hypothesis attests that most symptoms of DS are the result of a non-specific disturbance of chromosome balance which disrupts developmental homeostasis (AMANO 2004; EPSTEIN 1990; PRITCHARD and KOLA 1999).

Regardless of which hypothesis is true, it is most commonly thought that triplicated genes will exhibit a 1.5 fold increase in expression (EPSTEIN 1990; KAHLEM *et al.* 2004). Since this theory was first introduced, many experiments have both supported and contradicted this hypothesis. For example, one study performed a microarray on lymphoblastoid cells and determined that Hsa21 gene expression in individuals with DS could be grouped into four different classes. Class I contained 30 genes with an expression ratio of DS/control close to 1.5 which supports the original gene dosage hypothesis. Class II had only 9 genes with an expression ratio greater than 1.64, and it is hypothesized that these genes may have a more dominant role in creating the DS phenotype. Class III consisted of 77 genes that had an expression ratio below 1.4. It is thought that these genes may be compensated for by negative feedback systems (AIT YAHYA-GRAISON *et al.* 2007; LYLE *et al.* 2004). Class IV genes had differing expression rates between individuals with trisomy 21 which could possibly explain the variability in DS phenotypes. Other studies have discovered a global up-regulation of chromosome 21 gene expression ranging from 1.37 fold in fetal cerebellum and heart tissues, 1.27 in blood, and 1.28 in amniocytes (CHOU *et al.* 2008; MAO *et al.* 2005; TANG *et al.* 2004). According to these studies, approximately 20% of Hsa21 genes are significantly dysregulated in human fetal cells while 10.2% of individual genes are dysregulated in fetal cerebellum and heart tissues (FITZPATRICK *et al.* 2002; MAO *et al.* 2005). In DS amniocytes, euploid gene expression is close to 1.00 fold, but approximately 17 individual euploid genes in trisomic individuals are significantly dysregulated (CHOU *et al.* 2008).

Because of the difficulty in accessing trisomic human tissue, DS mouse models have provided a useful alternative for examining gene expression with microarray technology. Currently, most microarray studies on mice have been performed to determine the genetic etiology of cognitive disabilities that occur in DS. In Ts1Cje mice, trisomic genes in the cerebellum have an average 1.5 fold gene expression ratio when compared euploid mice (DAUPHINOT *et al.* 2005; LAFFAIRE *et al.* 2009; POTIER *et al.* 2006). Approximately 2.4-7.5% of non-trisomic genes are also significantly dysregulated in the cerebellum of trisomic mice (LAFFAIRE *et al.* 2009; POTIER *et al.* 2006). Interestingly, six non-trisomic homeobox genes were severely repressed in the cerebellum, but there was no noticeable developmental delay in the Ts1Cje mice (DAUPHINOT *et al.* 2005). Another study examined gene expression in the brain of P0 Ts1Cje mice and found approximately a 1.5 fold expression level of trisomic genes (AMANO 2004). In the Ts65Dn mouse model, a study of the cerebellum revealed an expression level of 1.45 fold in trisomic genes which is similar to what was found in the cerebellum of the Ts1Cje model (SARAN *et al.* 2003). More specifically, microarray analysis revealed that the cerebellum of trisomic mice had a significantly decreased expression level of Cyclin B1, which regulates cell cycle elongation and affects neurogenesis in the cerebellum (CONTESTABILE 2009b).

Furthermore, another study on the Ts65Dn mouse model examined nine separate tissues and found a general upregulation of trisomic genes by approximately 1.5 fold. Similar to the study on human lymphoblastoid cells, it was revealed that the expression level of 1.5 fold was a general trend in trisomic genes, but that many genes were actually expressed at significantly lower or higher levels (AIT YAHYA-GRAISON *et al.* 2007;

KAHLEM *et al.* 2004). It was also discovered that some disomic genes were significantly

dysregulated in the Ts65Dn tissues (KAHLEM *et al.* 2004).

1.7   Gene Ontology Organizes Genes According to Functions

Recent advances in genomic sequencing have indicated that many genes and their

functions are conserved between eukaryotes. This suggests that the discovery of a gene or

protein in one species could have implications for its function in another species. With

the constant influx of new information about genes and their functions, an organized

database with all known information would be invaluable to scientists. Gene ontology

(GO) is a concept that was created with the intentions of creating a common vocabulary

for genes and protein sequences between different species. GO organizes current

biological knowledge and also serves as a guide for organizing new data. The GO

database organizes genes based on their biological function, molecular function, and

cellular component. The database provides a centralized source of known information

which allows scientists from many different research backgrounds to effectively share

information (ASHBURNER *et al.* 2000).

The GO database has been particularly helpful in Down syndrome research. Many

DS researchers use microarrays to determine abnormal expression of genes in certain

tissues, and the GO database enables scientists to quickly determine the known function

of dysregulated genes. Knowledge of a dysregulated gene's function in a certain tissue

allows experimenters to formulate potential biochemical pathways that are affected by

trisomy 21. For example, one experiment analyzed gene expression in human fetal

cerebellum and heart tissues with DNA microarrays. The GO database allowed for the

functional grouping of dysregulated genes which provided indications of possible

biological pathways affected by DS (MAO *et al.* 2005). Another experiment analyzed

gene expression in Ts1Cje mice and determined that *Girk2* was over-expressed in

postnatal cerebellar development. Use of the GO database revealed *Girk2*'s role in

cerebellar development and allowed the researchers to hypothesize a potential cause of

the hypoplastic cerebellum in Ts1Cje mice (LAFFAIRE *et al.* 2009). Because the GO

database is constantly accruing new information, it will continue to be a beneficial tool

for scientists.

1.8   Thesis Hypothesis

Since the PA1, or mandibular precursor, is significantly smaller at E9.5 and the

mandible is reduced at P0, it is hypothesized that the mandibular precursor at E13.5 will

also be significantly smaller in Ts65Dn mice (HILL 2007; ROPER 2009). Furthermore, it is

hypothesized that the CNC deficit at E9.5 will cause other neural crest derived structures

such as Meckel's cartilage, the hyoid cartilage, and the tongue to be significantly smaller

at E13.5 in trisomic embryos. Along with reduced CNC derived structures, it is

hypothesized that there will be an overall reduction in size at E13.5 in trisomic embryos

because both Ts65Dn mice and newborns with DS exhibit reduced birth weight.

Because of the reduced trisomic mandibular precursor at E13.5, it was originally

hypothesized that triplicated genes would exhibit altered expression and adversely affect

the growth of the mandible at E13.5. When the results from the microarray analysis

revealed only non-trisomic genes with abnormal expression, it was hypothesized that

triplicated genes were dysregulated earlier in development and consequently, altering the

expression of downstream non-trisomic genes at E13.5. Furthermore, it was hypothesized that the dysregulated non-triplicated gene *Sox9* would be expressed in Meckel's and the hyoid cartilage which would further delay mandibular growth.

CHAPTER 2   MATERIALS AND EXPERIMENTAL METHODS

2.1   Ts65Dn and B6C3F$_1$ Breeding

Female B6EiC3Sn a/A-Ts(17^{16})65Dn (Ts65Dn) and female and male B6CBA-Tg(Wnt1-lacZ)206Amc/J (Wnt1-lacZ), B6.129S4-Gt(ROSA)26Sor^{tm1Sor}/J (B6.R26R) and C3H/HeJ (C3H) mice were purchased from the Jackson Laboratory (Bar Harbor, ME). Wnt1-Cre mice came from the lab of Dr. Yang Chai of the University of Southern California and backcrossed >6 generations to C57BL/6J (B6) mice. Wnt1-lacZ mice were brother-sister mated and mice homozygous for the Wnt1-lacZ transgene were identified and maintained in our colonies on an approximate B6 background. B6(R26R)C3F$_1$ mice were created by mating B6.R26R females with C3H males. The Ts65Dn and euploid embryos used in this study were generated at Indiana University-Purdue University Indianapolis (IUPUI) by crossing Ts65Dn females with B6(R26R)C3F$_1$ males. All animal use and protocols were reviewed and approved by the IACUC committee at IUPUI.

2.2   Ts65Dn Genotyping

Ts65Dn mice were prescreened through a restriction digest of a polymerase chain reaction (PCR) product amplified from the small translocation marker chromosome (17^{16}). The mouse DNA was isolated and PCR was performed and followed with a *SacI*

(New England BioLabs, Ipswich, MA) restriction digest. *SacI* cuts the DNA from the

B6C3F$_1$ background but not from the DBA background which causes the trisomic pups to

be represented by two bands since they contain the digestion site (LORENZI 2010). The

ploidy was confirmed through fluorescent in situ hybridization (FISH) after three weeks

of age (MOORE 1999).

2.3   E13.5 Dissections

Pregnant female mice were sacrificed thirteen and a half days after a vaginal plug

had been confirmed. The mice were then anesthetized with isoflurane (Webster

Veterinary Supply, Inc., USA) and euthanized through cervical dislocation. Embryos

were then dissected out of the uterus and placed onto ice to induce hypothermia. Embryos

were dissected in Phosphate Buffered Saline (PBS) (Mediatech, Herndon, VA), and yolk

sacs were removed for later genotyping. After the dissection, embryos were rinsed twice

in PBS and photographed with a Nikon Digital Sight Camera at 0.75X. Embryos that

originated from a mother without the R26R transgene were then fixed in 4%

paraformaldehyde (MP Biomedicals, Solon, OH) at 4°C overnight.

If the mother was either R26R +/- or +/+, then the embryos were only fixed in 4%

paraformaldehyde for two hours before being rinsed with β-gal buffer. They were then

placed in β-gal overnight at 4°C. The following day the embryos were first washed with

β-gal and then were placed in X-gal substrate (Fisher Science Education, Rochester, NY)

and allowed to incubate at 37°C for 72 hours. After the first 24 hours, the X-gal substrate

was replaced in all stained embryos. After the total 72 hours incubation the embryos were

washed twice in β-gal and then pictures were once again taken at 0.75X. Finally, embryos

were fixed in 4% paraformaldehyde overnight before processing.

Whether or not originating from an R26R positive mother, all embryos began

processing after they had been fixed in 4% paraformaldehyde overnight. Processing of

the embryos began with a dehydration step. Embryos were placed in 50%, 70%, 70%,

95%, 95%, 100%, and 100% ethanol for 20 minutes each. After dehydration, the embryos

were cleared by being placed in a 1:1 mixture of 100% ethanol and xylenes (Fisher

Scientific, Fair Lawn, NJ) for 20 minutes. They were then placed in xylenes twice for 20

minutes. Finally the embryos went through the embedding process by first incubating the

embryos in 1:1 xylenes and paraplast at 56°C for one hour. This was followed by a 20

minute incubation in paraplast and then an overnight incubation in paraplast at 56°C. The

following day embryos were placed in a mold for later sectioning. Embryos were allowed

to cure at 4°C before sectioning.

2.4   Sectioning E13.5 Embryos

Embryos were sectioned after they had been embedded for at least one week.

Embryos were first removed from the plastic mold and then melted onto a small block

that fits into the microtome. Embryos were sectioned at 22 µm and then placed into a

40°C water bath to allow the sections to smooth out. While the sections were in the water

bath, slides were prepared with the embryo's number, date of dissection, and the numbers

of the sections. Five sections were then placed onto each slide (Fisher Scientific, Fair

Lawn, NJ). The five sections were ribboned off the microtome together to ensure the

order of the sections. After the entire embryo was sectioned, slides dried on a 55°C slide

warmer overnight.

2.5   Staining E13.5 Sections

Following sectioning, slides were melted in a 56°C incubator for at least an hour

or until the paraplast was melted. Slides then went through an Eosin staining protocol.

The slides were placed in citrisolve (Fisher Scientific, Fair Lawn, NJ) three times for four

minutes each. They were placed in 100% ethanol twice for two minutes and then placed

into 90%, 70%, and 50% ethanol for two minutes each. Next they were placed into a 1%

eosin (Fisher Scientific Company, LLC, Kalamazoo, MI) 100% ethanol solution for two

minutes to stain them. This was followed by two rounds of 95% ethanol for 30 seconds

each and then two rounds of 95% ethanol for two minutes each. Finally, the slides went

through three rounds of citrisolve for three minutes each. After the staining process, the

slides were carefully dried and then coverslipped with dibutyl phthalate with xylenes

(DPX mounting medium) (Electron Microscopy Sciences, Hatfield, PA). Slides were

allowed to cure for a least one week before being examined.

2.6   Unbiased Stereology

All calculations of volume were made with the program Stereologer 2000 on a

Nikon Eclipse 80i microscope. For all regions measured, the region volume fraction and

a Cavaleri point grid were used to determine the measurements. The thickness of all

sections was viewed at 100X magnification. The slab sampling interval was one, and the

common probe information for all measurements was the same. The frame area was

25.00% screen height and the screen height was 0.01 mm. The frame spacing was 0.002

mm and the dissector placement was centered. Also, all measurements were made with

systematic random sampling and the measurements were made with blind knowledge

toward the genotype of the embryo. The measurements of each structure were performed

by the same experimenter to reduce possibility of procedural error and all structures were

defined with an atlas for mouse development (KAUFMAN 2003). Random starting

numbers were produced by the Stereologer 2000 program. The volume, thickness, and

coefficient of error (CE) were recorded for each measurement.

To determine the total volume of each embryo, a random sampling of every 15th

section was examined. The area per point was 0.1 mm². The area of each embryo was

determined at 4X magnification. For mandibular analysis, the mandible was defined so

that it included Meckel's cartilage but not the hyoid bone or the tongue. (Figure 2.6.1 C).

Once the mandibular precursor was defined, a random sampling of every 5th section was

examined to determine the total volume of the precursor. The area per point was 0.01

mm² and was determined at 4X magnification.

When measuring brain volume, the area inside the ventricles was included in the

calculation (Figure 2.6.1 A). A random sampling of every 10th section was measured.

The area per point was 0.009 mm² and examined at 4X magnification. For neocortical

examination, the neocortical precursor was considered to be the outer lining around the

lateral ventricles and was bound by the choroid plexus on one side and the ganglionic

eminences on the other (Figure 2.6.1 B). Measurements were taken at every 7th section.

The area per point was 1.5E-06 mm² and was measured at 10X magnification.

2.7 Statistics for Volume Measurements

Results from embryos that were marked as being damaged or questionable were

removed from the analysis. Data from the stereological results was analyzed with either a

one-tailed or two-tailed student's t-test to determine significance. Measurements that

were hypothesized to be smaller (total volume, mandibular precursor, tongue, Meckel's

cartilage, hyoid cartilage, neocortex, brain/total volume, neocortex/total volume, and

mandibular precursor/total volume) were analyzed with a one-tailed student's t-test.

Structures that were not hypothesized to be either larger or smaller (heart, liver, brain,

and heart/total volume) were analyzed with a two-tailed student's t-test. A p-value of

0.05 or below was considered statistically significant.

For the comparison of total embryonic size, differences between offspring from

$B6C3F_1$, euploid control, Ts65Dn euploid, and Ts65Dn trisomic mothers were

determined using analysis of variance in PROC GLM (SAS, Cary, NC). Least significant

difference post hoc comparisons (contrasts) were used to determine differences between

strains. A significance level of $\alpha = 0.05$ was used in all multiple comparison tests.

Correlation between E13.5 CRL, area, and volume was determined using PROC CORR

in SAS. A one-tailed t-test was performed to determine genotypic and phenotypic

differences between two strains of offspring.

2.8   Fluorescent In Situ Hybridization (FISH)

2.8.1 Processing the Yolk Sac for FISH Analysis

Yolk sacs were removed from E13.5 embryos and placed in 0.5 ml of Dulbecco's PBS (DPBS) (Mediatech, Inc., Herndon, VA) in a 1.5 ml tube. Yolk sacs were then centrifuged at 12,000 rpm for one minute. The supernatant was discarded and yolk sacs were resuspended in DPBS and vortexed. Once again, the yolk sacs were centrifuged at 12,000 rpm for one minute. The supernatant was removed and 0.5 ml of collagenase (type X1-S, 1000 U/mL in HBSS) (Sigma, St. Louis, MO) was added to each yolk sac and vortexed. The yolk sacs were then incubated in a 37°C water bath for 30 minutes. After incubation, yolk sacs were centrifuged at 12,000 rpm for one minute and then the supernatant was removed. Next, 0.5 ml of KCl (Invitrogen, Carlsbad, CA) was added and resuspended by vortexing. Yolk sacs were once again incubated in a 37°C water bath for 30 minutes. After incubation, one drop of 3:1 methanol: acetic acid (Fisher Scientific, Fair Lawn, NJ and J.T. Baker, USA) fix was added to each tube. The yolk sacs were then centrifuged at 13,000 rpm for one minute and then the supernatant was removed. Finally, the yolk sacs were resuspended in 0.5 ml of 3:1 methanol: acetic acid fix. Pellets were resuspended with a pipette tip and then were stored at 4°C for up to a week before dropping (ROPER 2009).

2.8.2 Dropping of Yolk Sacs

At least 24 hours after processing, the yolk sacs were then prepared to be "dropped" onto a VCE slide. The yolk sacs were centrifuged at 12,000 RPM for five

minutes. In the meantime, a 250 ml beaker was half-filled with water and heated until boiling. Two slides for each embryo were prepared by labeling each slide with the embryo number and the date dissected. Once the yolk sacs finished centrifuging, a single drop of distilled water was placed onto the "C" portion of the slide. Then a glass pipette was used to resuspend the yolk sac and then to place one drop of the yolk sac mixture onto each slide. It was best to avoid getting large samples of tissue on the slide. The slides were then placed on top of the beaker of boiling water for 30 seconds. While the first slides were being heat fixed, the same process would be repeated for the next slide. After all slides were heat fixed with cells from the yolk sac, they were fixed to the slide with 1 ml of a 3:1 methanol: acetic acid. Finally, they were allowed to dry at room temperature for 24 hours before the hybridization process could begin.

2.8.3 Hybridization

Before beginning the process, a humidified box was made and placed into a 37°C incubator. The slides that were previously fixed with the yolk sac cells were placed into a Coplin jar filled with 2X sodium chloride and sodium citrate solution (SSC) and were incubated in a 37°C water bath for 30 minutes. While slides were incubating, the probe and Denhyb (Insitus Biotechnologies, Albuquerque, NM) were warmed to room temperature. A 10:1 Denhyb/probe solution was made and warmed in the 37°C water bath. After the 30 minute incubation, the slides were dehydrated in cold 70%, 85%, and 100% ethanol for two minutes each. The slides were taken to a dark room and placed on a 37°C dry bath for three minutes. Next 7 µl of the Denhyb/probe solution was added to each slide. An 18 x 18 coverslip was then placed on the slide and sealed with rubber

cement. Slides were then quickly moved to an 85°C dry bath for five minutes. Finally,

the slides were placed in the humidified box and allowed to incubate overnight.

2.8.4 Viewing of FISH Slides

The day following the hybridization step, slides were removed from the

humidified box in a dark room. The rubber cement was removed and the slides were

placed in a solution of 2X SSC for five minutes at 68°C. The slides were placed into

another solution of 2X SSC set at room temperature for seven minutes. Then 8 µl of

Antifade/4',6-diamidino-2-phenylindole (DAPI) (Chemicon International, Temecula,

CA) was placed onto each slide and sealed with a 22 X 22 coverslip. Slides were then

immediately viewed with a Nikon Eclipse 80i microscope and fluorescent light. Trisomic

mice were then able to be identified because the specific probe used was created from the

BAC clones 401C2 and 433G17 which bind to the distal triplicated portion of Mmu16

(MOORE *et al.* 1999). The embryos were then able to be genotyped based on the number

of markers found in each nucleus. Trisomic mice would have three signals in the nucleus

of each cell while the euploid mice would only have two. A genotype was confirmed

after ten separate cells had been examined and determined to have the same number of

markers in the nuclei.

2.9   Sox9 Immunohistochemistry

E13.5 embryos used for immunohistochemistry (IHC) were processed similarly to

the embryos used for the volumetric measurements, but embryos used for IHC were not

incubated with X-gal. After the washing steps they were immediately placed into 4%

paraformaldehyde overnight and were processed the next day instead of incubating in X-gal for 72 hours.

After allowing to cure in paraplast for one week, embryos were sectioned at 10 µm and melted at 45°C for five hours before the IHC process. To deparaffinize the embryos they were placed in xylene twice for three minutes, 1:1 xylene/100% ethanol for three minutes, 100% ethanol twice for three minutes, and 95%, 70%, and 50% ethanol for three minutes each. They were then placed in running tap water to rinse.

To perform the antigen retrieval step, a water bath was heated to 100°C. Then 75 ml of a 10 mM Sodium Citrate (pH 6.0) buffer was brought to boiling in a microwave and then immediately poured into a glass Coplin jar. The Coplin jar was then placed into the 100°C water bath and the slides were then placed in to the Coplin jar for 20 minutes. The slides were then removed and allowed to cool before rinsing them with tap water for 10 minutes.

A PAP pen (Research Products International, Corp., Japan) was used to create a barrier around the sections. The slides were then washed with a mixture of PBS and 0.025% Triton (PBST) (Promega Corporation, Madison, WI) twice for 5 minutes each. Next, the sections were blocked with 10% donkey serum (MP Biomedicals, Solon, OH) with 1% Bovine Serum Albumin (BSA) (Invitrogen, Carlsbad, CA) in PBS for two hours at room temperature. While the donkey serum mixture was on the slides, the primary antibody (Sox9 (H-90) anti-mouse rabbit polyclonal IgG, 200 µg/ml) (Santa Cruz Biotechnology, Santa Cruz, CA) was diluted 1:500 in PBS with 1% BSA. After the two hour blocking period, the donkey serum was removed and the diluted Sox9 antibody was pipetted onto the slide. The slides were then incubated overnight at 4°C.

The following day, the primary antibody was removed and the sections were washed twice with PBST for five minutes each. The secondary antibody (Alexa Fluor 594 donkey anti-rabbit IgG (H+L), 2 mg/ml) (Invitrogen, Eugene, OR) was then diluted 1:500 in PBST. The secondary antibody was applied to the sections in a dark room and then allowed to incubate for one hour at room temperature. After the incubation, the secondary antibody was removed and the slides were rinsed three times with PBS for five minutes each rinse. The hydrophobic barrier created by the PAP was then carefully removed with a razor blade and then 3 µl of Antifade/DAPI was then added to each individual section. The slides were then coverslipped and sealed with clear nail polish.

2.10 Image Capturing and Quantification of DAPI and *Sox9* Expression

Sections that included both hyoid and Meckel's cartilage were chosen for IHC. All chosen sections had a fully developed tongue and were closely matched so that each sample came from approximately the same sectioned area. Two sections from each embryo were chosen to be quantified. All images were taken with an Olympus FV 1000 confocal microscope. For the DAPI images, a laser emitting light with a wavelength of 405 nm was used. For the secondary antibody (Alexafluor 594) a laser with a wavelength of 548 nm was used. Images were taken with a 20X water lens and image was zoomed in 2.5X for a total of 50X magnification. There was an average of four scans per image.

DAPI and antibody images for each animal were opened in ImageJ. The "Image" type was set to "RGB" and then "Image--->Composition" was selected. The DAPI picture was set as blue and the antibody was red. Files were then saved as a "tif" file. Images were then opened and quantified with Adobe Photoshop CS4 with a procedure

based on previous work by Kirkeby and Matkowskyj (KIRKEBY 2005; MATKOWSKYJ 2000). To start, either Meckel's or the hyoid cartilage was selected with the lasso tool with care to only select cells within the perichondrium, but not including the perichondrium. Once the selection was created, two copies of the selection were made to produce two new layers. On one layer, the background was painted black with the paint bucket tool. This was to allow for objective selection with the wand tool. Previous studies have used the wand tool to select a dark background which would slightly vary in color and affect the areas selected, but selecting a completely black background allows for exactly the same selection each time.

After the background was "painted" black, the channels tool was selected and the red and green channels were deselected. This allowed for only the blue DAPI expression to be visualized. Next, the wand tool was selected with a tolerance set to 35 and "anti-alias" was checked. Using the wand tool, the artificial "black background" was selected. This selection would then be inverted and then only cells expressing DAPI were selected. The histogram tool was then set to "blue" channel and the source image was set to "selected layer". The values for mean intensity, standard deviation, median intensity, and pixel area could then be recorded. To determine *Sox9* expression within the DAPI selected region, the histogram channel was simply changed to red and the values recorded.

To analyze *Sox9* expression, each Sox9 value was divided by DAPI intensity to control for experimental variations such as sectioning differences and signal fading. Then the values were simply compared with a student's t-test with a p value of 0.05 or below determining significance. To determine that DAPI was an effective control, a correlation

analysis was performed with PROC CORR in SAS. Cell density was calculated by counting the number of selected nuclei and dividing by the area of either Meckel's or the hyoid cartilage.

2.11   Gene Ontology

The 155 genes that were found to be dysregulated at E13.5 in the mandibular precursor were inputted into a gene ontology database (http://www.genetools.microarray.ntnu.no/common/intro.php). The site then organized the genes based on molecular function, biological process, and cellular component. The biological process category was divided into 18 different subcategories. Each of these categories was then further divided into subsequent categories. Each category had a gene ontology number and then identifiers for each gene in the category. Selecting the identifier for a particular gene would bring up all known processes related to that particular gene and links to PubMed (http://www.ncbi.nlm.nih.gov/pubmed/) where the information could be verified.

CHAPTER 3   RESULTS

3.1   <u>Volumetric Measurements Show Reduced Volume and Relative Macroglossia in E13.5</u>

<u>Ts65Dn Embryos</u>

Both neonatal and adult Ts65Dn mice have a reduced anterior face, palate, and

mandible (HILL 2007). Recent research has also shown that at E9.5, Ts65Dn mice have a

significantly smaller PA1, or mandibular precursor, with fewer CNC (ROPER 2009)

(Figure 3.1.1). To examine how early developmental changes at E9.5 affect mandibular

growth at later stages, the mandibular precursor and other structures of 19 Ts65Dn and 21

euploid littermates were examined at E13.5. Using unbiased stereology, it was

determined that the Ts65Dn mandibular precursor was significantly reduced when

compared to euploid littermates (p= 0.005) (Figure 3.1.2). Contrary to the reduced size of

the mandibular precursor, the Ts65Dn tongue was not significantly different from euploid

littermates (p= 0.17) (Figure 3.1.3). This data indicates that the early developmental

changes found in the PA1 at E9.5 continue to affect the development of the mandible at

E13.5. These results also indicate an embryonic origin for relative macroglossia (normal

tongue size in smaller oral cavity) that has been seen in individuals with trisomy 21

(GUIMARAES 2008).

3.2   <u>Trisomic Structures Derived from CNC Reduced While Partial or Non-CNC Derived</u>

<u>Structures Similar in Size to Euploid</u>

It was originally hypothesized that the reduction of CNC in the PA1 and PA2 of

E9.5 Ts65Dn embryos would affect the development of CNC derived structures at E13.5.

As expected, the mandibular precursor, which is mostly CNC derived (KNIGHT 2006),

was significantly smaller in trisomic mice, but the tongue, which is partially CNC derived

(YAMANE 2005), was not significantly different between Ts65Dn and euploid embryos.

Since the CNC deficit did not seem to adversely affect the growth of the tongue as

expected, other CNC derived structures, such as Meckel's cartilage and the hyoid

cartilage, were evaluated to further understand the role of CNC in the developing

embryo.

Meckel's cartilage and the hyoid cartilage primordium are CNC derived structures

that are located within and posterior to the mandibular precursor, respectively. Meckel's

cartilage develops from the PA1 and provides a template for mandibular growth (KNIGHT

2006; RAMAESH 2003) while the hyoid cartilage primordium develops mainly from the

PA2 and later becomes the hyoid bone (LIEBERMAN *et al.* 2001). As hypothesized, the

volumes of the trisomic hyoid cartilage primordium and Meckel's cartilage were

significantly reduced when compared to euploid littermates (p= 0.0002 and 0.05,

respectively) (Figure 3.2.1 and 3.2.2). Cardiac tissue, which has minimal NC contribution

(MORIKAWA 2008), was also examined to understand the development of a structure with

little NC contribution. The cardiac tissue volume was not significantly different between

trisomic and euploid littermates (p= 0.90) (Figure 3.2.3). The data indicate that, of the

examined tissues, most of the structures that are derived mainly from CNC are smaller in

Ts65Dn embryos while trisomic structures that are non-CNC derived, or only have

minimal NC contribution, are similar in size to the corresponding structures in the

euploid mice.

3.3 Abnormal Neurological Development in E13.5 Trisomic Embryos

Adults with Down syndrome have hypoplastic brains and neocortexes with

enlarged lateral ventricles (PEARLSON 1998; SCHAPIRO 1987; WEIS *et al.* 1991).

Similarly, human fetuses with trisomy 21 exhibit decreased brain weight when

normalized for total body weight (GUIHARD-COSTA 2006). Contrary to what is found in

humans with DS, adult Ts65Dn mice do not have reduced overall brain volume, but

embryonic Ts65Dn mice have demonstrated reduced brain weight (ALDRIDGE 2007;

BAXTER 2000; CHAKRABARTI 2007). Since the size of the embryonic Ts65Dn brain has

only been evaluated by weight without normalization for size differences, 19 Ts65Dn and

21 euploid littermates were examined with unbiased stereology to determine brain

volume at E13.5. Although there was shown to be a significant difference in brain weight

at E13.5 (CHAKRABARTI 2007), the volume of the Ts65Dn brain was not significantly

different from the euploid brain (p= 0.49) (Figure 3.3.1). The similar total brain volume

found between E13.5 trisomic and euploid littermates correlates with the similar total

brain size reported in adult Ts65Dn mice (ALDRIDGE 2007; BAXTER 2000).

Individuals with DS have reduced cerebral cortex volumes (WEIS *et al.* 1991), and

it has recently been shown that E13.5 Ts65Dn mice have a reduced thickness of

neocortical layers (CHAKRABARTI 2007). To determine if the entire volume of the

developing neocortex was reduced in E13.5 trisomic embryos, evaluation of total

neocortical volume with unbiased stereology was performed. As expected, the total

volume of the trisomic neocortex was significantly reduced when compared to euploid

littermates (p= 0.05) (Figure 3.3.2). When normalized for total brain volume, the volume

of the Ts65Dn neocortex remained significantly reduced (p= 0.02) (Figure 3.3.3).

3.4   Reduced E9.5 and E13.5 Ts65Dn Embryos Related to Trisomic, not Maternal,

Trisomy

    To determine that differences in tissue size were a direct cause of embryonic

trisomy and not related to a trisomic mother's uterine environment, the total area of E9.5

and E13.5 embryos from Ts65Dn, euploid control, and B6C3F$_1$ mothers was examined.

Average somite number of 117 trisomic, 158 euploid, 120 euploid control, and 105 E9.5

B6C3F$_1$ embryos was measured. From Ts65Dn mothers, trisomic embryos had an

average of 19.12 somites (SEM= ± 0.29) which was significantly less than the average of

20.41 (± 0.24) somites in euploid littermates. Embryos from euploid control mothers had

an average somite number of 20.67 (± 0.31) and did not differ significantly from euploid

embryos from Ts65Dn mothers. Embryos from B6C3F$_1$ mothers had a significantly larger

number of somites (23.10 ± 0.18) (Figure 3.4.1). The similar somite number between

euploid embryos from Ts65Dn mothers and embryos from euploid control mothers

indicates that trisomy of the mother does not affect embryonic growth of the embryos.

The significantly smaller somite number in trisomic mice indicates embryonic trisomy,

and not maternal trisomy, affects development of embryos.

Because it is difficult to determine somite number at E13.5, total area measurements were taken to evaluate embryonic size at E13.5. Once again, trisomic embryos (49.26 ± 0.96 mm²; n= 14) were significantly smaller than euploid littermates (52.00 ± 0.59 mm²; n= 20), and euploid embryos from Ts65Dn mothers were not significantly different from euploid control embryos (53.47 ± 0.83 mm²; n= 89). Embryos from B6C3F$_1$ were still significantly larger than all other embryo types (59.08 ± 0.38 mm²; n= 89) (Figure 3.4.2). These results further strengthen the argument that maternal trisomy does not affect embryonic development or growth.

3.5   Area Better Determinant of Embryonic Size than CRL

Because some of the E13.5 embryos included in the area measurements already had total volume measurements determined through unbiased stereology, a comparison of area and crown rump length (CRL) measurements was performed to determine if area would be a better determinant of embryonic size than CRL. Analysis of 49 E13.5 embryos (34 non-trisomic and 15 trisomic with similar genetic backgrounds) determined embryo volume had a higher correlation to area (r= 0.43; p= 0.0023) than CRL (r= 0.26; p= 0.0770). CRL is most commonly used to determine embryonic size, but these results indicate that evaluation of embryonic area would more accurately determine total embryonic size.

To obtain the most accurate evaluation of total embryonic size, unbiased stereology was performed on 40 E13.5 embryos (19 trisomic, 21 euploid) to determine total volume of each embryo. Correlating with the results from the area calculation,

trisomic mice were found to be significantly smaller than euploid littermates (p= 0.02) (Figure 3.5.1).

Because of the significant reduction in trisomic embryonic size, it was hypothesized that specific tissues may be smaller in Ts65Dn mice because of the overall size difference. To account for this, all tissues were normalized to each specific embryo volume. Both trisomic cardiac and brain tissues were not significantly different in size when compared directly to euploid embryos, but when normalized for total embryonic volume, the trisomic cardiac tissue was significantly larger (p= 0.03) (Figure 3.5.2) while the brain tissue was almost significantly larger in Ts65Dn embryos (p= 0.054) (Figure 3.5.3). Interestingly, the mandibular precursor was significantly smaller when directly compared to euploid littermates, but when normalized for total embryonic volume, no significant difference was found (p= 0.17) (Figure 3.5.4).

3.6 Microarray Analysis on E13.5 Mandibular Precursor Reveals Dysregulated Non- trisomic Genes

A microarray analysis of RNA from 13 Ts65Dn and 11 euploid mandibular precursors was previously performed to elucidate the molecular pathways that alter the development of the Ts65Dn mandible. Interestingly, 155 genes were differentially expressed in the Ts65Dn mandibular precursor at E13.5, but none of these genes were triplicated in the Ts65Dn mouse model or homologous to genes found on Hsa21. Of the 155 differentially expressed genes, 75 genes exhibited increased expression levels while 80 genes were down regulated in Ts65Dn embryos.

To understand how these dysregulated genes affect development of the Ts65Dn mandibular precursor, the biological functionality of each gene was examined through the use of the GeneTools database (http://www.genetools.microarray.ntnu.no/adb/index.php). The database automatically categorized genes based on their known functions. It is important to note that the database sorts genes based on their known functions at any developmental stage and in any organism. Therefore, functional groups that were not directly related to the developing mouse mandible, such as "multicellular organismal", were not of particular interest to this study. Functional groups that were relevant to the developing mouse mandible were more closely examined.

Initial examination of the functional groups revealed 80 dysregulated genes in the mandible that were involved with biological processes (Figure 3.6.1). When these genes were further categorized, it was revealed that 53 were involved with cellular processes while 40 had roles in development processes (Figure 3.6.2 and 3.6.3). Other notable functional groups were cell differentiation, cell proliferation, and apoptosis (Figure 3.6.4, 3.6.5, and 3.6.6). Closer examination of these groups revealed that many genes did not have known functions directly related to mandibular development. For example, *Gata3* has known functions in kidney and sympathetic neuron development, trophoblast gene expression, and T helper 2 cell differentiation. *Lyz1*, another gene in the cell differentiation group, has primarily a bacteriolytic function and no known effect on mandibular development.

To try and focus on genes that would have a direct effect on mandibular growth, genes that were involved in cartilage and skeletal development were more closely examined (Figure 3.6.7 and 3.6.8). Since stereological measurements revealed a reduced

hyoid cartilage primordium and Meckel's cartilage, these groups were of particular

interest. Two genes with cartilage related functions and 14 genes involved with skeletal

development were significantly dysregulated in the trisomic mandible. Interestingly, the

transcription factor *Sox9* had roles in cartilage condensation, skeletal development, cell

proliferation, and cell differentiation. Seeming to correlate with *Sox9* expression, *Col2a1*

was present in many of the same functional groups. Both *Sox9* and *Col2a1* were found to

be upregulated in the trisomic mandibular precursor by 1.19 and 1.16 fold, respectively.

The transcription factor *Six2* was also upregulated (1.17 fold) and had known functions in

craniofacial skeletal development. Also of notable interest, there were 11 down regulated

Hox genes in the skeletal development group, six of which were in the top 20 most

dysregulated genes (Figure 3.6.9). Further examination of these genes and their functions

will provide additional insight into the biological processes that are affected by trisomy in

the developing mandible.

3.7   *Sox9* Overexpressed in Meckel's Cartilage and Hyoid Cartilage Primordium of E13.5

Trisomic Embryos

To further verify the overexpression of *Sox9* shown in the microarray and to

determine the specific location of *Sox9* expression, immunohistochemistry was

performed on E13.5 embryos. Because *Sox9* is known to be expressed in chondrocytes,

expression in Meckel's and the hyoid cartilage was examined.

Even though the IHC procedure was performed as uniformly as possible, variation

in intensity caused by differences in sections or fading of signals was unavoidable. To

control for these variations, DAPI intensity was measured for each section and used to

normalize the Sox9 intensity. Because DAPI fluoresces by binding to DNA and because the Sox9 protein is located inside the nucleus, comparing Sox9 to DAPI would control for differences in sections that might affect either DAPI or the Sox9 antibody penetration into the nucleus. Using DAPI as a control also controlled for potential fading of the signals that may have occurred.

To confirm that DAPI would be a good control for *Sox9* expression, a correlation analysis was performed. There was significant correlation between Sox9 and DAPI intensity in both euploid and trisomic samples, in both Meckel's and the hyoid cartilages. (Euploid Meckel's cartilage p= 0.0513; Trisomic Meckel's cartilage p= 0.0077; Euploid Hyoid cartilage p= 0.0207; Trisomic Hyoid Cartilage p= 0.0035) (Figure 3.7.1).

After excluding sections that were damaged or that did not produce usable photos, analysis of nine samples from euploid Meckel's cartilage and eight from trisomic embryos was performed. (A total of five different animals provided euploid samples and four for trisomic samples). When normalized for DAPI intensity, *Sox9* expression was significantly higher in the trisomic Meckel's cartilage (p= 0.02) (Figure 3.7.2). Similarly, *Sox9* expression was also significantly higher in the trisomic hyoid cartilage when compared to euploid littermates (p= 0.02) (four euploid animals provided eight samples and five trisomic animals provided eight samples) (Figure 3.7.3). The results from the Sox9 IHC confirm what was found in the microarray analysis and also show the specific structures where *Sox9* overexpression is located in the mandibular precursor (Figures 3.7.4, 3.7.5, 3.7.6).

To determine that the *Sox9* overexpression found in both Meckel's and hyoid cartilages was from an actual increase in the level of expression and not from an

increased number of cells expressing Sox9, the cell density was measured for each sample. There was no significant difference between the cell density of euploid and trisomic Meckel's or hyoid cartilages which suggests the overexpression is caused by an actual increase in expression in the cells (Meckel's cartilage: $p= 0.35$, hyoid cartilage: $p= 0.75$) (Figure 3.7.7).

CHAPTER 4   DISCUSSION

4.1   Relative Macroglossia and Reduced Mandibular Precursor, Meckel's Cartilage,

and Hyoid Cartilage in E13.5 Ts65Dn Embryos

The mandibular precursor was measured at E13.5 to determine whether the reduced PA1 found at E9.5 affected mandibular development at later stages. As hypothesized, the trisomic mandibular precursor was significantly reduced at E13.5. The CNC deficit found in both the PA1 and PA2 of E9.5 Ts65Dn embryos seems to negatively affect the growth of the mandibular precursor at E13.5 (ROPER 2009). This suggests that other structures derived from the PA1 and PA2 CNC may also be significantly reduced.

Both Meckel's and the hyoid cartilage are derived from CNC from the PA1 and PA2, respectively (KNIGHT 2006; MINA 2001). These structures were also measured at E13.5 to determine if the CNC deficit found at E9.5 negatively altered their growth as well as the mandibular precursor. As hypothesized, both of these structures were significantly reduced in Ts65Dn embryos. Since later growth and function of the mandible is dependent upon both Meckel's and the hyoid cartilage, a reduction in these cartilages at E13.5 could indicate developmental and functional difficulties at later stages of development. Specifically, a reduced Meckel's cartilage would result in a smaller template for mandibular growth which could further exacerbate the already altered growth of the mandible.

A reduced hyoid cartilage may not specifically affect mandibular growth, but it has the potential to negatively affect mandibular function. The hyoid cartilage later develops into the hyoid bone which interacts with the tongue and overall craniofacial function. The hyoid cartilage is located posterior to the mandibular precursor and is derived from PA2 and PA3 NC (KNIGHT 2006). Since the hyoid bone develops through endochondral ossification, the reduced size of the hyoid cartilage primordium at E13.5 suggests there will be a smaller cartilage matrix for bone development which could result in a reduced hyoid bone postnatally (KNIGHT 2006). The hyoid bone serves as an insertion point for more than a dozen muscles that control functions such as deglutination, phonation, and respiration (VAN DE GRAAFF *et al.* 1984). A reduced hyoid bone might have deleterious effects on the control of these muscles which would further complicate the difficulties that individuals with DS have with swallowing, speaking, and breathing.

Also of interest, in post-natal human life, the hyoid descends concurrently with the enlargement of the oral cavity and mandible (LIEBERMAN *et al.* 2001). Since the oral cavity and mandible have reduced growth in individuals and mice with trisomy, it seems likely that the position of the hyoid would be also altered (HILL 2007; RICHTSMEIER 2000). This is supported by a study that has shown that the location of the hyoid bone is positioned farther from the mandibular symphysis and more posteriorly located in brachyfacial subjects (PAE *et al.* 2008). A lower positioned hyoid causes the epiglottis to lose the ability to form a seal with the soft palate which increases the risk of aspirating food and of developing dysphagia from poor intermuscular coordination during swallowing (LIEBERMAN *et al.* 2001). Difficulties in swallowing and the aspiration of

food are common functional difficulties in newborns with DS and can be explained by

the small oral cavity and subsequent altered hyoid descent (VAN CLEVE and COHEN

2006).

As with the mandibular precursor, Meckel's cartilage, and the hyoid cartilage

primordium, the tongue is mostly CNC derived. Since the tongue is mainly CNC derived,

it was hypothesized that the tongue would be smaller in size between trisomic and

euploid embryos but relatively larger when compared to the significantly reduced

mandibular volume (YAMANE 2005) . Evaluation of the E13.5 tongue volume revealed no

significant difference between trisomic and euploid littermates. These results indicate that

trisomic and euploid tongues are developing at a similar rate at E13.5 while the

mandibular precursor, Meckel's cartilage, and hyoid cartilage are reduced in trisomic

embryos (KNIGHT 2006). The reduced mandible with the "normal" sized tongue also

seems to support the development and occurrence of relative macroglossia in Ts65Dn

mice. These findings are important to the DS community because they indicate trisomy is

severely affecting the size of the oral cavity while the tongue seems to be relatively

normal in size. This indicates that many functional difficulties with sleeping and eating

are caused by a smaller oral cavity and a relatively larger tongue. Oral-facial functional

capabilities in individuals with DS are further complicated by hypotonia which makes it

more difficult to control tongue movements in a reduced oral cavity.

4.2   Abnormal Neurological Development in E13.5 Ts65Dn Embryos

Along with craniofacial dysmorphology, essentially all individuals with Down

syndrome have some degree of cognitive impairment and have also been shown to have

hypoplastic brains (CROME 1966; PEARLSON 1998; PINTER 2001; RAZ 1995; SCHAPIRO 1987; WEIS *et al.* 1991). Similarly, the Ts65Dn mouse model has been shown to have reduced cognitive abilities, but at 12 weeks they have slightly larger brains when compared to their euploid littermates, although the difference is not significant (ALDRIDGE 2007; LORENZI 2006). At E13.5, the wet brain weight was found to be significantly reduced in trisomic mice in comparison to their euploid littermates, but these results were not normalized for the variation in total size of the embryos (CHAKRABARTI 2007).

To determine if the reduced brain weight found at E13.5 was indicative of overall brain volume reduction, the total volume of the brain was measured. It was hypothesized that the total brain volume would be reduced, but the results show no significant differences between trisomic and euploid brains. These results do not correlate with the reduced brain weight found at E13.5 but do coincide with the volume measurements of Ts65Dn mice at 12 weeks. When normalized for total embryonic volume, the trisomic brains were found to be larger than euploid brains, although the difference was not significant. The differing results between the weight and volume of embryonic brains can be explained with two different factors. In measuring the brain weight, it is likely the lateral ventricles did not contribute a significant amount of weight even though they take up a significant amount of space (PEARLSON 1998). Another study which used the Ts2Cje mouse, which carries a trisomic segment similar to that found in Ts65Dn mice, found that Ts2Cje mice have significantly enlarged brain ventricles (ISHIHARA 2009). In our own volumetric measurements of the brain, the lateral ventricles were included in the

calculation which could make a significant difference in the measurement of the brain if there is a significant alteration in ventricular size between Ts6Dn and euploid mice.

In a previous study, the total thickness of the neocortical wall was determined to be significantly thinner in the brains of E13.5 Ts65Dn mice when compared to the brains of euploid littermates and a delay in neocortical expansion was also found (CHAKRABARTI 2007). To further corroborate those results, the total volume of the neocortex was examined in E13.5 Ts65Dn and euploid embryos. In our own study, it was determined that there was a significant difference in the total volume of the neocortex. To account for individual variations in brain size, the measurements of the neocortex were normalized for total brain volume and the trisomic neocortex was proportionally smaller. Our results correlate with previous research and further suggest the occurrence of brain abnormalities early in embryonic development. This indicates that the origin of mental impairment begins early in the development of the DS brain.

4.3   Embryonic and not Maternal Trisomy Causes Developmental Attenuation in Ts65Dn Embryos

Both individuals with Down syndrome and Ts65Dn mice exhibit reduced birth weight and display developmental attenuation of many structures (ROPER 2006a). During embryonic development of Ts65Dn mice, the PA1 is significantly smaller, and both the cerebral cortex and hippocampus display abnormal growth caused by reduced proliferation of neural precursor cells (CHAKRABARTI 2007; ROPER 2009). Because of low birth weight and hypoplastic embryonic structures, it was hypothesized that E13.5 Ts65Dn mice would be significantly smaller than euploid littermates. Volumetric

analysis of 19 trisomic and 21 euploid embryos confirmed that hypothesis. Since trisomic

mice were significantly smaller than euploid littermates, specific structures were

normalized for total body volume. Interestingly, the trisomic mandibular precursor was

not smaller when controlled for overall body size.

Because CNC contribute to the development of a wide array of structures

including bone, cartilage, and connective tissue, a reduced number of proliferating CNC,

as seen in the PA1 and PA2 at E9.5, may affect enough structures to present as an overall

reduction in embryonic size (MINA 2001). This might explain why the CNC derived

mandibular precursor is significantly smaller when compared directly to euploid

littermates but not when normalized for total embryonic volume. This theory also

explains why trisomic cardiac tissue, which has minimal CNC contribution, is not

significantly different when directly compared to non-trisomic embryos but is larger

when normalized to the significantly smaller total embryonic volume (MORIKAWA 2008).

Similarly, when controlled for total embryonic volume, the Ts65Dn brain was slightly

larger than in euploid littermates, although not significantly.

While performing the stereological experiments to determine size differences

between Ts65Dn embryos and their euploid littermates, it was generally assumed that

embryonic trisomy was the main contributor to the abnormal development in Ts65Dn

embryos. To verify that embryonic trisomy was the main cause of the developmental

abnormalities seen at E9.5 and E13.5, and not a trisomic mother's uterine environment,

total embryonic area of several different types of embryos was examined. Embryos from

Ts65Dn, euploid control, and B6C3F$_1$ mothers were evaluated for size differences. As

expected, trisomic embryos from Ts65Dn mothers were significantly smaller than all

other embryos. Interestingly, there was no significant difference between euploid embryos from Ts65Dn mothers and embryos from euploid controls which indicates that a trisomic uterine environment does not affect overall growth of embryos. This verifies the differences seen in the stereological experiments are a result of embryonic trisomy and not maternal trisomy.

Although volumetric and area measurements revealed a significant difference in the size of E13.5 Ts65Dn and euploid embryos, previous studies using CRL have found no significant difference in size (CHAKRABARTI 2007). CRL is a one-dimensional linear measurement that is commonly used to determine developmental size of embryos (BROWN 2006; MU 2008). Previous studies have used CRL to determine that no significant size difference exists between E13.5 Ts65Dn and euploid embryos (CHAKRABARTI 2007). Contrary to those results, volumetric analysis of 40 E13.5 Ts65Dn and euploid embryos has revealed a significant reduction in overall size of trisomic embryos when compared to euploid littermates ($p= 0.02$). Ideally, volumetric measurements would be the ultimate determinant of embryonic size, but unfortunately, gathering volumetric data often requires embedding and sectioning entire embryos that is often expensive and impractical in most experiments. In an attempt to find a practical, but accurate way to determine embryonic size, area measurements of the same 40 E13.5 embryos were quantified and compared to CRL measurements. As hypothesized, embryo volume had a higher correlation to embryo area ($r = 0.43$; $p= 0.0023$) than CRL ($r = 0.26$; $p= 0.0770$). These results indicate that an area measurement would be a better determinant of embryonic size than CRL. Area measurements are also practical because they can be simply calculated by quantifying the area on a single image of an embryo.

4.4   Microarray Analysis on E13.5 Mandibular Precursor Reveals 155 Non-trisomic

Dysregulated Genes

The original goal of this research was to further examine the abnormal

development of the mandible in Ts65Dn mice. Even though some interesting size

differences were found in the cardiac and neural tissue of E13.5 Ts65Dn mice, it was

decided to maintain focus on the developing craniofacial structures. In accordance with

this decision, a microarray analysis was performed on RNA isolated from the mandibular

precursor of several E13.5 trisomic and euploid embryos to elucidate the molecular

mechanisms behind the developing craniofacial dysmorphology. The analysis revealed

155 differentially expressed genes in the mandibular precursor of Ts65Dn embryos.

Surprisingly, out of these 155 genes, none are located on the triplicated mouse

chromosome 16 or were homologous to genes on Hsa21. Although it was surprising that

no trisomic genes were dysregulated at E13.5, it is thought that the triplicated genes are

differentially expressed at a developmental stage prior to E13.5 in the trisomic

mandibular precursor. It seems that the altered expression of the trisomic genes prior to

E13.5 affects the expression of non-trisomic at E13.5.

Using gene ontology (http://www.genetools.microarray.ntnu.no/adb/index.php)

the 155 dysregulated genes were categorized based on their specific functions in

biological processes. Genes involved in skeletal development, cartilage formation,

cellular proliferation, and cellular differentiation were of particular interest because of the

reduced Meckel's cartilage and hyoid cartilage primordium found within the developing

trisomic mandible at E13.5. Both of these structures develop through endochondral

ossification so any genes involved with this process might affect the growth of these two important mandibular cartilages (KNIGHT 2006).

Of the 14 dysregulated genes involved with skeletal development, 11 were down regulated *Hox* genes. *Hox* genes are important developmental regulators that specify segmental identity in the developing embryo but little is known about the molecular events that are directly controlled by these genes (CARROLL 1995; KUTEJOVA 2005). In the developing vertebrate embryo, the location and order of *Hox* genes on the chromosome determines their expression domains along the anteroposterior (A-P) axis (KRUMLAUF 1994). *Hoxa2* and *Hoxb2* are expressed in the CNC that migrate to the PA2 and exhibit the most anterior expression of the *Hox* genes (MALLO 1997; NONCHEV 1996; PRINCE 1994). Considering known functions of *Hox* genes, expression of the *Hox* genes (*c6,a5,b7,b5,b6,b4,a7,d4,a4,b9,b2,d8)* in the E13.5 mandible was unexpected. Interestingly, *Hoxa2,* the only *Hox* gene known to affect craniofacial skeletal development, was not dysregulated in the trisomic mandibular precursor. The presence of the other *Hox* genes indicates a possible function in mandibular development that has yet to be discovered.

Even though abnormal *Hoxa2* expression was not detected in the E13.5 mandibular precursor, over-expression of *Six2*, a gene known to be regulated by *Hoxa2*, was revealed by the microarray. *Hoxa2* has been shown to negatively regulate *Six2* expression during PA2 formation (KUTEJOVA 2005). *Hoxa2* expression is mainly confined to the PA2 and its expression at E13.5 in mice would not be expected (MALLO 1997; NONCHEV 1996; PRINCE 1994). However, *Six2* is widely expressed in the head mesenchyme and would be expected to be present at E13.5 (OLIVER 1995).

Overexpression of *Six2* has been shown to cause morphological abnormalities in the skeletal structures derived from the PA2 (stapes, styloid process and lesser horn of the hyoid bone (KUTEJOVA 2005). Results from our microarray performed on E13.5 Ts65Dn and euploid embryos revealed an overexpression of *Six2* by 1.17 fold in the trisomic mouse. Considering the expression of all 12 *Hox* genes expressed at E13.5 was downregulated, it is plausible that *Hoxa2* expression may have been downregulated as well but at an earlier time period in development. Since *Hoxa2* negatively regulates *Six2*, a reduction in *Hoxa2* earlier in development would explain the increase of *Six2* found at E13.5. The overexpression of *Six2* found at E13.5 may be negatively affecting the development of the hyoid and could partially explain the smaller hyoid found in trisomic embryos.

4.5 *Sox9* Dysregulated in Trisomic Mandibular Precursor

Although many genes contribute to the abnormal phenotypes found in E13.5 trisomic embryos, *Sox9*, like the *Hox* genes, was of particular interest because of its involvement in many different functional groups such as cartilage condensation, cell proliferation, skeletal development, and cell differentiation. As previously mentioned, *Sox9* and *Col2a1* control chondrogenesis, which is a necessary precursor for the formation of endochondral bones (PROVOT and SCHIPANI 2005). Although the mandible is mainly formed through intramembranous ossification, which does not require a cartilaginous template, both Meckel's cartilage and the hyoid cartilage undergo endochondral ossification (ISHIZEKI 1999; RAMAESH 2003). Since Meckel's cartilage and the hyoid cartilage primordium were both found to be reduced at E13.5, overexpression

of both *Sox9* and *Col2a1* may be responsible for the altered growth of these cartilages in trisomic embryos.

It was recently demonstrated that a 1.2 fold overexpression of *Sox9* in chondrocytes caused shortened endochondral bones, reduced chondrocyte proliferation, and delayed hypertrophy of chondrocytes (AKIYAMA 2004). More specifically, the hyoid cartilage exhibited delayed endochondral ossification. In our own experiment, the microarray revealed a 1.19 fold overexpression of *Sox9* in the trisomic mandibular precursor (including the hyoid cartilage). Based on the previous research by Akiyama, it was hypothesized that the overexpression of *Sox9* in the Ts65Dn mandibular precursor would reduce chondrocyte proliferation and delay hypertrophy of chondrocytes which would negatively affect the growth of Meckel's cartilage and subsequently, the entire mandible.

To further examine the hypothesis that an overexpression of *Sox9* in the mandibular precursor would affect the development of both the hyoid and Meckel's cartilage, immunohistochemistry was performed to determine the precise location of *Sox9* expression in the mandibular precursor and to quantify its expression specifically in Meckel's and the hyoid cartilage. As hypothesized, immunohistochemistry revealed *Sox9* expression that was mainly isolated to Meckel's and hyoid cartilages. *Sox9* expression was found to be significantly higher in both Meckel's and the hyoid cartilage. Overexpression of *Sox9* in Meckel's cartilage would delay the chondrocytes from becoming hypertrophic and would cause a delay in bone formation. Along with the growth deficit caused by reduced CNC, overexpression of *Sox9* at E13.5 in Meckel's cartilage would further restrict the growth of the mandible in trisomic embryos since

Meckel's cartilage serves as the template for mandibular growth (MINA 2001). This may

further explain the reduced mandible seen in both neonatal and adult Ts65Dn mice (HILL

2007). Similarly, the overexpression of *Sox9* found in the trisomic hyoid cartilage would

most likely result in a reduced hyoid bone which could negatively affect craniofacial

functions. The combined effects of reduced CNC in the mandibular precursor at E9.5

with the overexpression of *Sox9* found at E13.5 explain the craniofacial abnormalities

that have been found postnatally in both Ts65Dn mice and individuals with DS.

4.6   Future Work

This research mainly focused on the abnormal development of the mandible in

Ts65Dn mice through both structural and genetic analyses. Although the mandible was

the main focus, stereological evaluations revealed a reduced neocortex and enlarged

cardiac tissue. Microarray analysis could be performed on these structures to further

elucidate the genetic anomalies that are causing the abnormal phenotypes. Alternatively,

many genes were found to be dysregulated in the trisomic mandibular precursor that have

yet to be analyzed in depth. Further research and the application of

immunohistochemistry could further explain the functions and locations of other genes in

mandibular development. Specifically, the expression of *Six2* should be analyzed because

of its known role in hyoid development. The hyoid had a much more pronounced

reduction in size than other CNC derived structures. Altered expression of *Six2* may be

further exacerbating the growth reduction caused by a reduction of CNC.

Because the microarray did not reveal altered expression of any triplicated genes

at E13.5 in the mandibular precursor, a microarray analysis should be performed at an

earlier stage of development to determine which trisomic genes are affecting the expression levels of euploid genes at E13.5. This would elucidate the molecular pathways that are affected by trisomy and causing altered mandibular development.

Furthermore, previous research has shown that the overexpression of *Sox9* causes reduced growth in all endochondral bones (AKIYAMA 2004) which suggests that the overexpression of *Sox9* in Ts65Dn mice may not be localized to just the mandibular precursor. A generalized overexpression of *Sox9* could potentially explain the reduced size of Ts65Dn mice. A microarray or q-PCR could be performed on specific structures to see if *Sox9* is overexpressed in other tissues. Analysis of *Sox9* expression in the somites would be of particular interest because of their role in vertebrae cartilage development. The developing femur would also be of interest. Smaller vertebrae and shortened femurs resulting from a *Sox9* overexpression would explain the reduced size of Ts65Dn mice.

Finally, examination of the hyoid bone in postnatal Ts65Dn mice could potentially show that a reduced oral cavity affects the location of the hyoid. The distance between the hyoid and previously defined craniofacial landmarks could be measured to determine if the hyoid is abnormally located in Ts65Dn mice (RICHTSMEIER 2000). If the hyoid is found to be more posteriorly located in Ts65Dn mice, then this could potentially explain some of the feeding and breathing problems found in individuals with DS.

LITERATURE CITED

LITERATURE CITED

AIT YAHYA-GRAISON, E., J. AUBERT, L. DAUPHINOT, I. RIVALS, M. PRIEUR *et al.*, 2007 Classification of human chromosome 21 gene-expression variations in Down syndrome: impact on disease phenotypes. Am J Hum Genet **81:** 475-491.

AKIYAMA, H., M. C. CHABOISSIER, J. F. MARTIN, A. SCHEDL and B. DE CROMBRUGGHE, 2002 The transcription factor Sox9 has essential roles in successive steps of the chondrocyte differentiation pathway and is required for expression of Sox5 and Sox6. Genes Dev **16:** 2813-2828.

AKIYAMA, H., J.P. LYONS, Y. MORI-AKIYAMA, X. YANG, R. ZHANG, Z. ZHANG, J.M. DENG, M.M. TAKETO, T NAKAMURA, R.R. BEHRINGER P.D. MCCREA AND B. DE CROMBRUGGHE, 2004 Interactions between Sox9 and beta-catenin control chondrocyte differentiation. Genes Dev. **18:** 1072-1087.

ALDRIDGE, K., R.H. REEVES, L.E. OLSON AND J.T. RICHTSMEIER, 2007 Differential Effects of Trisomy on Brain Shape and Volume in Related Aneuploid Mouse Models. American Journal of Medical Genetics Part A **143A:** 1060-1070.

ALLANSON, J. E., P. O'HARA, L.G. FARKAS AND R.C. NAIR, 1993 Antropometric craniofacial pattern profiles in Down syndrome. Am J Med Genet **47:** 748-752.

ALLEN, E. G., S.B. FREEMAN, C. DRUSCHEL, C.A. HOBBS, L.A. O'LEARY, P.A. ROMITTI, M.H. ROYLE, C.P. TORFS, S.L. SHERMAN, 2009 Maternal age and risk for trisomy 21 assessed by the origin of chromosome nondisjunction: a report from the Atlanta and National Down Syndrome Projects. Hum Genet. **125:** 41-52.

ALLISON, D. B., J. E. GOMEZ, S. HESHKA, R. L. BABBITT, A. GELIEBTER *et al.*, 1995 Decreased resting metabolic rate among persons with Down Syndrome. Int J Obes Relat Metab Disord **19:** 858-861.

AMANO, K., H. SAGO, C. UCHIKAWA, T. SUZUKI, S.E. KOTLIAROVA, N. NUKINA, C.J. EPSTEIN, K. YAMAKAWA, 2004 Dosage-dependent over-expression of genes in the trisomic region of Ts1Cje mouse model for Down syndrome. Hum Mol Genet. **13:** 1333-1340.

ANTONARAKIS, S. E., R. LYLE, E. T. DERMITZAKIS, A. REYMOND and S. DEUTSCH, 2004 Chromosome 21 and down syndrome: from genomics to pathophysiology. Nat Rev Genet **5:** 725-738.

ASHBURNER, M., C. A. BALL, J. A. BLAKE, D. BOTSTEIN, H. BUTLER *et al.*, 2000 Gene ontology: tool for the unification of biology. The Gene Ontology Consortium. Nat Genet **25:** 25-29.

ASLING, S.-A. I. A. C. W., 1973 Resorption of calcified cartilage as seen in Meckel's cartilage of rats. Anat. Rec **176:** 345-359.

AYLWARD, E. H., Q. LI, N. A. HONEYCUTT, A. C. WARREN, M. B. PULSIFER *et al.*, 1999 MRI volumes of the hippocampus and amygdala in adults with Down's syndrome with and without dementia. Am J Psychiatry **156:** 564-568.

BALKANY, T. J., M.P. DOWNS, B.W. JAFEK, M.J. KRAJICEK, 1979 Hearing loss in Down's syndrome. A treatable handicap more common than generally recognized. Clin Pediatr (Phila) **18:** 116-118.

BARNHART, R. C., and B. CONNOLLY, 2007 Aging and Down syndrome: implications for physical therapy. Phys Ther **87:** 1399-1406.

BAXTER, L. L., T.H. MORAN, J.T. RICHTSMEIER, J. TRONCOSO, R.H. REEVES, 2000 Discovery and genetic localization of Down syndrome cerebellar phenotypes using the Ts65Dn mouse. Hum Mol Genet. **9:** 195-202.

BELICHENKO, P. V., E. MASLIAH, A.M. KLESCHEVNIKOV, A.J. VILLAR, C.J. EPSTEIN, A. SALEHI, W.C. MOBLEY, 2004 Synaptic structural abnormalities in the Ts65Dn mouse model of Down Syndrome. J Comp Neurol **480:** 281-298.

BELL, D. M., K. K. LEUNG, S. C. WHEATLEY, L. J. NG, S. ZHOU *et al.*, 1997 SOX9 directly regulates the type-II collagen gene. Nat Genet **16:** 174-178.

BEREND, S. A., S.L. PAGE, W. ATKINSON, C. MCCASKILL, N.E. LAMB, S.L. SHERMAN, L.G. SHAFFER, 2003 Obligate short-arm exchange in de novo Robertsonian translocation formation influences placement of crossovers in chromosome 21 nondisjunction. Am J Hum Genet. **72:** 488-495.

BERESFORD, W. A., 1975 Schemes of zonation in the mandibular condyle. Am J Orthod. **68:** 189-195.

BERNAL, J. E., I. BRICENO, 2006 Genetic and other diseases in the pottery of Tumaco-La Tolita culture in Colombia-Ecuador. Clin Genet **70:** 188-191.

BHASKAR, S. N., J.P. WEINMANN AND I. SCHOUR, 1953 Role of Meckel's cartilage in the development and growth of the rat mandible. J Den. Res. **32:** 398-410.

BI, W., W. HUANG, D. J. WHITWORTH, J. M. DENG, Z. ZHANG *et al.*, 2001 Haploinsufficiency of Sox9 results in defective cartilage primordia and premature skeletal mineralization. Proc Natl Acad Sci U S A **98:** 6698-6703.

BI, W., J.M. DENG, Z. ZHANG, R.R. BEHRINGER AND B. DE CROMBRUGGHE, 1999 Sox9 is required for cartilage formation. Nat Genet. **22:** 85-89.

BILITEWSKI, U., 2009 DNA microarrays: an introduction to the technology. Methods Mol Biol **509:** 1-14.

BITTLES, A. H., and E. J. GLASSON, 2004 Clinical, social, and ethical implications of changing life expectancy in Down syndrome. Dev Med Child Neurol **46:** 282-286.

BLAZEK, J. D., C.N. BILLINGSLEY, A. NEWBAUER, R.J. ROPER, 2010 Embryonic and Not Maternal Trisomy Causes Developmental Attenuation in the Ts65Dn Mouse Model for Down Syndrome. Dev. Dyn. **239:** 1645-1653.

BROWN, F. R. R., M.K. GREER, E.H. AYLWARD, H.H. HUNT, 1990 Intellectual and adaptive functioning in individuals with Down syndrome in relation to age and environmental placement. Pediatrics **85:** 450-452.

BROWN, S. D., D. ZURAKOWSKI, D.P. RODRIGUEZ, P.S. DUNNING, R.J. HURLEY, G.A. TAYLOR, , 2006 Ultrasound diagnosis of mouse pregnancy and gestational staging Comp Med **56:** 262-271.

CANFIELD, M. A., T.A. RAMADHANI, M.J. DAVIDOFF, J.R. PETRINI, C.A. HOBBS, R.S. KIRBY, P.A. ROMITTI, 2006 Improved national prevalence estimates for 18 selected major birth defects--United States, 1999-2001. MMWR Morb Mortal Wkly Rep **54:** 1301-1305.

CARLESIMO, G. A., L. MAROTTA, S. VICARI, 1997 Long-term memory in mental retardation: evidence for a specific impairment in subjects with Down's syndrome. Neuropsychologia **35:** 71-79.

CARROLL, S. B., 1995 Homeotic genes and the evolution of arthropods and chordates. Nature **376:** 479-485.

CHAKRABARTI, L., Z. GALDZICKI AND T.F. HAYDAR, 2007 Defects in Embryonic Neurogenesis and Initial Synapse Formation in the Forebrain of the Ts65Dn Mouse Model of Down Syndrome. The Journal of Neuroscience **27:** 11483-11495.

CHAPMAN, R. S., L.J. HESKETH, 2000 Behavioral phenotype of individuals with Down syndrome. Ment Retard Dev Disabil Res Rev. **6:** 84-95.

CHOU, C. Y., L. Y. LIU, C. Y. CHEN, C. H. TSAI, H. L. HWA *et al.*, 2008 Gene expression variation increase in trisomy 21 tissues. Mamm Genome **19:** 398-405.

CHRISTIANSON, A., C.P. HOWSON AND B. MODEL, 2006 March of Dimes Global Report on Birth Defects: The Hidden Toll of Dying and Disabled Children. 1-98.

CONTESTABILE, A., T. FILA, A. CAPPELLINI, R. BARTESAGHI, E. CIANI, 2009a Widespread impairment of cell proliferation in the neonate Ts65Dn mouse, a model for Down syndrome. Cell Prolif. **42:** 171-181.

CONTESTABILE, A., T. FILA, C. CECCARELLI, P. BONASONI, L. BONAPACE, D. SANTINI, R. BARTESAGHI, E. CIANI, 2007 Cell cycle alteration and decreased cell proliferation in the hippocampal dentate gyrus and in the neocortical germinal matrix of fetuses with Down syndrome and in Ts65Dn mice. Hippocampus **17:** 665-678.

CONTESTABILE, A., T. FILA, R. BARTESAGHI AND E. CIANI, 2009b Cell cycle elongation impairs proliferation of cerebellar granule cell precursors in the Ts65Dn mouse, an animal model for Down syndrome. Brain Pathol. **19:** 224-237.

CROME, 1966 A statistical note on cerebellar and brain stem weight in mongolism. J Ment Defic Res**:** 69-72.

CUNNIFF, C., 2001 American Academy of Pediatrics: Health supervision for children with Down syndrome. Pediatrics **107:** 442-449.

DAGKLIS, T., M. BORENSTEIN, C. F. PERALTA, C. FARO and K. H. NICOLAIDES, 2006 Three-dimensional evaluation of mid-facial hypoplasia in fetuses with trisomy 21 at 11 + 0 to 13 + 6 weeks of gestation. Ultrasound Obstet Gynecol **28:** 261-265.

DAHLE, A. J., F.P. MCCOLLISTER, 1986 Hearing and otologic disorders in children with Down syndrome. Am J Ment Defic **90:** 636-642.

DALTON, A. J., D.R. CRAPPER-MCHLACHLAN, 1986 Clinical expression of Alzheimer's disease in Down's syndrome. Psychiatr Clin North Am. **9:** 659-670.

DAUPHINOT, L., R. LYLE, I. RIVALS, M. T. DANG, R. X. MOLDRICH *et al.*, 2005 The cerebellar transcriptome during postnatal development of the Ts1Cje mouse, a segmental trisomy model for Down syndrome. Hum Mol Genet **14:** 373-384.

DAVISSON, M. T., C. SCHMIDT, R.H. REEVES, N.G. IRVING, E.C. AKESON, B.S. HARRIS, R.T. BRONSON, 1993 Segmental trisomy as a mouse model for Down syndrome. Prog Clin Biol Res. **384:** 117-133.

DIERSSEN, M., C. FILLAT, L. CRNIC, M. ARBONES, J. FLOREZ, X. ESTIVILL, 2001 Murine models for Down syndrome. Physiol Behav. **73:** 859-871.

DIETRICH, W. F., J. C. MILLER, R. G. STEEN, M. MERCHANT, D. DAMRON *et al.*, 1994 A genetic map of the mouse with 4,006 simple sequence length polymorphisms. Nat Genet **7:** 220-245.

DOWN, J. L., 1866 Observations on an ethnic classification of idiots. 1866. Ment Retard **33:** 54-56.

EPSTEIN, C. J., 1990 The consequences of chromosome imbalance. Am J Med Genet Suppl **7:** 31-37.

EPSTEIN, C. J., 2001 *Down Syndrome (Trisomy 21)*. McGraw-Hill, New York.

FERENCZ, C., C. A. NEILL, J. A. BOUGHMAN, J. D. RUBIN, J. I. BRENNER *et al.*, 1989 Congenital cardiovascular malformations associated with chromosome abnormalities: an epidemiologic study. J Pediatr **114:** 79-86.

FITZPATRICK, D. R., J. RAMSAY, N. I. MCGILL, M. SHADE, A. D. CAROTHERS *et al.*, 2002 Transcriptome analysis of human autosomal trisomy. Hum Mol Genet **11:** 3249-3256.

FOSTER, J. W., M. A. DOMINGUEZ-STEGLICH, S. GUIOLI, C. KWOK, P. A. WELLER *et al.*, 1994 Campomelic dysplasia and autosomal sex reversal caused by mutations in an SRY-related gene. Nature **372:** 525-530.

FRACCARO, M., K. KAIJSER, J. LINDSTEN, 1960 Chromosomal abnormalities in father and Mongol child. Lancet **1:** 724-727.

FREEMAN, S. B., E.G. ALLEN, C.L. OXFORD-WRIGHT, S.W. TINKER, C. DRUSCHEL, C.A. HOBBS, L.A. O'LEARY, P.A. ROMITTI, M.H. ROYLE, C.P. TORFS, S.L. SHERMAN, 2007 The National Down Syndrome Project: design and implementation. Public Health Rep. **122:** 62-72.

FREEMAN, S. B., L.F. TAFT, K.J. DOOLEY, K. ALLRAN, S.L. SHERMAN, T.J. HASSOLD, M.J. KHOURY AND D.M. SAKER, 1998 Population-based study of congenital heart defects in Down syndrome. Am J Med Genet **87:** 195-196.

FROMMER, J. A. M. R. M., 1971 Contribution of Meckel's cartilage to ossification of the mandible in mice. J Dent Res. **50:** 1260-1267.

GARDINER, K., A. FORTNA, L. BECHTEL, M.T. DAVISSON, 2003 Mouse models of Down syndrome: how useful can they be? Comparison of the gene content of human chromosome 21 with orthologous mouse genomic regions. Gene **318:** 137-147.

GIRAUD, F., J.F. MATTEI, 1975 [Epidemiological aspects of trisomy 21]. J Genet Hum **SUPPL:** 1-30.

GUIHARD-COSTA, A. M., S. KHUNG, K. DELBECQUE, F. MENEZ AND A.L. DELEZOIDE, 2006 Biometry of face and brain in fetuses with trisomy 21. Pediatr Res **59:** 33-38.

GUIMARAES, C. V., L.F. DONNELLY, S.R. SHOTT, R.S. AMIN AND M. KALRA 2008 Relative rather than absolute macroglossia in patients with Down syndrome: implications for treatment of obstructive sleep apnea. Pediatr Radiol. **38:** 1062-1067.

HARGUS, G., R. KIST, J. KRAMER, D. GERSTEL, A. NEITZ *et al.*, 2008 Loss of Sox9 function results in defective chondrocyte differentiation of mouse embryonic stem cells in vitro. Int J Dev Biol **52:** 323-332.

HASSOLD, T., D. CHIU, 1985 Maternal age-specific rates of numerical chromosome abnormalities with special reference to trisomy. Hum Genet. **70:** 11-17.

HATTORI, M., A. FUJIYAMA, T.D. TAYLOR, H. WATANABE, T. YADA, H.S. PARK, A. TOYODA, K. ISHII, ET AL, 2000 The DNA sequence of human chromosome 21. Nature **405:** 311-319.

HILL, C. A., R.H. REEVES AND J.T. RICHTSMEIER, 2007 Effects of aneuploidy on skull growth in a mouse model of Down syndrome. J. Anat. **210:** 394-405.

HOLTZMAN, D. M., D. SANTUCCI, J. KILBRIDGE, J. CHUA-COUZENS, D.J. FONTANA, S.E. DANIELS, R.M. JOHNSON, K. CHEN, Y. SUN, E. CARLSON, E. ALLEVA, C.J. EPSTEIN, W.C. MOBLEY, 1996 Developmental abnormalities and age-related neurodegeneration in a mouse model of Down syndrome. Proc Natl Acad Sci U S A. **93:** 13333-13338.

ISHIHARA, K., K. AMANO, E. TAKAKI, A. SHIMOHATA, H. SAGO, C.J. EPSTEIN AND K. YAMAKAWA 2009 Enlarged Brain Ventricles and Impaired Neurogenesis in the Ts1Cje and Ts2Cje Mouse Models of Down Syndrome. Cerebral Cortex.

ISHIZEKI, K., H. SAITO, T. SHINAGAWA, N. FUJIWARA AND T. NAWA, 1999 Histochemical and immunohistochemical analysis of calcification of Meckel's cartilage during mandible development in rodents. J Anat. **194** 265-277.

JACOBS, P. A., A.G. BAIKIE, W.M. COURT BROWN, J.A. STRONG, 1959 The somatic chromosomes in mongolism. Lancet **1:** 710.

KAHLEM, P., M. SULTAN, R. HERWIG, M. STEINFATH, D. BALZEREIT *et al.*, 2004 Transcript level alterations reflect gene dosage effects across multiple tissues in a mouse model of down syndrome. Genome Res **14:** 1258-1267.

KAUFMAN, M. H., 2003 *The Atlas of Mouse Development*. El Sevier Academic Press.

KIMMEL, C. B., B. ULLMANN, M. WALKER, C. T. MILLER and J. G. CRUMP, 2003 Endothelin 1-mediated regulation of pharyngeal bone development in zebrafish. Development **130:** 1339-1351.

KIRKEBY, S., C.E. THOMSEN, 2005 Quantitative immunohistochemistry of fluorescence labelled probes using low-cost software. J Immunol Methods **301:** 102-113.

KNECHT, A. K., and M. BRONNER-FRASER, 2002 Induction of the neural crest: a multigene process. Nat Rev Genet **3:** 453-461.

KNIGHT, R. D. A. R. F. S., 2006 Cranial neural crest and development of the head skeleton. Adv. Exp. Med. Biol. **589:** 120-133.

KRUMLAUF, R., 1994 *Hox* genes in vertebrate development. Cell Tissue Res **78:** 191-201.

KURAKU, S., Y. TAKIO, F. SUGAHARA, M. TAKECHI and S. KURATANI, 2010 Evolution of oropharyngeal patterning mechanisms involving Dlx and endothelins in vertebrates. Dev Biol **341:** 315-323.

KUTEJOVA, E., B. ENGIST, M. MALLO, B. KANZLER, N. BOBOLA, 2005 Hoxa2 downregulates Six2 in the neural crest-derived mesenchyme. Development **132:** 469-478.

LAFFAIRE, J., I. RIVALS, L. DAUPHINOT, F. PASTEAU, R. WEHRLE *et al.*, 2009 Gene expression signature of cerebellar hypoplasia in a mouse model of Down syndrome during postnatal development. BMC Genomics **10:** 138.

LEFEBVRE, V., W. HUANG, V. R. HARLEY, P. N. GOODFELLOW and B. DE CROMBRUGGHE, 1997 SOX9 is a potent activator of the chondrocyte-specific enhancer of the pro alpha1(II) collagen gene. Mol Cell Biol **17:** 2336-2346.

LEJEUNE, J., M. GAUTIER, R. TURPIN, 1959 [Study of somatic chromosomes from 9 mongoloid children]. C R Hebd Seances Acad Sci. **248:** 1721-1722.

LI, Z., T. YU, M. MORISHIMA, A. PAO, J. LADUCA, J. CONROY, N. NOWAK, S. ATSUI, I. SHIRAISHI, Y.E. YU, 2007 Duplication of the entire 22.9 Mb human chromosome 21 syntenic region on mouse chromosome 16 causes cardiovascular and gastrointestinal abnormalities. Hum Mol Genet. **16:** 1359-1366.

LIEBERMAN, D. E., R. C. MCCARTHY, K. M. HIIEMAE and J. B. PALMER, 2001 Ontogeny of postnatal hyoid and larynx descent in humans. Arch Oral Biol **46:** 117-128.

LORENZI, H., N. DUVALL, S.M. CHERRY, R.H. REEVES AND R.J. ROPER, 2010 PCR prescreen for genotyping the Ts65Dn mouse model of Down syndrome. Biotechniques **48:** 35-38.

LORENZI, H. A. A. R. H. R., 2006 Hippocampal hypocellularity in the Ts65Dn mouse originates early in development. Brain Res **1104:** 153-159.

LYLE, R., C. GEHRIG, C. NEERGAARD-HENRICHSEN, S. DEUTSCH and S. E. ANTONARAKIS, 2004 Gene expression from the aneuploid chromosome in a trisomy mouse model of down syndrome. Genome Res **14:** 1268-1274.

MALLO, M., 1997 Retinoic Acid Disturbs Mouse Middle Ear Development in a Stage-Dependent Fashion. Dev Bio **184:** 175-186.

MAO, R., X. WANG, E. L. SPITZNAGEL, JR., L. P. FRELIN, J. C. TING *et al.*, 2005 Primary and secondary transcriptional effects in the developing human Down syndrome brain and heart. Genome Biol **6:** R107.

MARCUS, C. L., T.G. KEENS, D.B. BAUTISTA, W.S. VON PECHMANN, S.L. WARD, 1991 Obstructive sleep apnea in children with Down syndrome. Pediatrics **88:** 132-139.

MATKOWSKYJ, K. A., D. SCHONFELD, R.V. BENYA, 2000 Quantitative immunohistochemistry by measuring cumulative signal strength using commercially available software photoshop and matlab. J Histochem Cytochem **48:** 303-312.

MERRILL, A. E., B. F. EAMES, S. J. WESTON, T. HEATH and R. A. SCHNEIDER, 2008 Mesenchyme-dependent BMP signaling directs the timing of mandibular osteogenesis. Development **135:** 1223-1234.

MINA, M., 2001 Regulation of Mandibular Growth and Morphogenesis. Crit Rev Oral Biol Med **12:** 276-300.

MOORE, C. S., 2006 Postnatal lethality and cardiac anomalies in the Ts65Dn Down syndrome mouse model. Mamm Genome **17:** 1005-1012.

MOORE, C. S., J. S. LEE, B. BIRREN, G. STETTEN, L. L. BAXTER *et al.*, 1999 Integration of cytogenetic with recombinational and physical maps of mouse chromosome 16. Genomics **59:** 1-5.

MOORE, C. S., R.J. ROPER, 2007 The power of comparative and developmental studies for mouse models of Down syndrome. Mamm Genome **18:** 431-443.

MORI-AKIYAMA, Y., H. AKIYAMA, D. H. ROWITCH and B. DE CROMBRUGGHE, 2003 Sox9 is required for determination of the chondrogenic cell lineage in the cranial neural crest. Proc Natl Acad Sci U S A **100:** 9360-9365.

MORIKAWA, Y., CSERJESI, P., 2008 Cardiac neural crest expression of Hand2 regulates outflow and second heart field development. Circ Res **103:** 1422-1429.

MU, J., J.C. SLEVIN, S. MCCORMICK, S.L. ADAMSON, 2008 In vivo quantification of embryonic and placental growth during gestation in mice using micro-ultrasound Reprod Biol Endocrinol **6:** 34.

MUTTON, D., E. ALBERMAN, E.B. HOOK, 1996 Cytogenetic and epidemiological findings in Down syndrome, England and Wales 1989 to 1993. National Down Syndrome Cytogenetic Register and the Association of Clinical Cytogeneticists. J Med Genet. **33:** 387-394.

NADEL, L., 2003 Down's syndrome: a genetic disorder in biobehavioral perspective. Genes Brain Behav. **2:** 156-166.

NG, L. J., S. WHEATLEY, G.E. MUSCAT, J. CONWAY-CAMPBELL, J. BOWLES, E. WRIGHT, D.M. BELL, P.P. TAM, K.S. CHEAH AND P. KOOPMAN, 1997 SOX9 binds DNA, activates transcription, and coexpresses with type II collagen during chondrogenesis in the mouse. Dev Biol. **183:** 108-121.

NONCHEV, S., C. VESQUE, M. MACONOCHIE, T. SEITANIDOU, L. ARIZA-MCNAUGHTON, M. FRAIN, H. MARSHALL, M.H. SHAM, R. KRUMLAUF, P. CHARNAY, 1996 Segmental expression of Hoxa-2 in the hindbrain is directly regulated by Krox-20. Development **122:** 543-554.

OLIVER, G., R. WEHR, N.A. JENKINS, N.G. COPELAND, B.N. CHEYETTE, V. HARTENSTEIN, S.L. ZIPURSKY, P. GRUSS, 1995 Homeobox genes and connective tissue patterning. Development **121:** 693-705.

PAE, E. K., C. QUAS, J. QUAS and N. GARRETT, 2008 Can facial type be used to predict changes in hyoid bone position with age? A perspective based on longitudinal data. Am J Orthod Dentofacial Orthop **134:** 792-797.

PEARLSON, G., S. BREITER, E. AYLWARD, A. WARREN, M. GRYGORCEWICZ, S. GRANGOU, P. BARTA AND M. PULSIFER, 1998 MRI brain changes in subjects with Down syndrome with and without dementia. Dev Med Child Neurol **40:** 326-334.

PINTER, J., S. ELIEZ, J. SCHMITT, G. CAPONE AND A. REISS, 2001 Neuroanatomy of Down's syndrome: A high-resolution MRI study. Am J Psychiatry **158:** 1659-1665.

POTIER, M. C., I. RIVALS, G. MERCIER, L. ETTWILLER, R. X. MOLDRICH *et al.*, 2006 Transcriptional disruptions in Down syndrome: a case study in the Ts1Cje mouse cerebellum during post-natal development. J Neurochem **97 Suppl 1:** 104-109.

PRINCE, V., LUMSDEN, A., 1994 Hoxa-2 expression in normal and transposed rhombomeres: independent regulation in the neural tube and neural crest. Development **120:** 911-923.

PRITCHARD, M. A., and I. KOLA, 1999 The "gene dosage effect" hypothesis versus the "amplified developmental instability" hypothesis in Down syndrome. J Neural Transm Suppl **57:** 293-303.

PROVOT, S., and E. SCHIPANI, 2005 Molecular mechanisms of endochondral bone development. Biochem Biophys Res Commun **328:** 658-665.

PUFFENBERGER, E. G., E. R. KAUFFMAN, S. BOLK, T. C. MATISE, S. S. WASHINGTON *et al.*, 1994 Identity-by-descent and association mapping of a recessive gene for Hirschsprung disease on human chromosome 13q22. Hum Mol Genet **3:** 1217-1225.

RAMAESH, T., AND J. BARD, 2003 The growth and morphogenesis of the early mouse mandible: a quantitative analysis. J. Anat. **203:** 213-222.

RAZ, N., I.J. TORRES, S.D. BRIGGS, W.D. SPENCER, A.E. THORNTON, W.J. LOKEN, F.M. GUNNING, J.D. MCQUAIN, N.R. DRIESEN AND J.D. ACKER, 1995 Selective neuroanatomic abnormalities in Down's syndrome and their cognitive correlates: Evidence from MRI morphometry. Neurology **45:** 356-366.

REEVES, R. H., N.G. IRVING, T.H. MORAN, A. WOHN, C. KITT, S.S. SISODIA, C. SCHMIDT, R.T. BRONSON, M.T. DAVISSON, 1995 A mouse model for Down syndrome exhibits learning and behaviour deficits. nat Genet. **11:** 177-184.

RICHTSMEIER, J. T., L.L. BAXTER AND R.H. REEVES, 2000 Parallels of Craniofacial Maldevelopment in Down Syndrome and Ts65Dn Mice. Developmental Dynamics **217:** 137-145.

ROGERS, S., and A. CAMBROSIO, 2007 Making a new technology work: the standardization and regulation of microarrays. Yale J Biol Med **80:** 165-178.

ROIZEN, N. J. A. D. P., 2003 Down's syndrome. Lancet **361:** 1281-1289.

ROPER, R., J.F. VANHORN, C.C. CAIN, AND R.H. REEVES, 2009 A neural crest deficit in Down syndrome mice is associated with deficient mitotic response to Sonic hedgehog. Mechanisms of Development **126:** 212-219.

ROPER, R. J., H.K. ST JOHN, J. PHILIP, A. LAWLER, R.H. REEVES, 2006a Perinatal loss of Ts65Dn Down syndrome mice. Genetics **172:** 437-443.

ROPER, R. J., L.L. BAXTER, N.G. SARAN, D.K. KLINEDINST, P.A. BEACHY, R.H. REEVES, 2006b Defective cerebellar response to mitogenic Hedgehog signaling in Down syndrome mice. Proc Natl Acad Sci U S A. **103:** 1452-1456.

RUBIN, S. S., J. H. RIMMER, B. CHICOINE, D. BRADDOCK and D. E. MCGUIRE, 1998 Overweight prevalence in persons with Down syndrome. Ment Retard **36:** 175-181.

SANTAGATI, F., and F. M. RIJLI, 2003 Cranial neural crest and the building of the vertebrate head. Nat Rev Neurosci **4:** 806-818.

SARAN, N. G., M. T. PLETCHER, J. E. NATALE, Y. CHENG and R. H. REEVES, 2003 Global disruption of the cerebellar transcriptome in a Down syndrome mouse model. Hum Mol Genet **12:** 2013-2019.

SCHAPIRO, M. B., H. CREASEY, M. SCHWARTZ, J.V. HAXBY, B. WHITE, A. MOORE AND S.I. RAPOPORT, 1987 Quantitative CT analysis of brain morphometry in adult Down's syndrome at different ages. Neurology **37:** 1424-1427.

SCHMITT, K., J. W. FOSTER, R. W. FEAKES, C. KNIGHTS, M. E. DAVIS *et al.*, 1996 Construction of a mouse whole-genome radiation hybrid panel and application to MMU11. Genomics **34:** 193-197.

SEO, H., O. ISACSON, 2005 Abnormal APP, cholinergic and cognitive function in Ts65Dn Down's model mice. Exp Neurol. **193:** 469-480.

SHOTT, S. R., 2006 Down syndrome: common otolaryngologic manifestations. Am J Med Genet C Semin Med Genet **142C:** 131-140.

SIAREY, R. J., J. STOLL, S.I. RAPOPORT, Z. GALDZICKI, 1997 Altered long-term potentiation in the young and old Ts65Dn mouse, a model for Down syndrome. Neuropharmocology **36:** 1549-1554.

TANG, Y., M. B. SCHAPIRO, D. N. FRANZ, B. J. PATTERSON, F. J. HICKEY *et al.*, 2004 Blood expression profiles for tuberous sclerosis complex 2, neurofibromatosis type 1, and Down's syndrome. Ann Neurol **56:** 808-814.

TRAINOR, P. A., D. SOBIESZCZUK, D. WILKINSON and R. KRUMLAUF, 2002 Signalling between the hindbrain and paraxial tissues dictates neural crest migration pathways. Development **129:** 433-442.

TROIS, M. S., G. T. CAPONE, J. A. LUTZ, M. C. MELENDRES, A. R. SCHWARTZ *et al.*, 2009 Obstructive sleep apnea in adults with Down syndrome. J Clin Sleep Med **5:** 317-323.

VAN CLEVE, S. N., S. CANNON and W. I. COHEN, 2006 Part II: Clinical Practice Guidelines for adolescents and young adults with Down Syndrome: 12 to 21 Years. J Pediatr Health Care **20:** 198-205.

VAN CLEVE, S. N., and W. I. COHEN, 2006 Part I: clinical practice guidelines for children with Down syndrome from birth to 12 years. J Pediatr Health Care **20:** 47-54.

VAN DE GRAAFF, W. B., S. B. GOTTFRIED, J. MITRA, E. VAN LUNTEREN, N. S. CHERNIACK *et al.*, 1984 Respiratory function of hyoid muscles and hyoid arch. J Appl Physiol **57:** 197-204.

VILLAR, A. J., P.V. BELICHENKO, A.M. GILLESPIE, H.M. KOZY, W.C. MOBLEY, C.J. EPSTEIN, 2005 Identification and characterization of a new Down syndrome model, Ts[Rb(12.1716)]2Cje, resulting from a spontaneous Robertsonian fusion between T(171)65Dn and mouse chromosome 12. Mamm Genome **16:** 79-90.

WAGNER, T., J. WIRTH, J. MEYER, B. ZABEL, M. HELD *et al.*, 1994 Autosomal sex reversal and campomelic dysplasia are caused by mutations in and around the SRY-related gene SOX9. Cell **79:** 1111-1120.

WEIJERMAN, M. E., A.M. VAN FURTH, A. VONK NOORDEGRAAF, J.P. VVAN WOUWE, C.J. BROERS, R.J. GEMKE, 2008 Prevalence, neonatal characteristics, and first-year mortality of Down syndrome: a national study. J Pediatr. **152:** 15-19.

WEIS, S., G. WEBER, A. NEUHOLD and A. RETT, 1991 Down syndrome: MR quantification of brain structures and comparison with normal control subjects. AJNR Am J Neuroradiol **12:** 1207-1211.

WILLIAMS, A. D., C.H. MJAATVEDT, C.S. MOORE, 2008 Characterization of the cardiac phenotype in neonatal Ts65Dn mice. Dev Dyn. **237:** 426-435.

WRIGHT, E., M.R. HARGRAVE, J. CHRISTIANSEN, L. COOPER, J. KUN, T. EVANS, U. GANGADHARAN, A. GREENFIELD P. AND KOOPMAN, 1995 The Sry-related gene Sox9 is expressed during chondrogenesis in mouse embryos. Nat Genet. **9:** 15-20.

YAMANE, A., 2005 Embryonic and postnatal development of masticatory and tongue muscles. Cell Tissue Res **322:** 183-189.

YU, T., Z. LI, Z. JIA, S. J. CLAPCOTE, C. LIU *et al.*, 2010 A mouse model of Down syndrome trisomic for all human chromosome 21 syntenic regions. Hum Mol Genet **19:** 2780-2791.

ZHAO, Q., H. EBERSPAECHER, V. LEFEBVRE AND B. DE CROMBRUGGHE, 1997 Parallel expression of Sox9 and Col2a1 in cells undergoing chondrogenesis. Dev Dyn. **209:** 377-386.

FIGURES
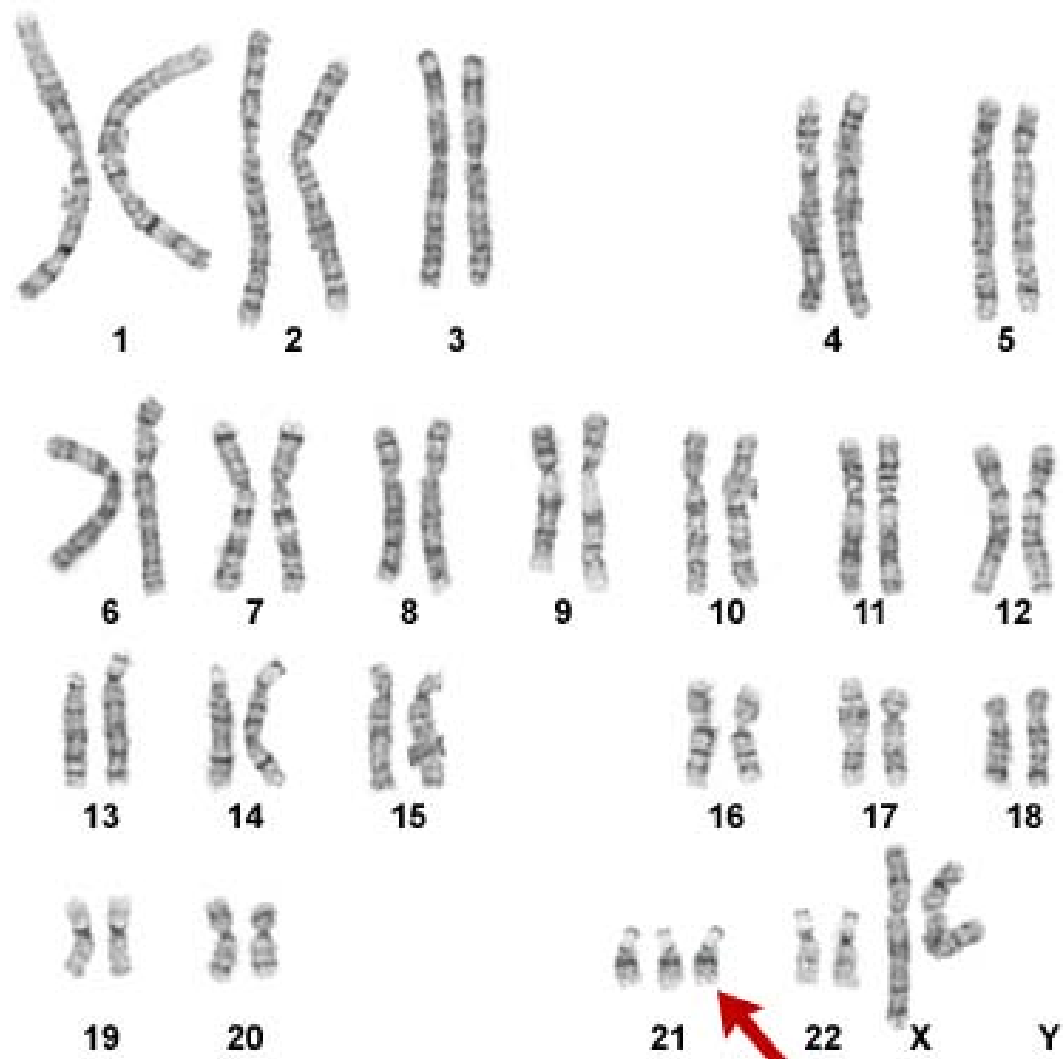
Figure 1.1.1: Down Syndrome Karyotype. Karyotypes show the number and appearance of chromosomes in the nucleus of eukaryote cells. Most cases of Down syndrome can be easily diagnosed by the presence of three copies of chromosome 21. (http://images1.clinicaltools.com/images/gene/karyotypes/trisomy21.jpg).
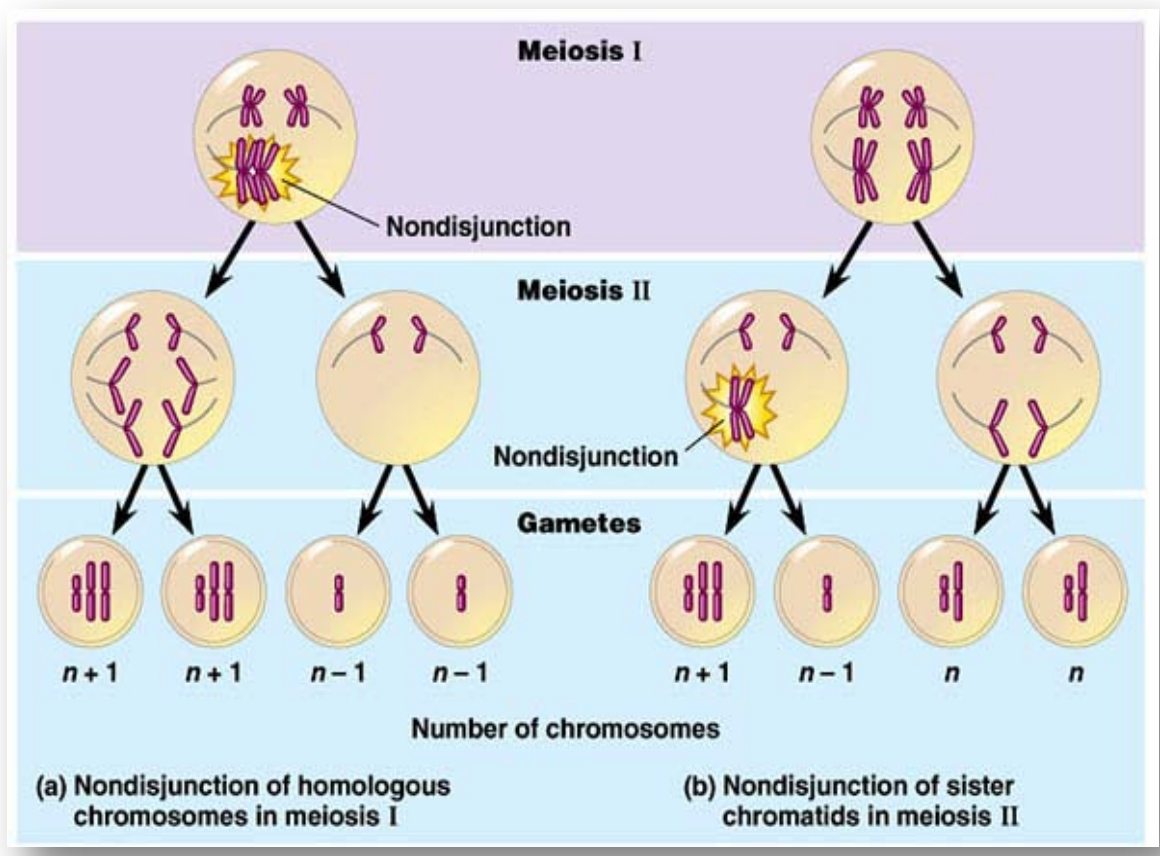
Figure 1.1.2: Nondisjunction in Meiosis I and Meiosis II. 95% of DS cases occur when homologous chromosomes fail to separate during meiosis. The majority of DS cases are caused by an error during meiosis I.
(http://www.bio.miami.edu/~cmallery/150/mendel/c15x11nondisjunction.jpg).
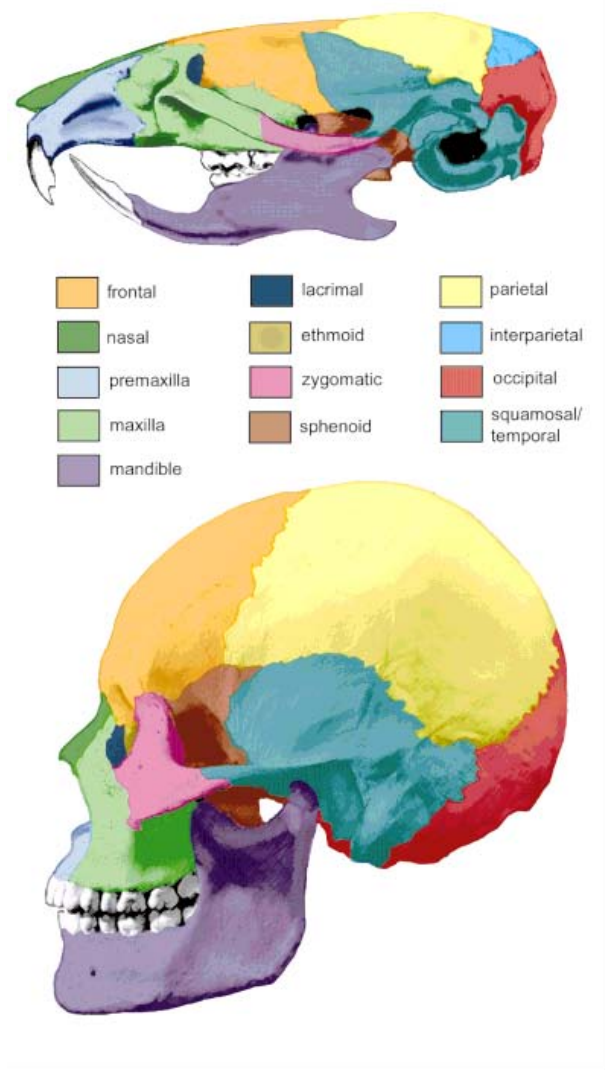
Figure 1.3.1: Conserved Skull Bone Structures between Humans and Mice.
Individual bony elements are conserved between mouse and human skulls. The colors show the parts of the human skull that are analogous to the mouse skull. The conservation in structure between humans and mice allows the comparison of skull development in Ts65Dn mice to humans with Down syndrome. (RICHTSMEIER 2000).
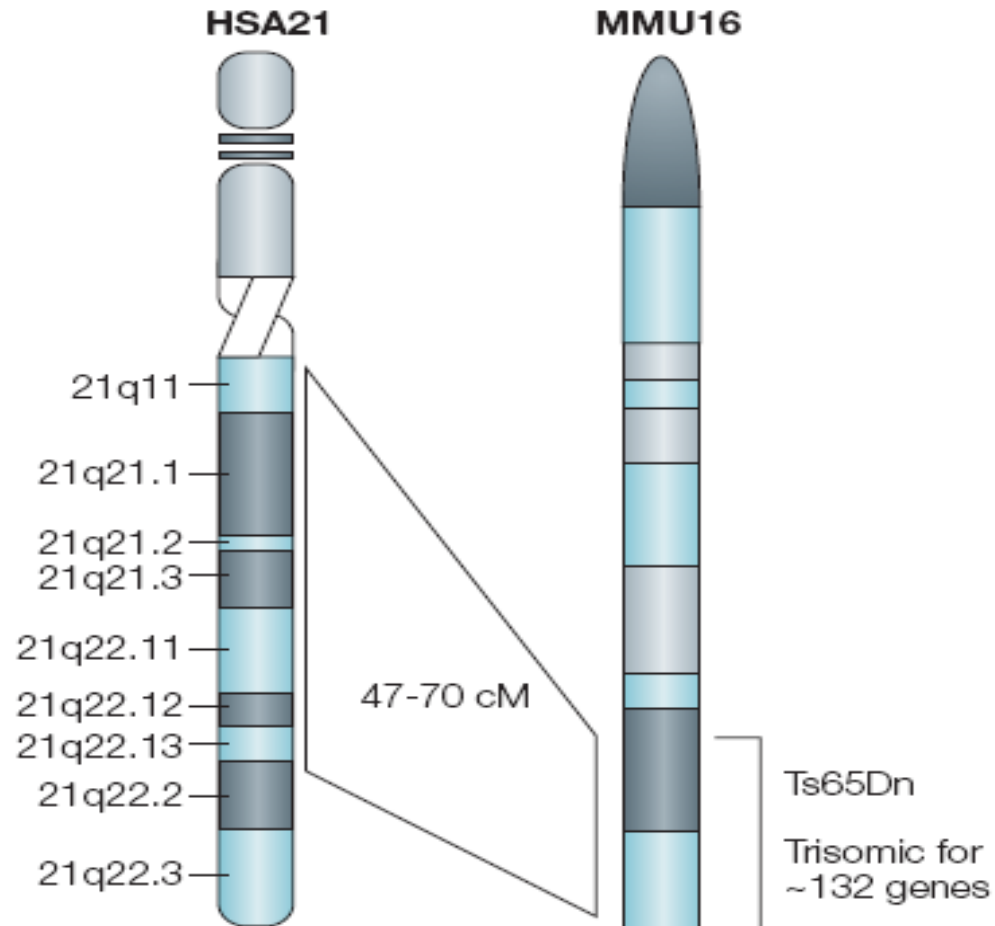
Figure 1.3.2: Human Chromosome 21 Gene Homologues in the Ts65Dn Mouse.
Genes found on Hsa21 are found on three different murine chromosomes (Mmu) 10, 16
and 17. The Ts65Dn mouse model displays many phenotypes similar to those found in
individuals with DS and is the most commonly used mouse model for Down syndrome. It
is trisomic for nearly half of the genes located on Hsa21 (ANTONARAKIS *et al.* 2004). This
figure shows the 132 genes in the Ts65Dn mouse that are orthologus to Hsa21.
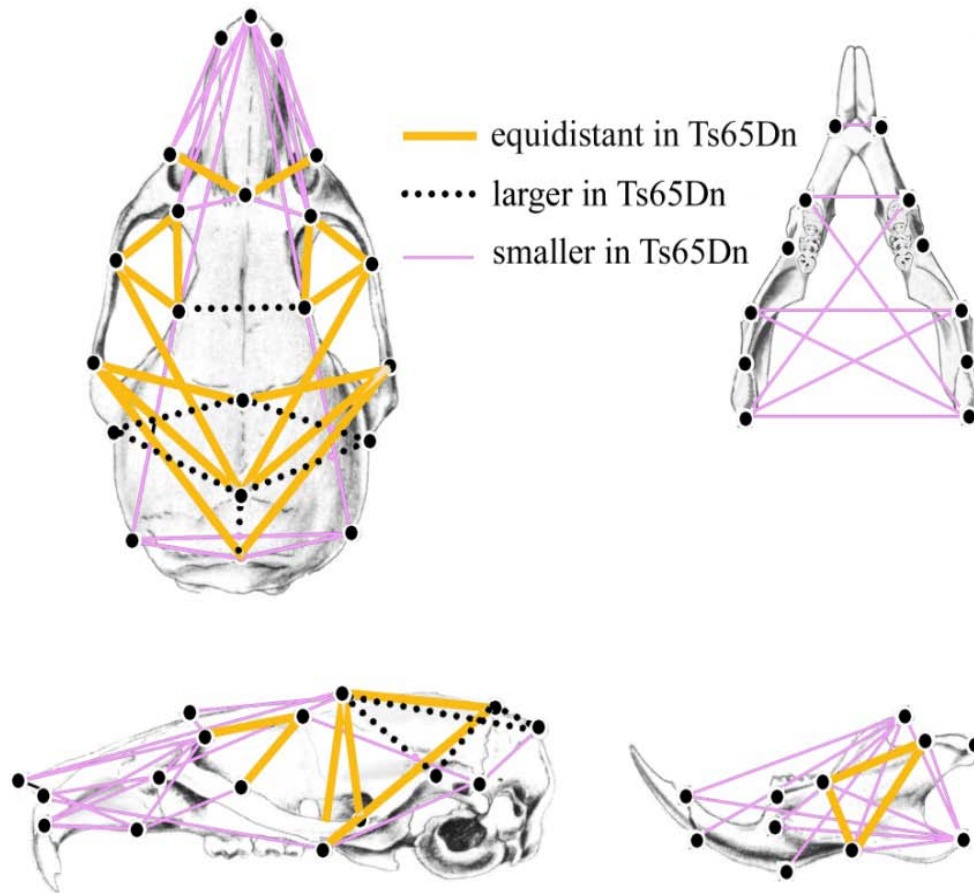
Figure 1.3.3: Ts65Dn Skulls Significantly Differ from Euploid Mice. Ts65Dn skulls differ significantly from euploid mice in patterns that parallel craniofacial dysmorphology found in individuals with DS. Biological landmarks were incorporated to make three-dimensional measurements of euploid and trisomic skulls. The mandible and maxilla were significantly smaller which is a common phenotype observed in individuals with DS. Ts65Dn mice also displayed a shorter, wider skull mice that also correlates to skull shape in humans with trisomy 21 (RICHTSMEIER 2000).
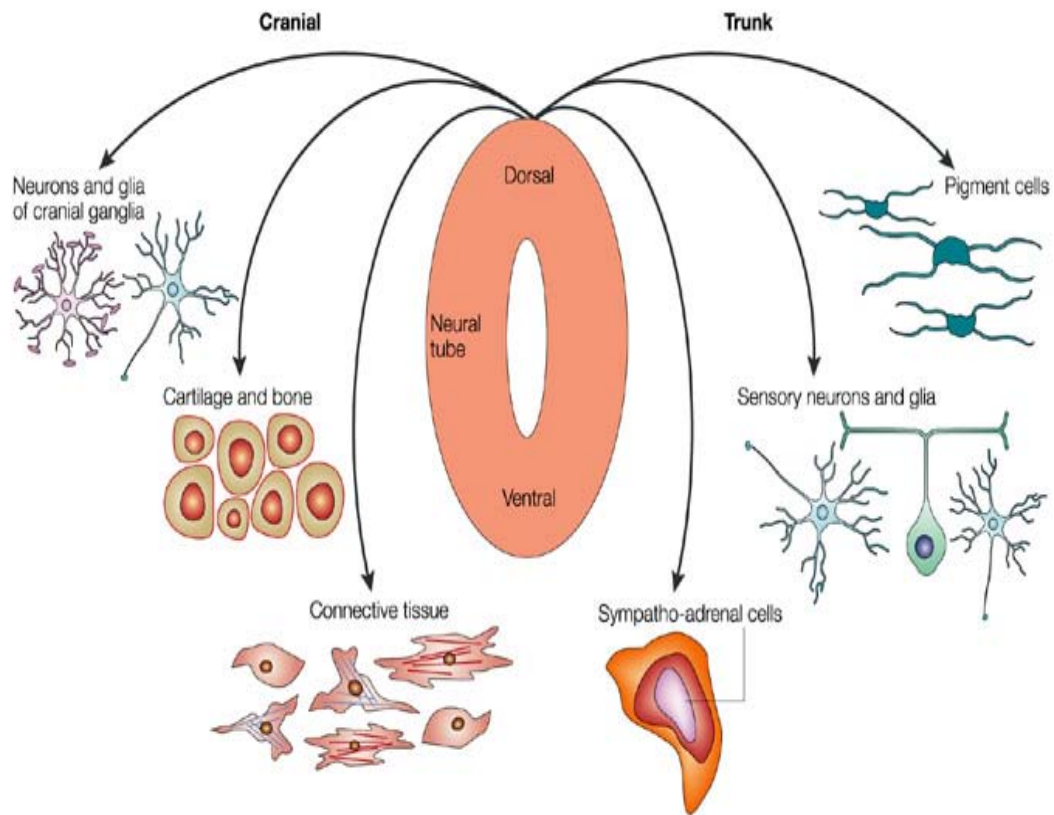
Figure 1.4.1: Neural Crest Derived Tissues. Neural crest (NC) are pluripotent cells that delaminate from the ectoderm overlying the dorsal neural tube and migrate to various locations. Cranial neural crest (CNC) migrate and become neurons, cartilage, bone, and connective tissue. Trunk neural crest migrate and become melanocytes or sensory neurons (KNECHT and BRONNER-FRASER 2002).
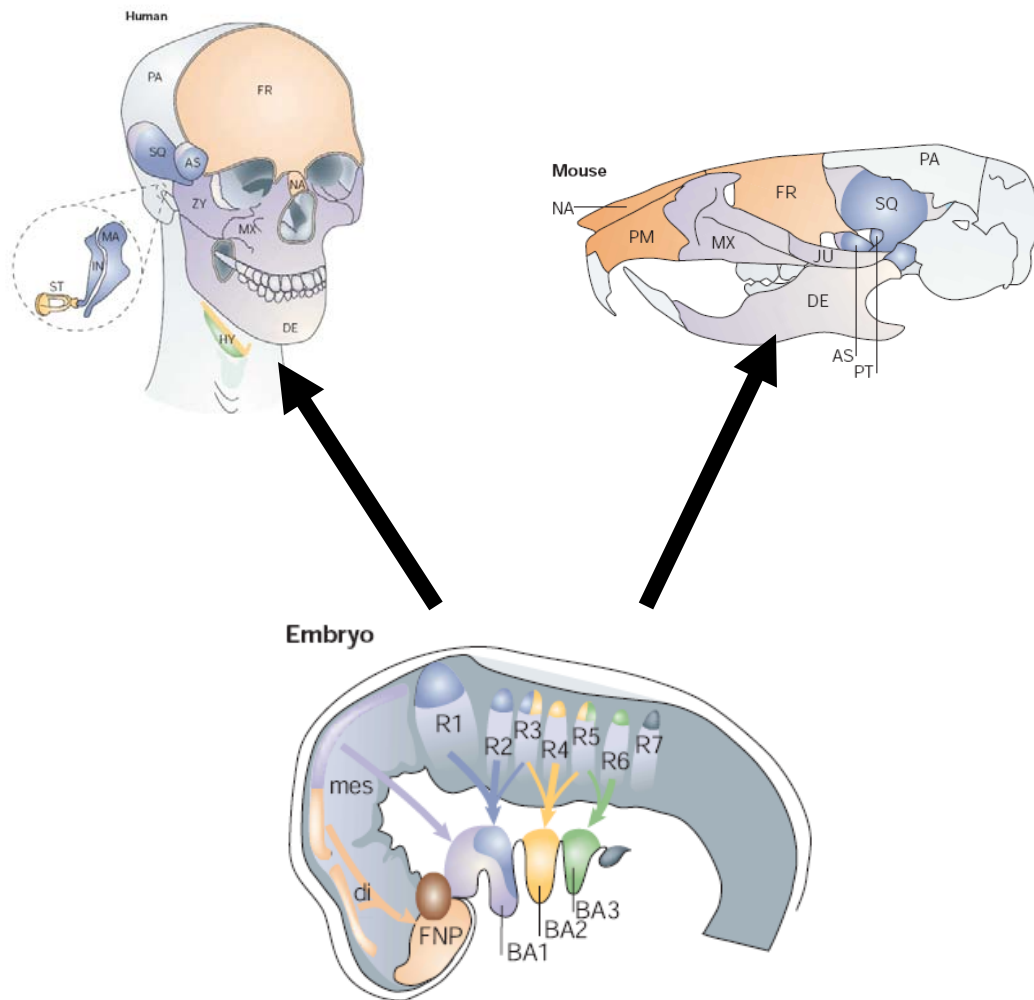
Figure 1.4.2: CNC Migration and Development of Vertebrate Head. This diagram illustrates the migration route of CNC from rhombomeres to branchial arches and then the subsequent craniofacial skeletal structures in both human and mice. (BA stands for branchial arch and is synonymous with pharyngeal arch. The BA will be referred to as PA for the explanation of this diagram). Purple and blue structures in the craniofacial skeleton are derived from the PA1 which is smaller in E9.5 Ts65Dn embryos. Yellow structures form from the PA2 which is also reduced in E9.5 Ts65Dn embryos. CNC migrate from rhombomeres 1, 2, and 3 migrate to the first branchial arch which then gives rise to the maxilla, mandible, incus, malleus, and Meckel's cartilage. CNC from rhombomeres 3, 4, and 5 migrate to the PA2 which forms the stapes, styloid process, hyoid, and Reichert's cartilage. Both the PA1 and PA2 form structures that are affected by trisomy 21 (SANTAGATI and RIJLI 2003)
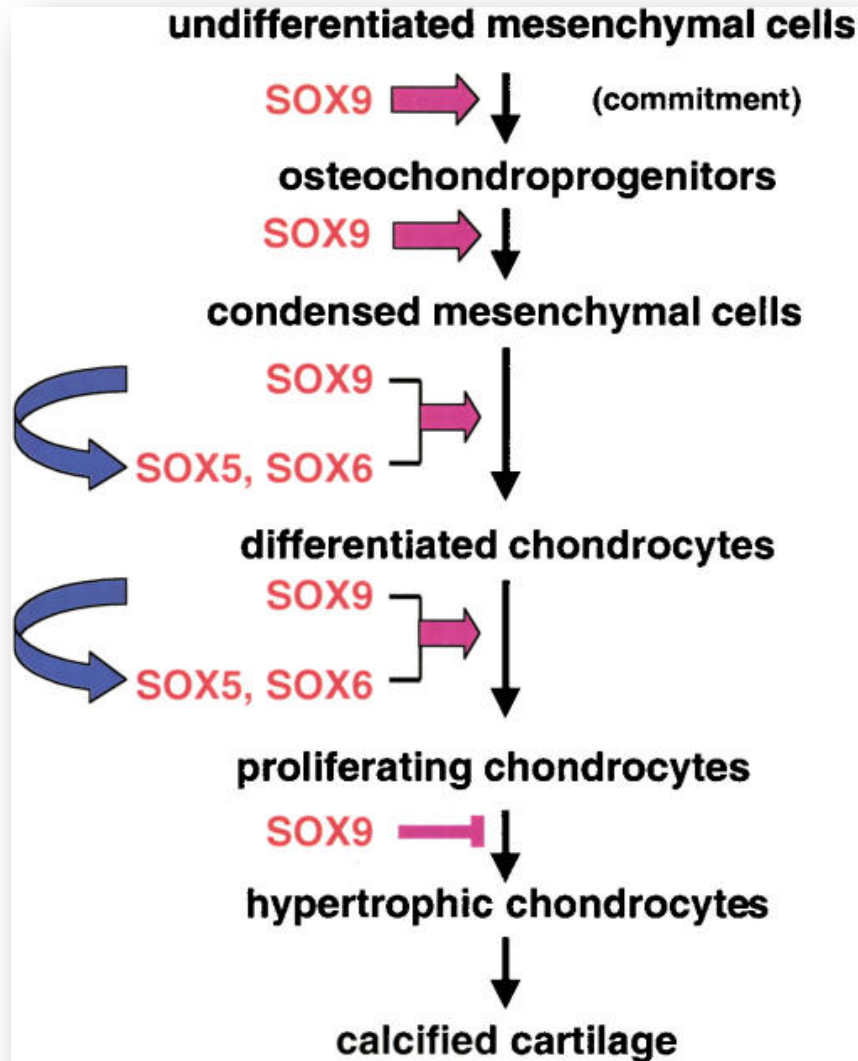
Figure 1.5.1: *Sox9* **Controls Chondrocyte Development**. *Sox9* expression causes undifferentiated mesenchymal cells to differentiate into osteochondroprogenitors and then to become condensed mesenchymal cells. With the help of Sox5 and Sox6, Sox9 causes the mesenchymal cells to differentiate into chondrocytes and then to proliferate. Sox9 presence inhibits proliferating chondrocytes from becoming hypertrophic. An over expression of *Sox9* delays cartilage formation and subsequent endochondral bone formation (AKIYAMA *et al.* 2002).
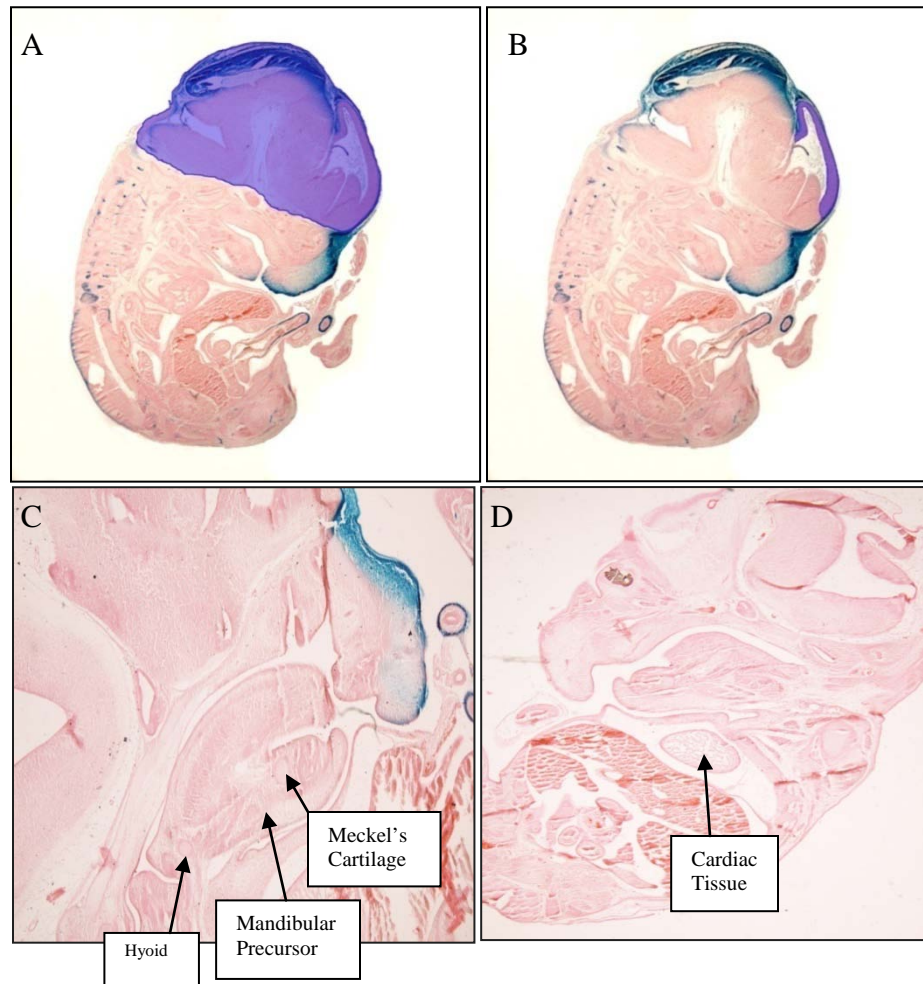
Figure 2.6.1: E13.5 Structures Measured with Unbiased Stereology. Parasagittal Sections of E13.5 embryos demonstrating measured structures.

A. Blue shading defines the brain which includes the ventricles.

B. Blue shading defines the neocortical precursor which was defined as lining the lateral ventricles and bordered by ganglionic eminences and choroid plexus.

C. Mandibular precursor was defined as including Meckel's cartilage and extending posteriorly to the hyoid cartilage. Meckel's cartilage was characteristically spherical or rod shaped. The hyoid cartilage was located posterior to the mandibular precursor and usually exhibited a spherical shape.

D. Cardiac was easily identified beneath the mandibular precursor and hepatic tissue was directly below the heart.
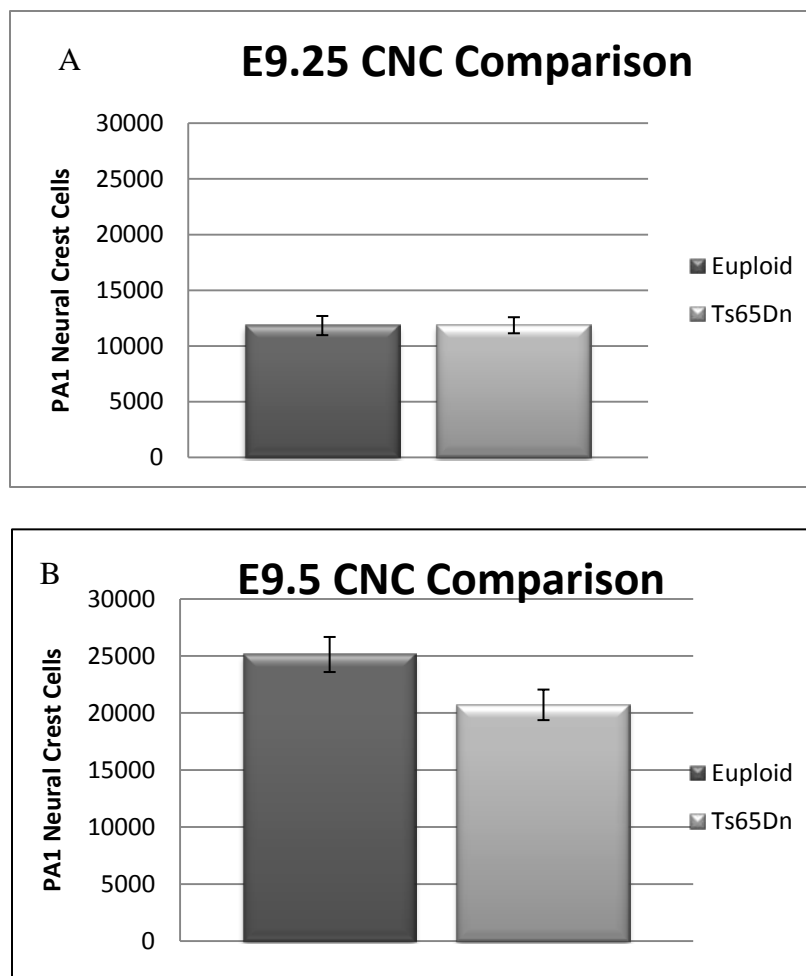
Figure 3.1.1: Reduced Cranial Neural Crest Cells in PA1 of Ts65Dn Mice. Reduced number of CNC in PA1 becomes apparent at E9.5 in Ts65Dn embryos. Error bars were calculated as standard error of the mean.

A. Evaluation of CNC in the PA1 of E9.25 trisomic and euploid littermates revealed no significant difference in CNC number.

B. At E9.5, there is a significant reduction in number of CNC in the PA1 of Ts65Dn mice when compared to euploid littermates (p= 0.03, n= 10 euploid, 8 trisomic).

This deficit is hypothesized to cause the reduced mandibular precursor seen at E13.5 and smaller mandible found at birth in Ts65Dn mice (ROPER 2009).
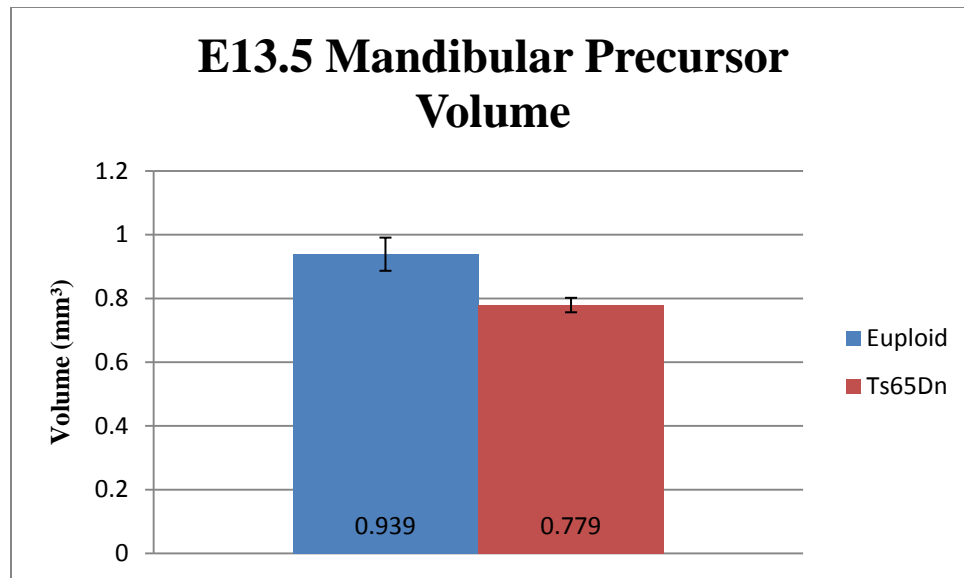
Figure 3.1.2: Reduced Mandibular Precursor in E13.5 Trisomic Embryos. Average size of trisomic mandibular precursor (0.779 mm³) compared to euploid mandibular precursor (0.939 mm³). Error bars were calculated as standard error of the mean. Trisomic mandibular precursor is significantly reduced (p= 0.005). This supports the hypothesis that a reduced PA1 at E9.5 affects later mandibular development.

E13.5 Tongue Volume
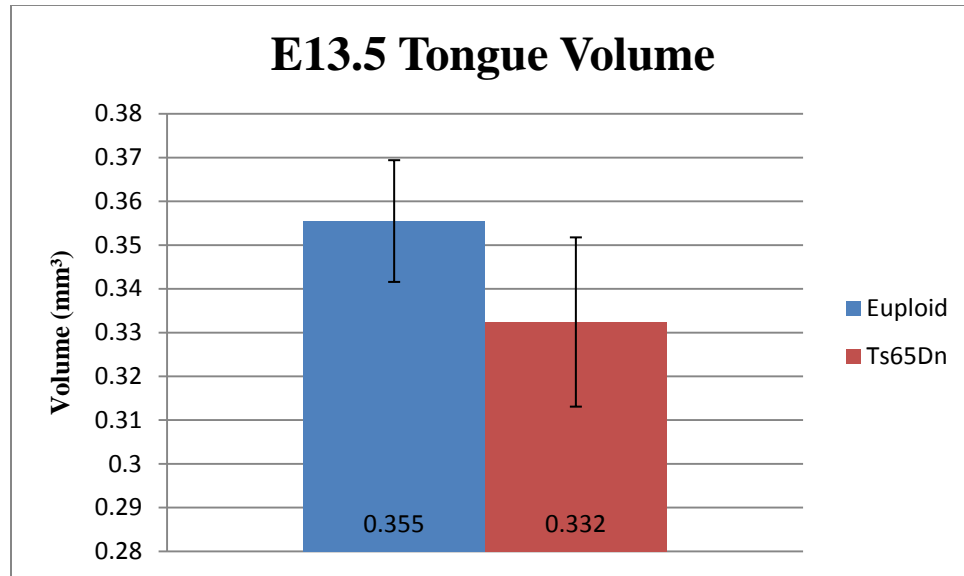
Figure 3.1.3: Similarly Sized Tongue in E13.5 Trisomic and Euploid Embryos.
Average size of trisomic tongue (0.332 mm³) compared to euploid tongue (0.355 mm³)
(p= 0.17). Error bars were calculated as standard error of the mean. No significant
difference between euploid and trisomic tongue volume. This indicates feeding,
breathing, and sleeping difficulties are caused by a smaller oral and a relatively larger
tongue (relative macroglossia).
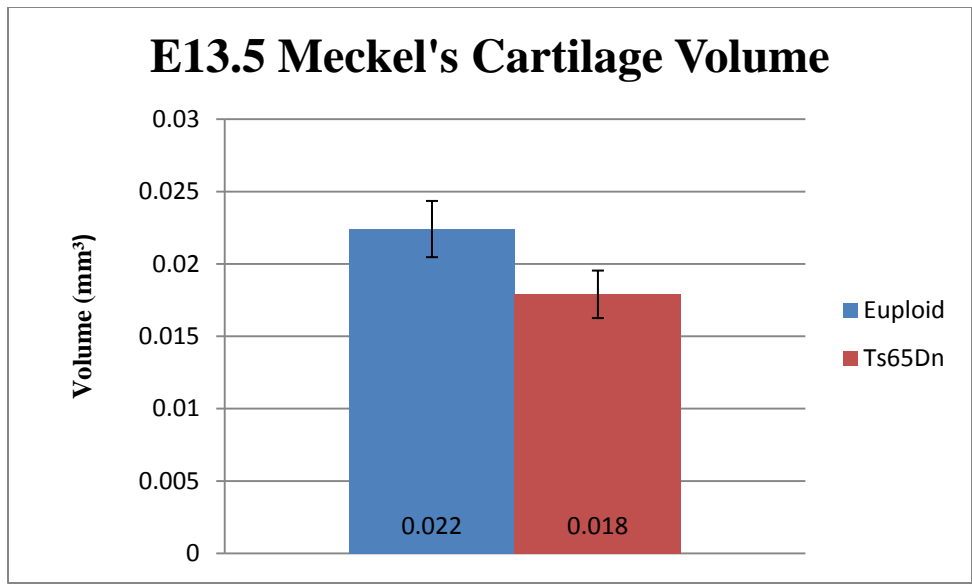
Figure 3.2.1: Reduced Meckel's Cartilage in E13.5 Trisomic Embryos. Average size of trisomic Meckel's cartilage (0.018 mm³) compared to euploid Meckel's cartilage (0.022 mm³). Error bars were calculated as standard error of the mean. Trisomic Meckel's cartilage is significantly reduced (p= 0.05). Meckel's cartilage serves as a template for mandibular growth and it is hypothesized that a reduced Meckel's cartilage at E13.5 will negatively influence the growth of the mandible.
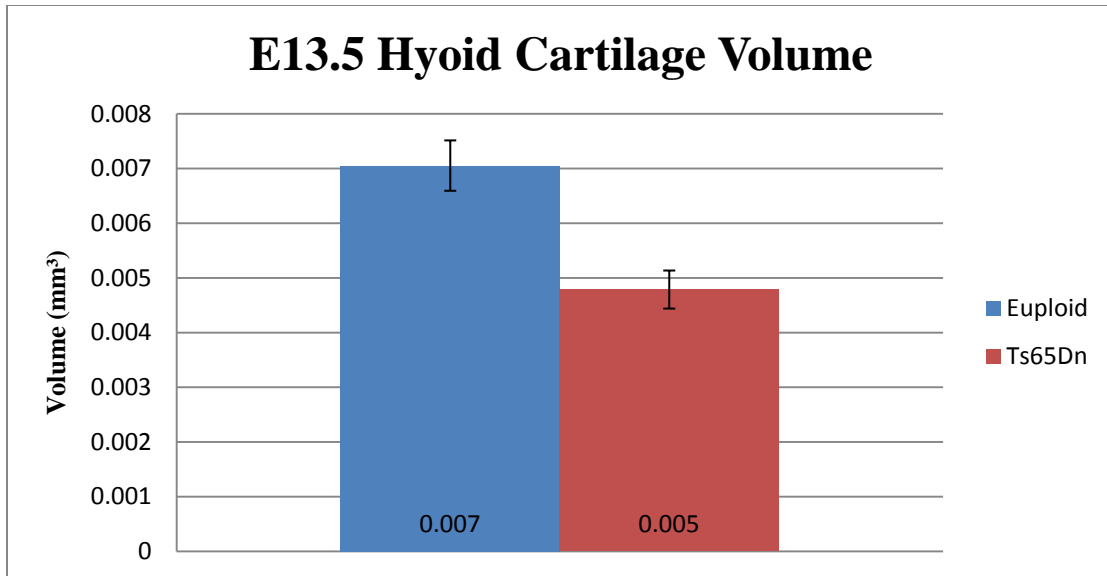
Figure 3.2.2: Reduced Hyoid Cartilage in E13.5 Trisomic Embryos. Average size of trisomic hyoid cartilage (0.005 mm³) compared to euploid hyoid cartilage (0.007 mm³). Error bars were calculated as standard error of the mean. Trisomic hyoid cartilage is significantly reduced (p= 0.0002).
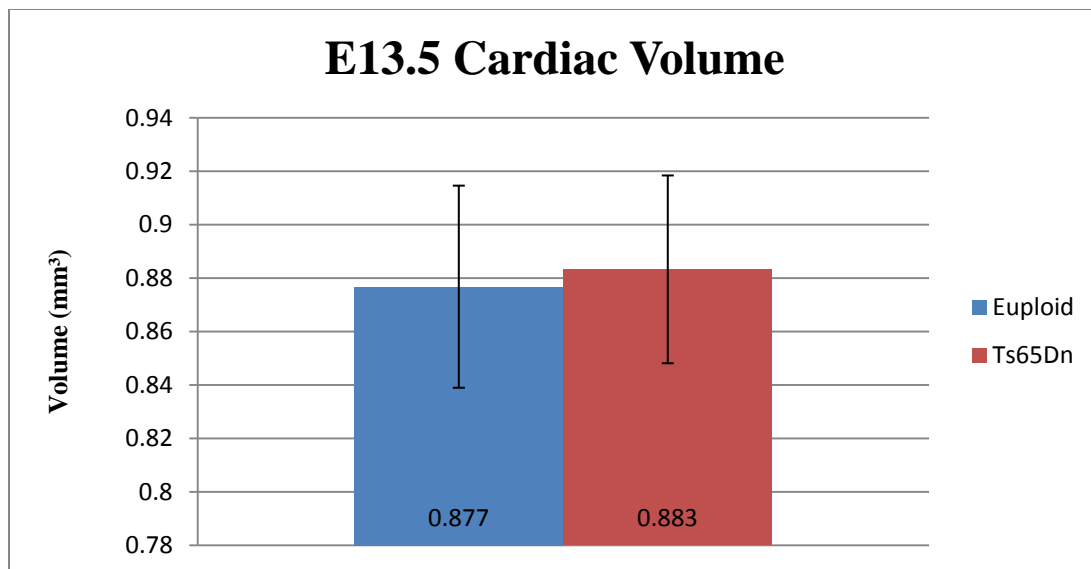
Figure 3.2.3: Similar Cardiac Volumes in E13.5 Euploid and Trisomic Embryos.
Average size of euploid (0.877 mm³) and trisomic (0.883 mm³) cardiac tissue. Error bars
were calculated as standard error of the mean. No significant difference in cardiac tissue
volume was found between euploid and trisomic littermates (p= 0.90).
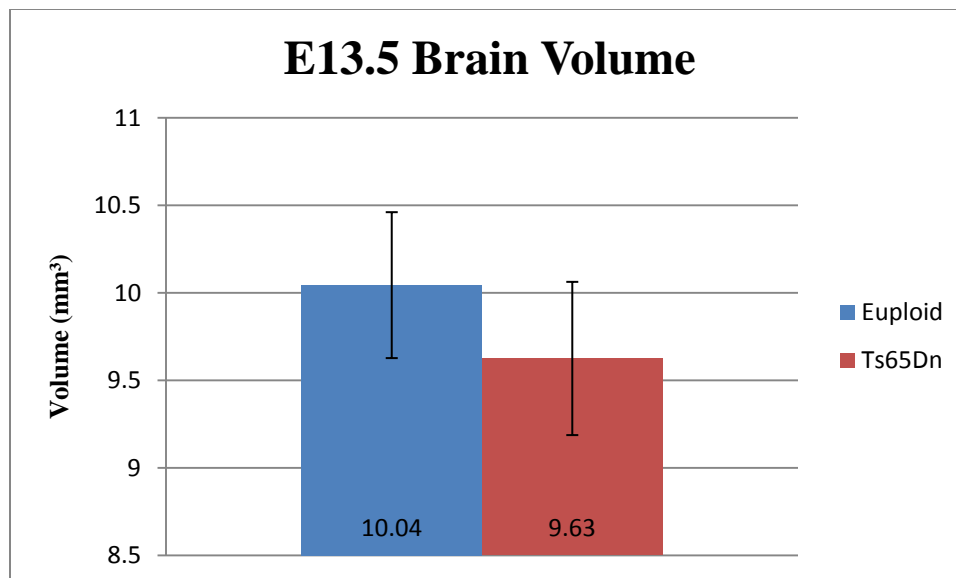
Figure 3.3.1: Similar Brain Volume in E13.5 Euploid and Ts65Dn Mice. Average size of euploid brain was 10.04 mm³ and 9.63 mm³ for Ts65Dn brain. Error bars were calculated as standard error of the mean. There was no significant difference in size (p= 0.49).
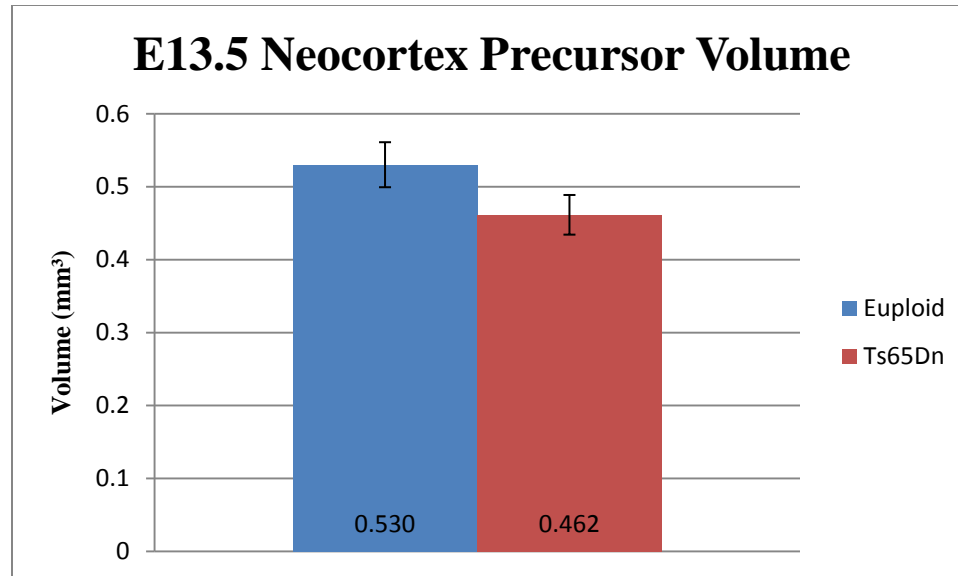
Figure 3.3.2: Reduced Neocortex Volume in E13.5 Trisomic Embryos. Average size of trisomic neocortex (0.462 mm³) compared to euploid neocortex (0.530 mm³). Error bars were calculated as standard error of the mean. Trisomic neocortex is significantly reduced when compared to euploid littermates ($p = 0.05$). This further corroborates the reduced neocortical thickness found in trisomic embryos.
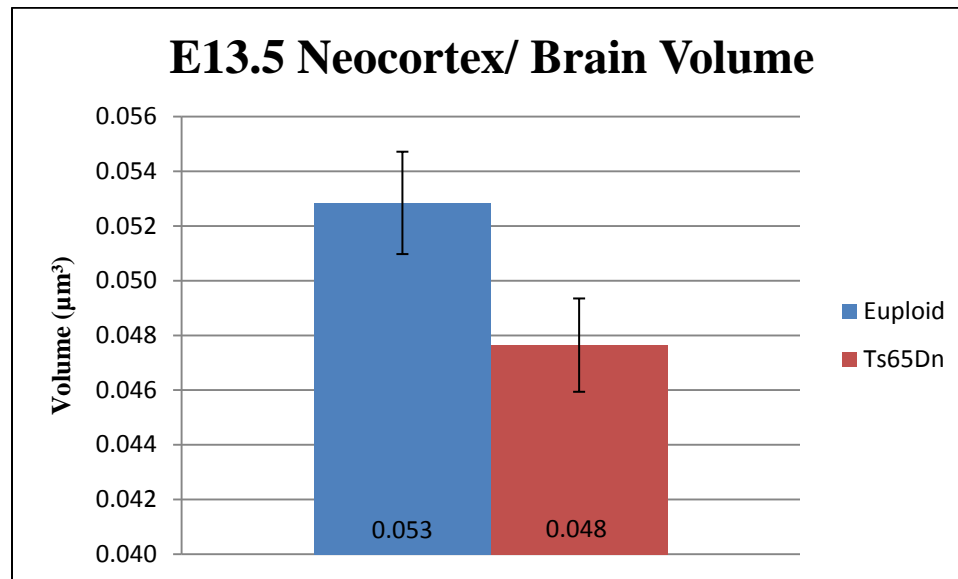
Figure 3.3.3: Reduced Neocortex when Normalized for Total Brain Volume in E13.5 Trisomic Embryos. Average size of trisomic normalized neocortex volume (0.048 mm³) compared to euploid normalized neocortex precursor (0.053 mm³). Error bars were calculated as standard error of the mean. Trisomic neocortex normalized for brain volume is significantly reduced (p= 0.02). This indicates the Ts65Dn neocortex is proportionally smaller when normalized for total brain volume.
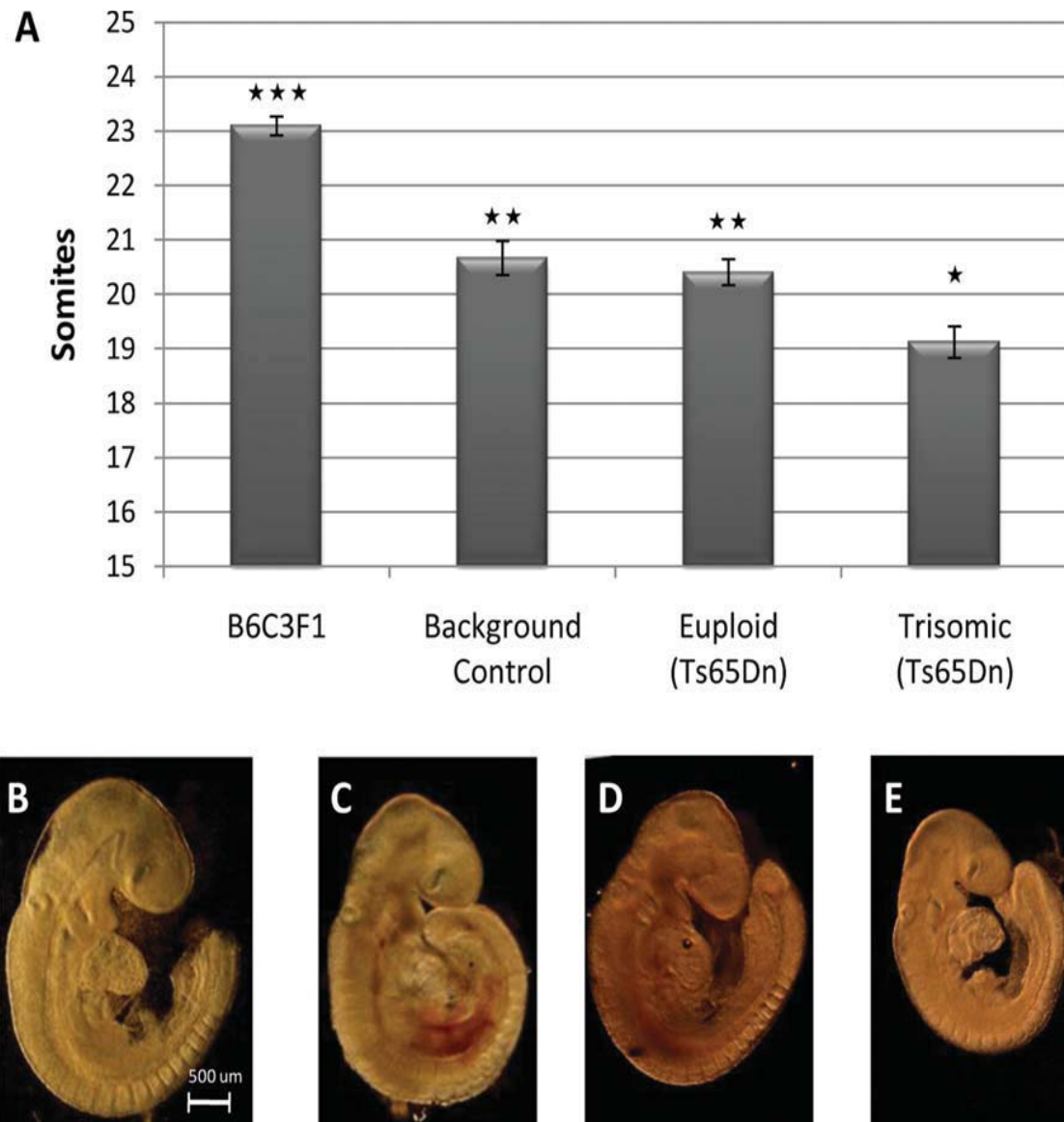
Figure: 3.4.1: Developmental Attenuation in Trisomic E9.5 Ts65Dn Embryos.
Average Somite numbers in E9.5 embryos from Ts65Dn and control mothers. A: Euploid
(Ts65Dn) and trisomic (Ts65Dn) indicates these embryos are offspring of Ts65Dn
mothers. (*) Trisomic embryos exhibit significantly fewer somites compared with their
euploid littermates and control embryos. (**) There is no significant difference between
Ts65Dn euploid somite number and euploid controls; however, both have significantly
fewer somites than B6C3F1 embryos (***). Stars represent significantly different
groupings from analysis of variance and post hoc. Error bars are calculated as standard
error of the mean. B-E Representative E9.5 offspring from B6C3F1 mother (B), a euploid
control mother (C), and a Ts65Dn mother (D,E). D is a euploid embryo, and E is a
trisomic embryo from a Ts65Dn mother. (BLAZEK 2010)
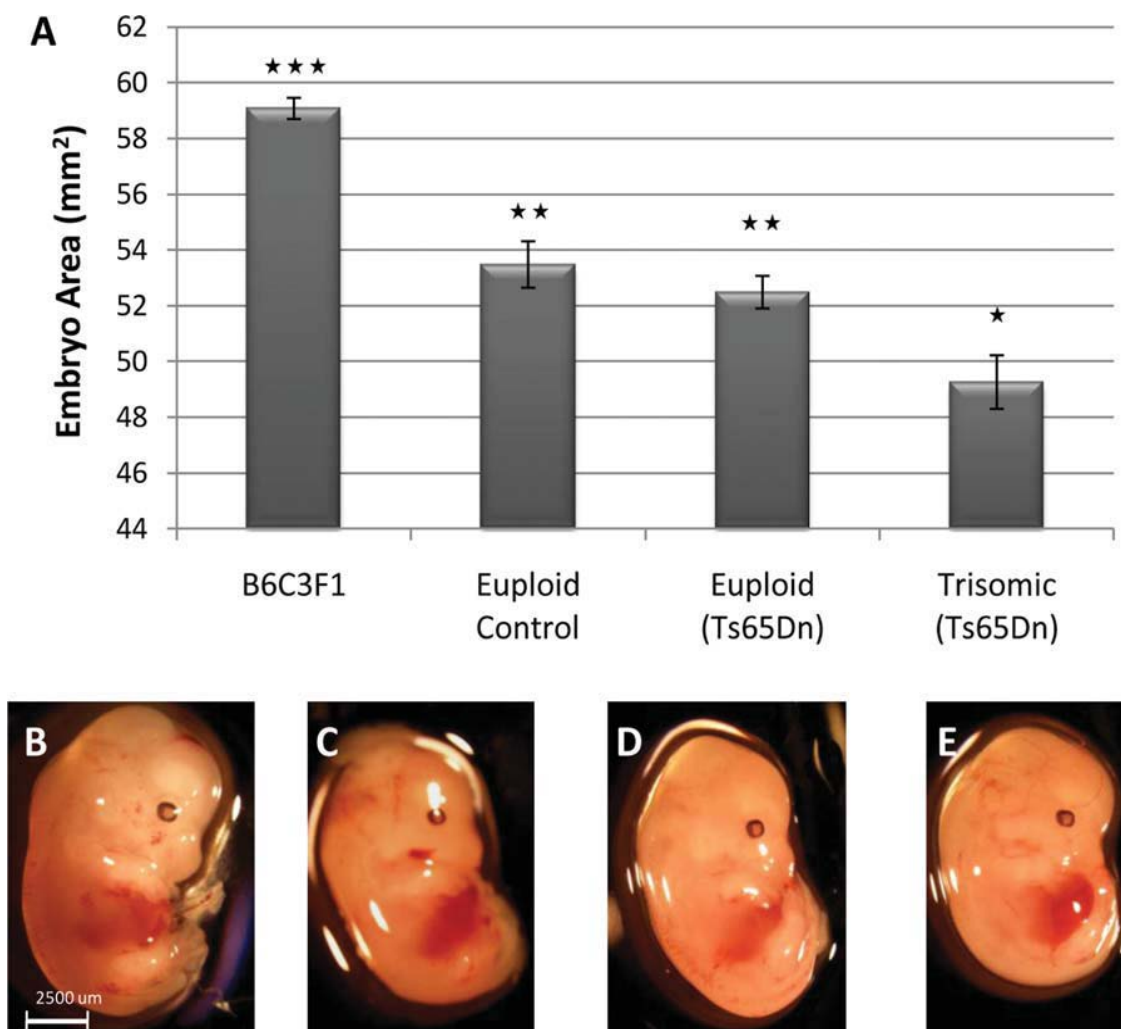
Figure 3.4.2: Developmental Size Alterations at E13.5 in Ts65Dn Trisomic Mice. A-E: Average area of E13.5 embryos from B6C3F1 mother (A), a euploid control mother (B), and a Ts65Dn mother (C); euploid embryo (D) and trisomic embryo (E). D,E: Euploid (Ts65Dn) and trisomic (Ts65Dn) indicates these embryos are offspring of Ts65Dn others. Average area of E13.5 trisomic embryos from Ts65Dn mothers is significantly less than euploid littermates and Ts65Dn background control and B6C3F1 mothers. There is no statistical difference in the area of euploid embryos from Ts65Dn trisomic mothers or background control mothers. The E13.5 embryos from B6C3F1 mothers are larger than all other embryos. Stars represent significantly different groupings from analysis of variance and post hoc. Error bars are calculated as standard error of the mean.(BLAZEK 2010).

E13.5 Total Volume
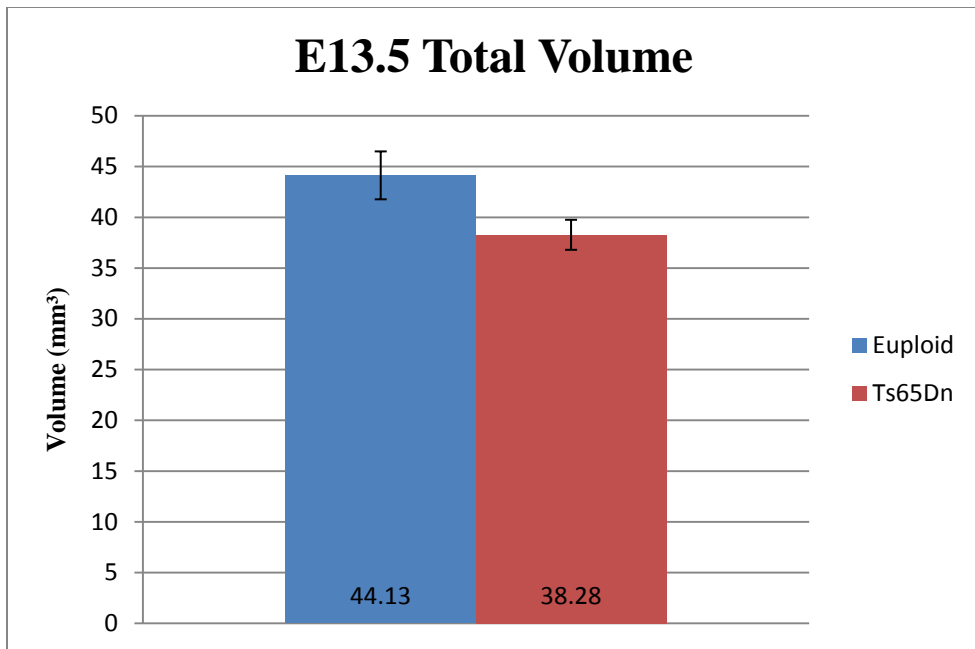
44.13
38.28

Figure 3.5.1: Reduced Total Volume in E13.5 Trisomic Embryos. Average size of trisomic embryos (38.28 mm³) compared to euploid (44.13 mm³). Error bars were calculated as standard error of the mean. Trisomic embryos are significantly reduced (p= 0.02). This supports the hypothesis of developmental attenuation in Ts65Dn embryos.
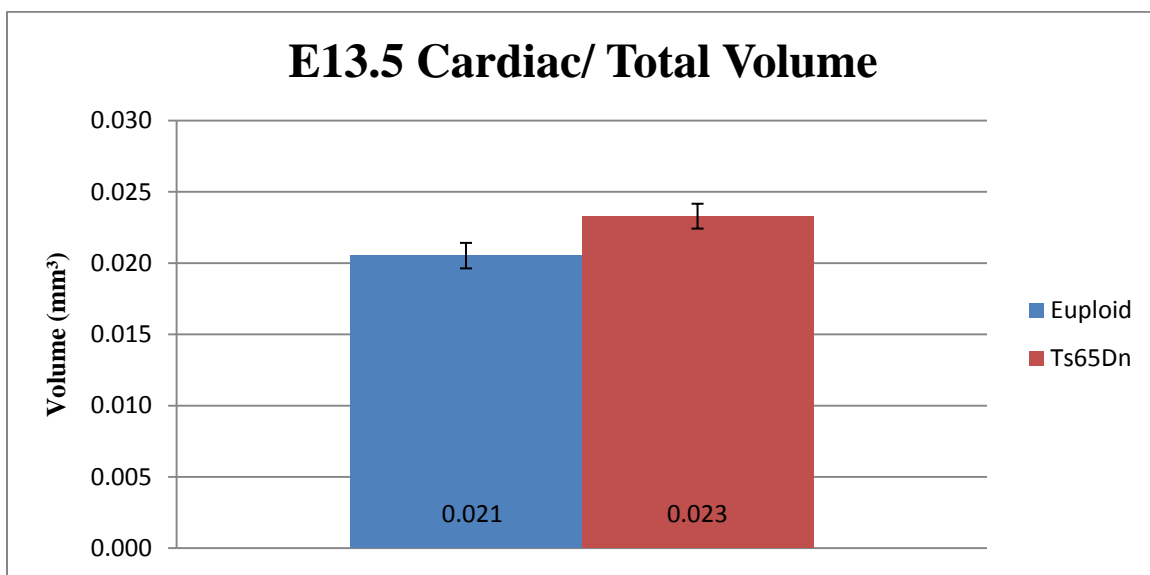
Figure 3.5.2: Enlarged Cardiac Tissue When Normalized for Total Embryonic Volume. Average size of trisomic heart normalized for total volume (0.023 mm³) compared to euploid normalized heart volume (0.021 mm³) indicates a larger heart in trisomic embryos (p= 0.03). Error bars were calculated as standard error of the mean.
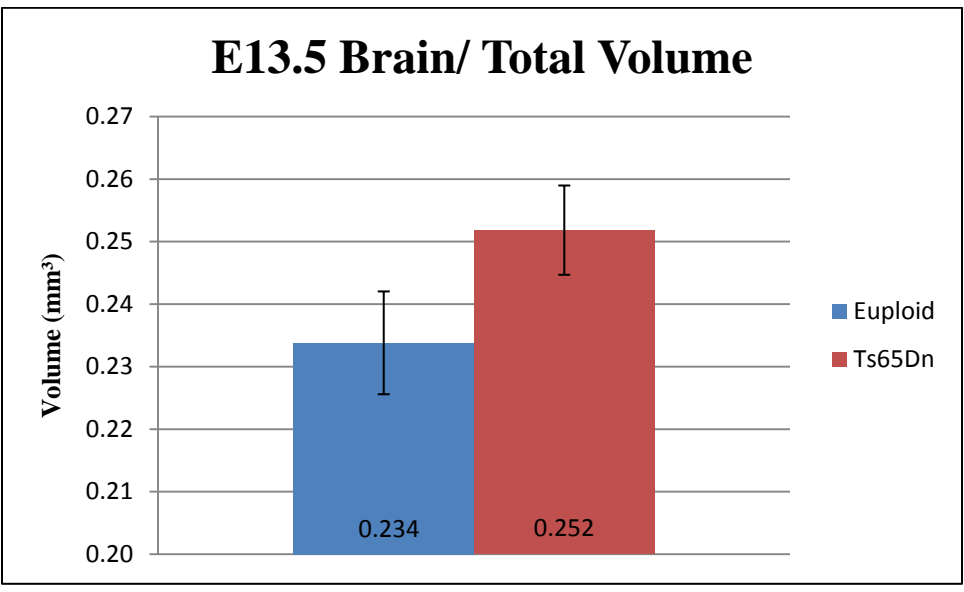
Figure 3.5.3: Slightly Enlarged Trisomic Brain When Normalized for Total Embryonic Volume. Average size of trisomic brain normalized for total volume (0.252 mm³) compared to euploid normalized brain volume (0.234 mm³) indicates a slightly larger brain in trisomic embryos, although not quite reaching statistical significance (p= 0.054). Error bars were calculated as standard error of the mean.
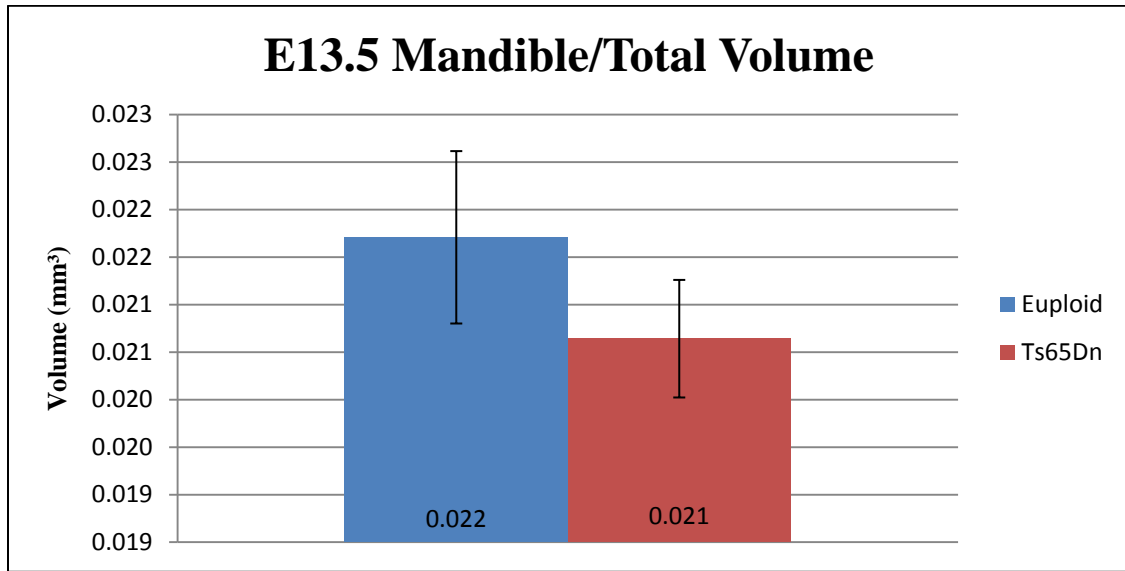
Figure 3.5.4: No Significant Difference Between Euploid and Ts65Dn Mandible when Normalized for Total Volume. This graph illustrates the similar size in euploid and Ts65Dn mandibles when normalized for total volume (p= 0.17). Error bars were calculated as standard error of the mean.
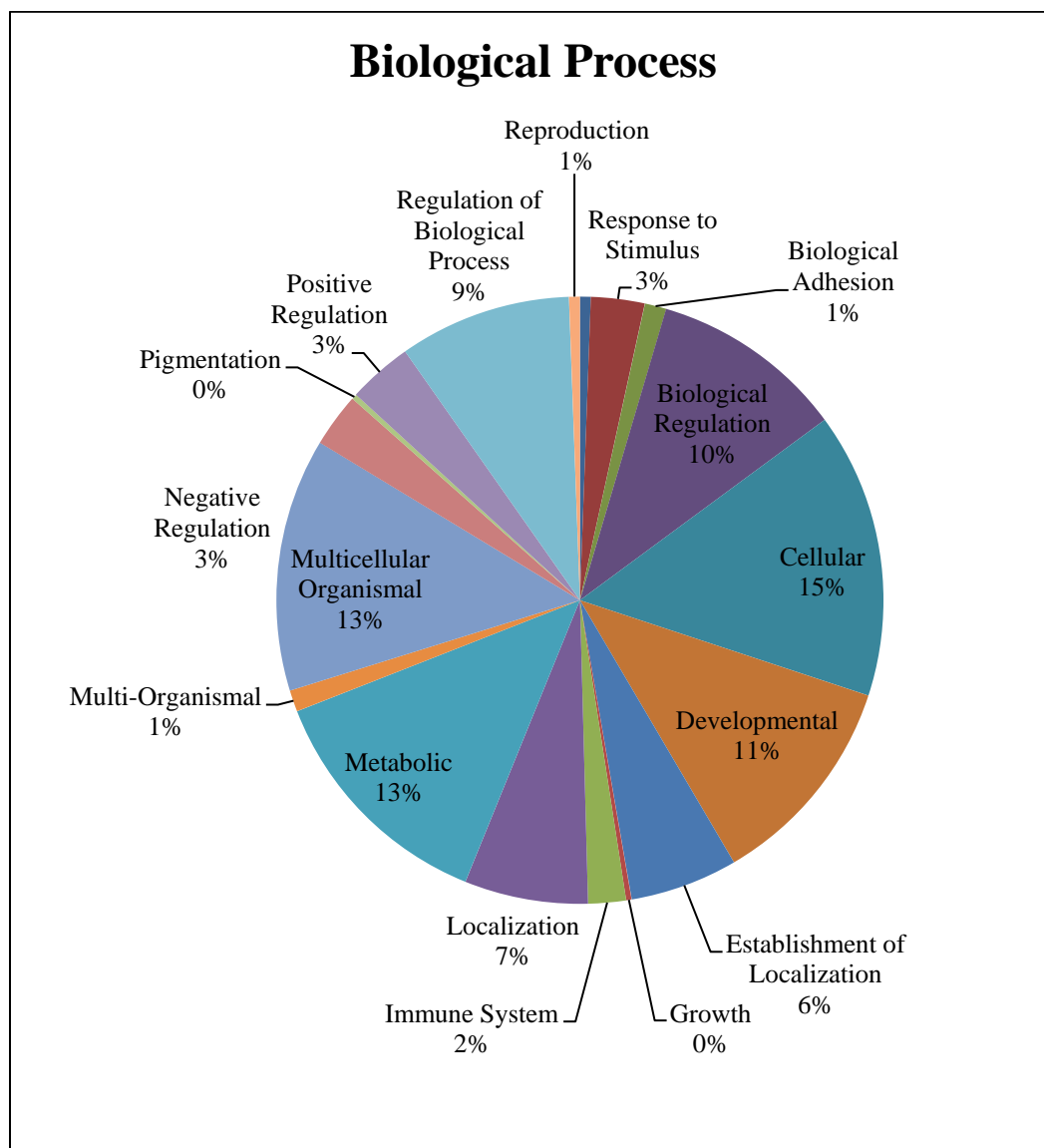
Figure 3.6.1: Dysregulated Genes Involved in Biological Processes. The dysregulated genes revealed through the microarray analysis on the E13.5 mandibular precursor were categorized through gene ontology. This graph reveals the percentage of genes in the "biological process" group that are involved with specific biological processes. The majority of genes in the biological process group had functions in cellular (15%), multicellular organismal (13%), metabolic (13%), or developmental processes (11%).
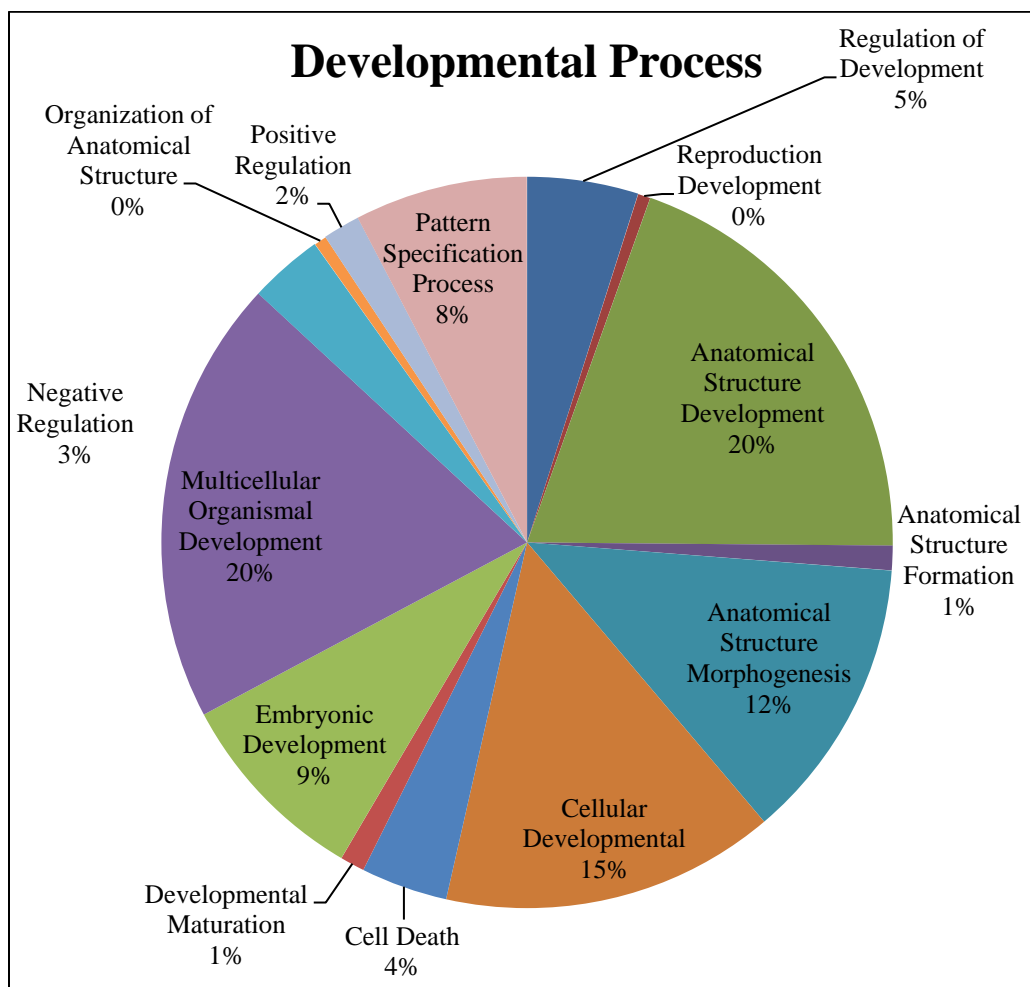
Figure 3.6.2: Dysregulated Genes Involved in Developmental Processes. The dysregulated genes from the microanalysis were initially categorized by their biological processes and then further subcategorized into their developmental processes. This graph reveals the percentage of genes in the "developmental processes" subcategory that are involved with different types of developmental functions. Most of the dysregulated genes with developmental process functions were involved with anatomical structure development (20%), multicellular organismal development (20%), or cellular developmental processes (15%).
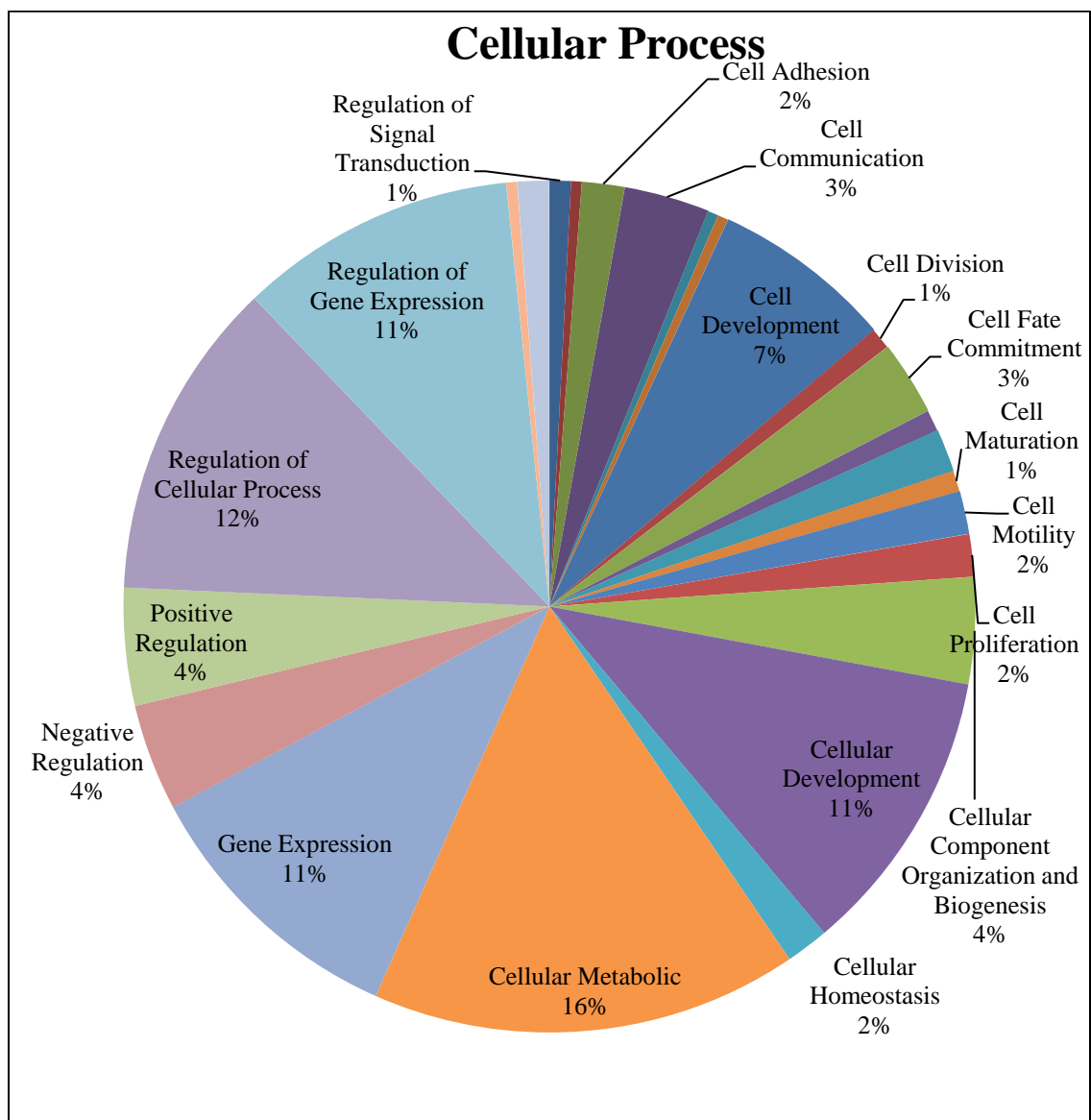
Figure 3.6.3: Dysregulated Genes Involved with Cellular Processes. The dysregulated genes from the microanalysis performed on E13.5 mandibular precursors were categorized by their biological processes and then further subcategorized by their cellular processes. This graph reveals the percentage of genes in the "cellular processes" subcategory that are involved with different types of cellular functions. Most of the dysregulated genes within the cellular process group had functions involved with cellular metabolic processes (16%), regulation of cellular processes (12%), or gene expression (11%).
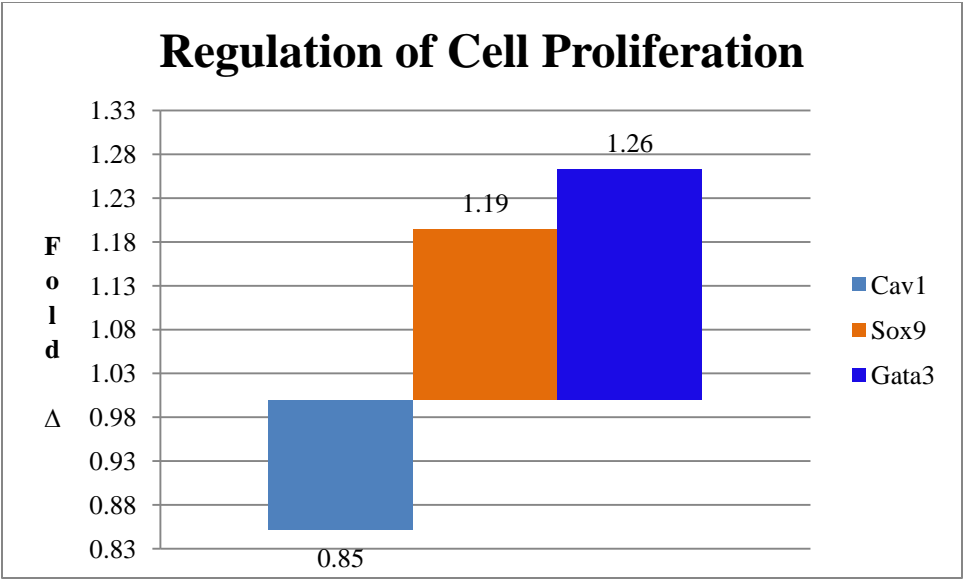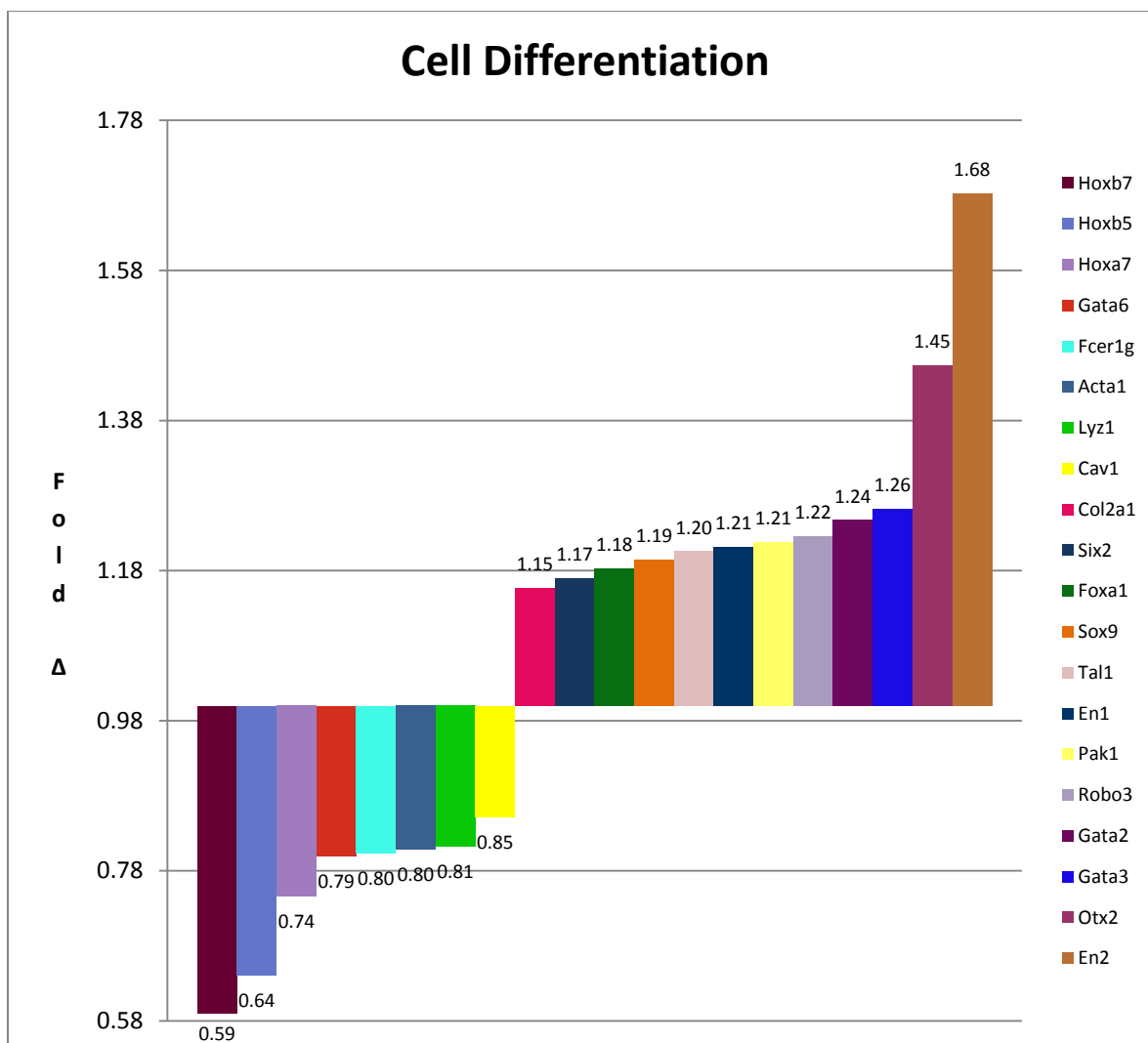
Figure 3.6.4: Dysregulated Genes Involved with Cell Proliferation. This graph shows dysregulated genes found in the microarray that are involved with cell proliferation. Genes that are downregulated are represented with a bar below 1.0 fold while upregulated genes are represented with a bar above 1.0 fold. Genes involved with cellular proliferation are of interest because decreased cellular proliferation would have an effect on mandibular growth.
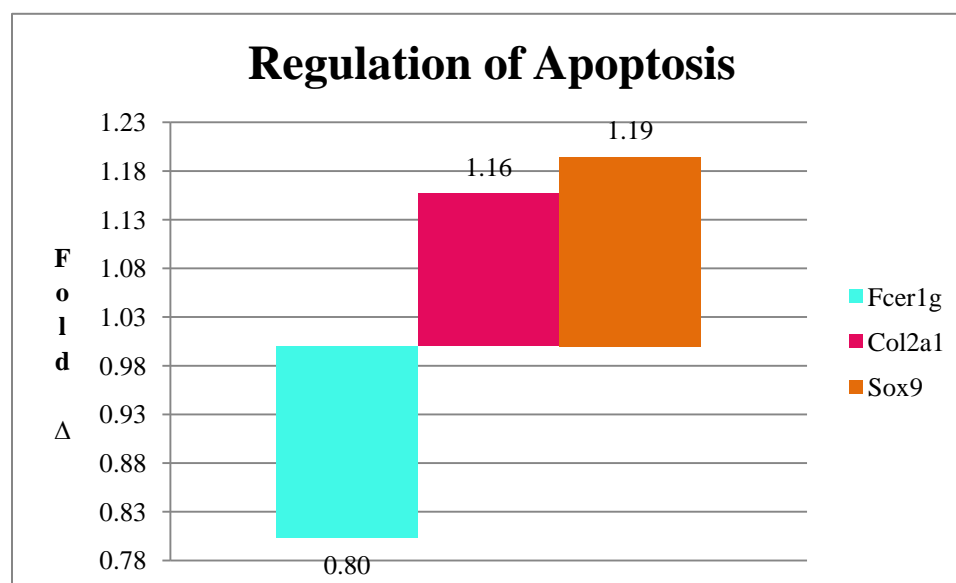
Figure 3.6.5: Dysregulated Genes Involved with Apoptosis. This graph shows dysregulated genes from the microarray that are involved with the regulation of apoptosis. Genes that are downregulated are represented with a bar below 1.0 fold while upregulated genes are represented with a bar above 1.0 fold. Genes involved in the regulation of apoptosis are important because misexpression of these genes could cause premature death of cells needs for the normal development of the mandible.

Figure 3.6.6: Dysregulated Genes Involved with Cell Differentiation. This graph shows dysregulated genes from the microarray analysis that are involved with cellular differentiation. Genes that are downregulated are represented with a bar below 1.0 fold while upregulated genes are represented with a bar above 1.0 fold. Genes involved with cellular differentiation are important in the developing mandible because mesenchymal cells need to differentiate into either chondrocytes or osteoblasts to allow for normal ossification of the mandible.
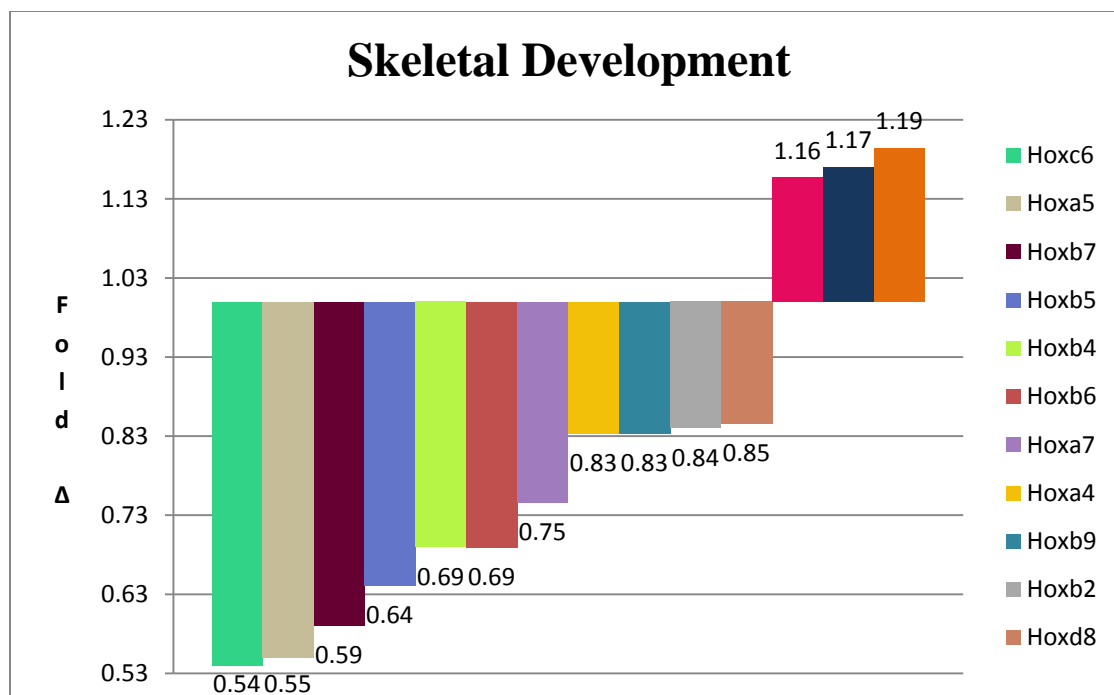
Figure 3.6.7: Dysregulated Genes with Skeletal Development Function. This graph shows genes that were dysregulated in the E13.5 trisomic mandibular precursor that have a function in skeletal development. Genes that are downregulated are represented by a bar beneath 1.0 fold whiles genes that are overexpressed have a bar above 1.0 fold. Genes of interest are the downregulated *Hox* genes and the upregulated *Sox9* and *Col2a1*. Genes involved with skeletal development are of particular interest because the mandibular precursor is preparing to undergo bone formation at E13.5.
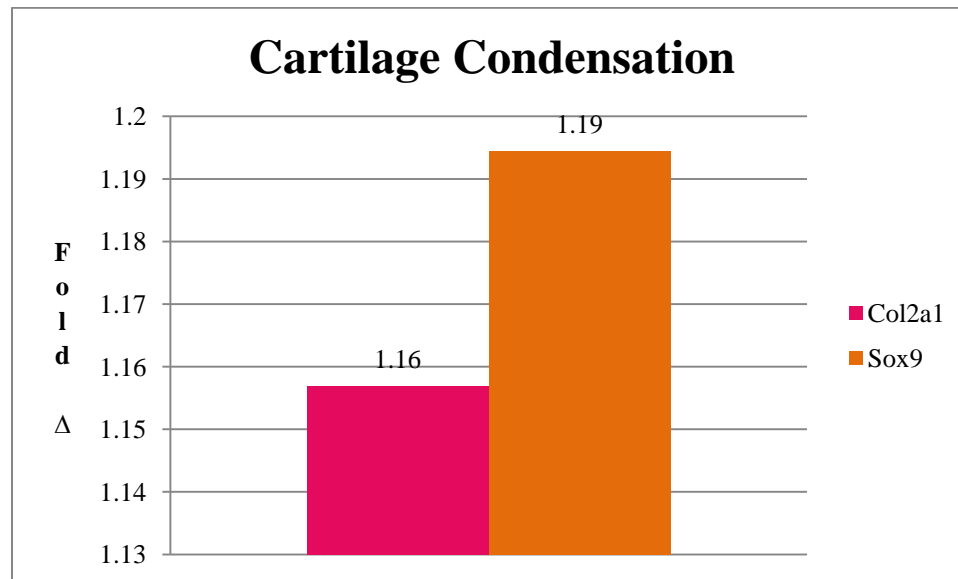
Figure 3.6.8: Dysregulated Genes Involved with Cartilage Condensation. This graph shows dysregulated genes that are involved in cartilage condensation. *Sox9* and *Col2a1* are the only genes involved with cartilage condensation and are both overexpressed in the E13.5 trisomic mandibular precursor. Genes involved with cartilage condensation are of interest because of their role in endochondral ossification.

Gene	Fold Change
HOXC6	0.540
HOXA5	0.550
PTH	0.584
XIST	0.586
HOXB7	0.590
GLRX1	0.602
S100A8	0.611
EG433016	0.633
HOXB5	0.641
S100A9	0.643
STFA1	0.662
TTC27	0.676
2310036D22RIK	1.335
PICALM	1.419
OTX2	1.453
TTR	1.483
LOC666403	1.493
ADAMTS9	1.657
EN2	1.683
OC90	1.962

Figure 3.6.9: Top Dysregulated Genes from E13.5 Mandibular Precursor. A fold change below 1.0 indicates the gene was downregulated while a change above one indicates upregulation.
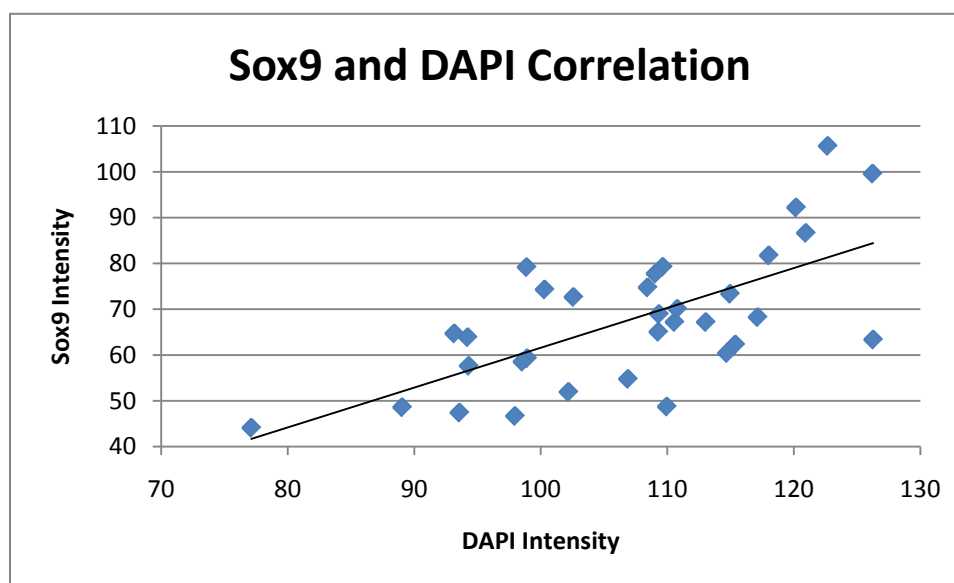
Figure 3.7.1: DAPI Intensity Correlates with *Sox9* Expression. This graph plots the trisomic and euploid DAPI and Sox9 intensity in both Meckel's and the hyoid cartilages. There is a significant correlation between DAPI and Sox9 intensity (R= 0.67, p= 0.0001). This suggests DAPI would be a good control for measuring Sox9 intensity in IHC sections.
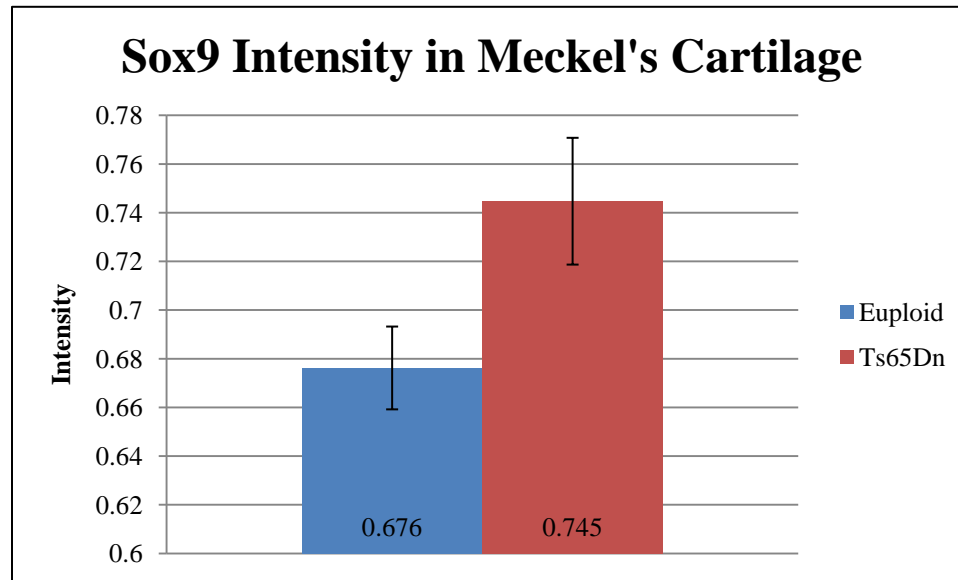
Figure 3.7.2: Increased *Sox9* Expression in Ts65Dn Meckel's Cartilage. After controlling Sox9 results for DAPI, *Sox9* expression was significantly higher in the trisomic Meckel's cartilage (p= 0.02). Error bars were calculated as standard error of the mean.
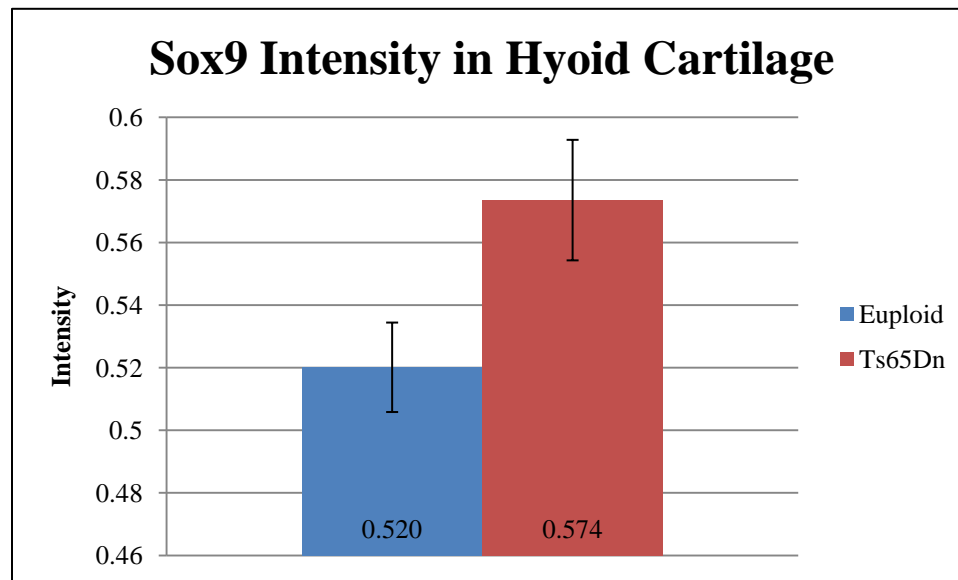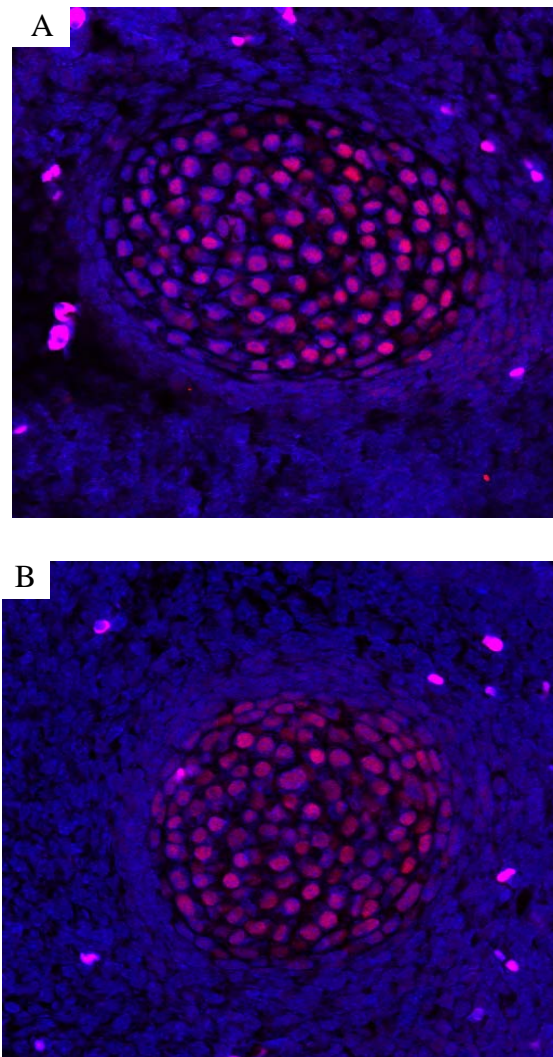
Figure 3.7.3: Increased *Sox9* Expression in Ts65Dn Hyoid Cartilage. After controlling Sox9 results for DAPI, *Sox9* expression was significantly higher in the trisomic hyoid cartilage (p= 0.02). Error bars were calculated as standard error of the mean.

Figure 3.7.4: *Sox9* **Expression in Euploid and Trisomic Meckel's Cartilage**.
Meckel's cartilage from E13.5 euploid (A) and trisomic (B) embryos with Sox9
antibody and DAPI stain. *Sox9* expression is indicated by red color while DAPI
expression is blue. Sox9 intensity (when controlled for DAPI) is significantly higher
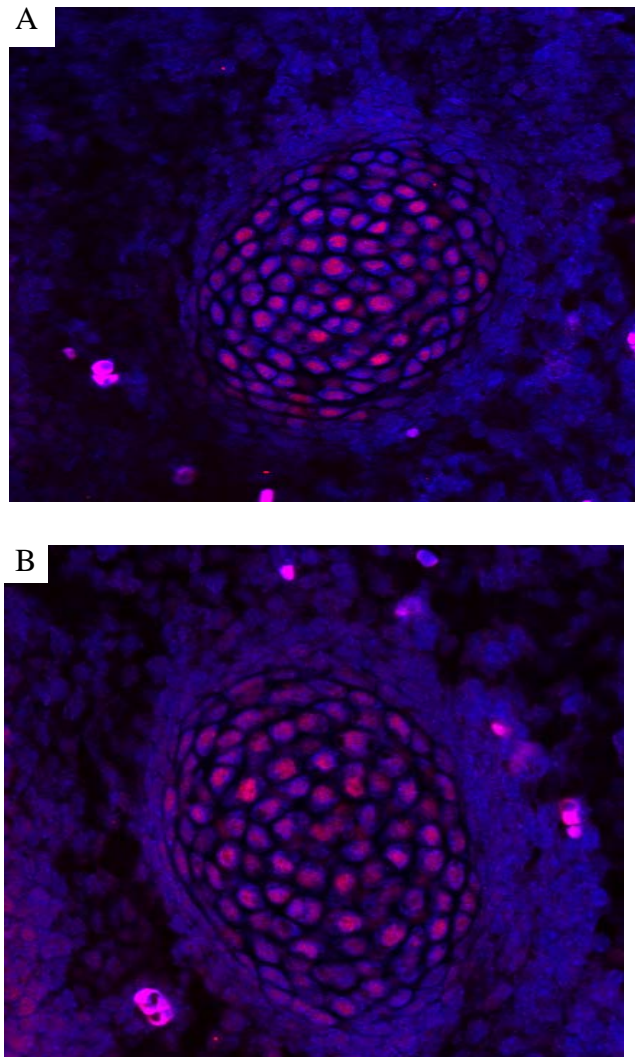in the trisomic Meckel's cartilage.

Figure 3.7.5: *Sox9* Expression in Euploid and Trisomic Hyoid Cartilage. The hyoid cartilage from E13.5 euploid (A) and trisomic (B) embryos with Sox9 antibody and DAPI stain. Sox9 expression is indicated by red color while DAPI expression is blue. Sox9 intensity (when controlled for DAPI) is significantly higher in the trisomic hyoid cartilage.
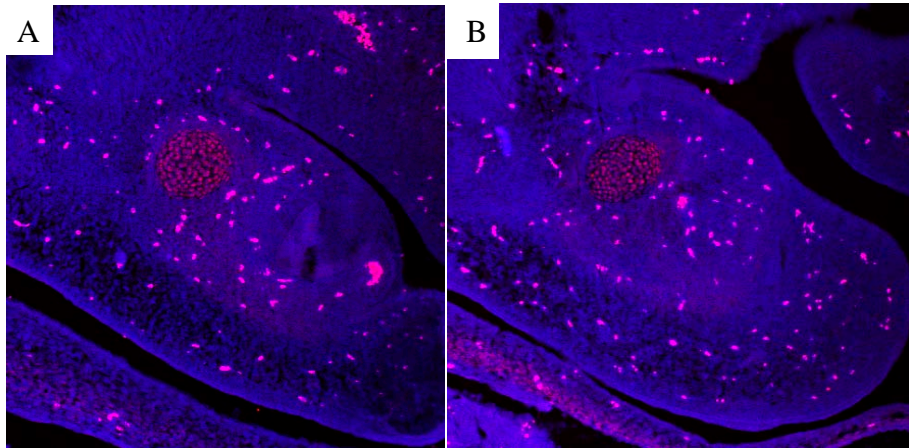
Figure 3.7.6: *Sox9* Expression in E13.5 Mandibular Precursor. E13.5 mandibular precursor with Sox9 antibody and DAPI stain. Red color indicates Sox9 protein and blue indicates nuclei. As hypothesized, *Sox9* expression is mainly localized to Meckel's cartilage in the mandibular precursor and is overexpressed in Ts65Dn embryos. (A) Trisomic (B) Euploid.
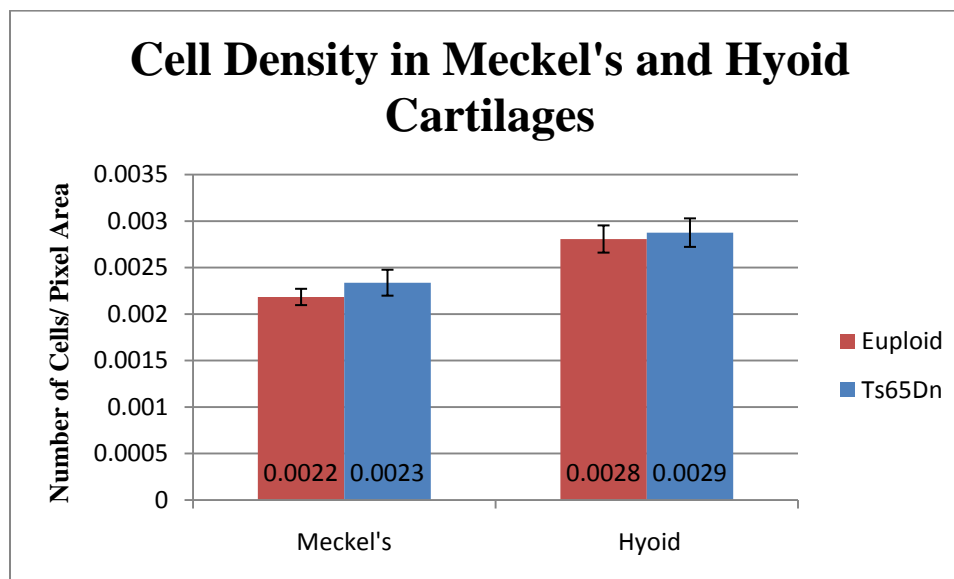
Figure 3.7.7: Cell Density in Meckel's and Hyoid Cartilages. There was no significant difference in the cell density of euploid and trisomic embryos in either Meckel's or hyoid cartilages (p= 0.35, n= 8 euploid and 8 trisomic; p= 0.75, n= 6 euploid, 5 trisomic). Error bars were calculated as standard error of the mean. These results indicate *Sox9* overexpression is not from an increased number of cells per area.